Supporting Information

Crystal Engineering in Oligorylenes: The Quest for Optimized Crystal Packing and Enhanced Charge Transport

Rahul Meena[1], Priya Pandey[1], Caterina Zuffa[2], Petr Brázda[3], Erika Samolova[3], Nemo McIntosh[4], Martina Volpi[1], Federico Modesti[5], Christos Gatsios[6], Nicholas Turetta[7], Luca Catalano[8,9], Wookjin Choi[10], Shu Seki[10], Jérôme Cornil[4] , Peter Erk[11], Norbert Koch[6], Paolo Samorì[7], Lucia Maini[2], Guillaume Schweicher[1*] and Yves Geerts[1, 12, 13*]

[1]Laboratory of Polymer Chemistry, Université Libre de Bruxelles (ULB), Boulevard du Triomphe, 1050, Bruxelles, Belgium
[2]Dipartimento di Chimica "G. Ciamician", via Selmi 2 − Università di Bologna, I-40126, Bologna, Italy
[3]Dept. of Structure Analysis, Institute of Physics, Czech Academy of Sciences Na Slovance 2/1999, Prague 8, 18221, Czech Republic
[4]Laboratory for Chemistry of Novel Materials, University of Mons, 7000 Mons, Belgium
[5]BASF SE RGD – J542S, 67056 Ludwigshafen am Rhein, Germany
[6]Institut für Physik and IRIS Adlershof Humboldt-Universitat zu Berlin 12489 Berlin, Germany
[7]University of Strasbourg, CNRS, ISIS UMR 7006, 8 Alleé Gaspard Monge, 67000 Strasbourg, France
[8]Dynamic Molecular Materials Laboratory, Dipartimento di Scienze della Vita, Università degli Studi di Modena e Reggio Emilia, Via Campi 103, 41125 Modena, Italy
[9]Department of Chemistry, University of Rochester, Rochester, New York 14627, United States
[10] Department of Molecular Engineering, Graduate School of Engineering, Kyoto University, Kyoto 615-8510, Japan
[11]erConTec GmbH, Roter-Turm-Weg 3, 67157 Wachenheim an der Weinstrasse, Germany
[12]International Solvay Institutes, ULB, CP 231 Boulevard du Triomphe, 1050, Bruxelles, Belgium
[13]WEL Research Institute, avenue Pasteur, 6, 1300 Wavre, Belgium

Table of Content

1.1 Methods and Materials:

1.1.1 Spectrometer for NMR and Mass sample

^{1}H NMR spectra recorded at 400 MHz, and the ^{13}C NMR spectra at 101 MHz, were either on a Varian VNMRS 400 device, or on a *JEOL JNM-ECZ400R / S3* device equipped with a 5 mm ROYAL HFX probe. $CDCl_3$ is used as solvent to record NMR spectra at 25 °C. Chemical shifts of ^{1}H NMR spectra are reported in units of parts per million (ppm) downfield from 1,1,1,1-tetramethylsilane (TMS) ($\delta = 0.0$) and relative to the signal of chloroform-d ($\delta = 7.260$, singlet) and couplings are expressed in Hertz. The multiplicities are expressed by the following usual abbreviations: s: singlet, brs (broad singlet), d: doublet, dd: doubled doublet, t: triplet, m: multiplet.

The mass spectra were recorded by the team of Professor Pascal Gerbaux from the Universite de Mons. MALDI-TOF spectra were recorded using *Waters QToF* device, and the EI-MS via a *Waters Autospec* EI Inner Ion Chamber device.

1.1.2 Experimental Procedure for Synthesis of Oligorylene series

a. Synthesis of 1,1,2,2-tetramethyl-1,2-dihydroacenaphthene (TMA)

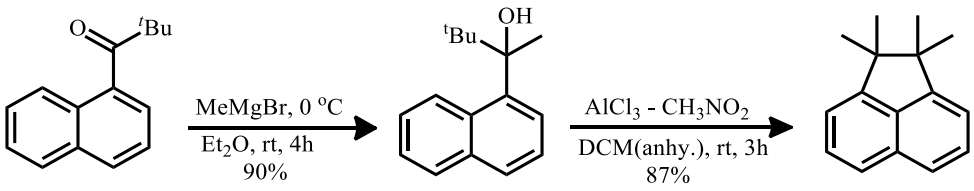

Following molecule had already been described by several groups.[1]

In an oven dried RB flask, anhydrous aluminum chloride (665 mg, 4.99 mmol, 1.2 equiv.) was weighed, mixed with nitromethane (2.2 ml, 41.6 mmol, 10 equiv.) and anhydrous DCM. In a separate RB flask, 3,3-Dimethyl-2-(naphthalen-4-yl)butan-2-ol (950 mg, 4.16 mmol, 1 equiv.) is dissolved in an equal volume of anhydrous DCM , which then added drop wise to the stirred aluminum chloride suspension. This addition takes 15-20 min. After addition is complete, reaction mixture is stirred at rt for 3h. It is decomposed by pouring into ice-water and extracted with DCM (3 x 10 ml), dried over $MgSO_4$, organic layer is collected and concentrated over rotary evaporator. Residue is purified over column chromatography on silica gel, using heptane to afford 898 mg with 87% yield as white solid product.

^{1}H NMR (400 MHz, $CDCl_3$) δ 7.86 (d, J = 8.2 Hz, 2H), 7.72 (dd, J = 8.3, 6.8 Hz, 2H), 7.43 (d, J = 6.9 Hz, 2H), 1.60 – 1.52 (m, 12H).

^{13}C NMR (101 MHz, $CDCl_3$) δ 153.62, 135.01, 131.46, 128.05, 122.71, 117.53, 49.92, 26.08.

GC-MS (EI) calcd for $C_{16}H_{18}$ 210.1 found 210.1

b. Synthesis of 5-bromo-1,1,2,2-tetramethyl-1,2-dihydroacenaphthlyene (5)

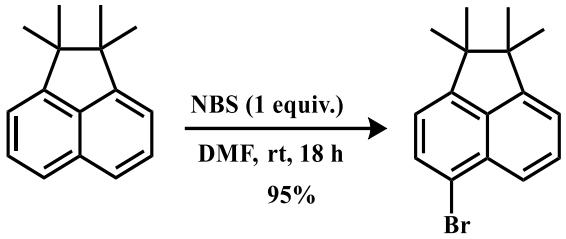

This compound was synthesized according to a protocol described.[2]

In a 250 mL flame-dried RB flask, 1,1,2,2-tetramethyl-1,2-dihydroacenaphthlyene (500 mg, 2.38 mol, 1.0 eq.) was dissolved in dry DMF. The reaction solution was cooled to 10 °C, and an NBS suspension (444 mg, 2.49 mmol, 1.05 eq.) in DMF was added dropwise over a time period of 20 min. The solution was stirred at room temperature for 18 h, protected from light, and mixture is poured over ice-cooled water to seize the reaction. The organic layer was washed with ether and concentrated over vacuum. Residue is purified over column chromatography on silica gel using heptane to afford 654 mg white solid product with 95% yield.

^{1}H NMR (400 MHz, $CDCl_3$) δ 7.88 (d, *J* = 8.5 Hz, 1H), 7.77 (d, *J* = 7.3 Hz, 1H), 7.65 (dd, *J* = 8.3, 6.9 Hz, 1H), 7.30 (d, *J* = 7.0 Hz, 1H), 7.11 (d, *J* = 7.4 Hz, 1H), 1.34 (s, 7H), 1.33 (d, *J* = 2.1 Hz, 6H).

^{13}C NMR (101 MHz, $CDCl_3$) δ 153.84, 153.62, 137.91, 136.09, 131.29, 130.84, 129.52, 122.32, 118.70, 118.68, 117.26, 50.21, 49.74, 26.17, 26.05.

HRMS (MALDI) – calcd for $C_{16}H_{17}Br$ 288.0514 found 288.0509, m/z: 288.0514 (100.0%), 290.0493 (97.3%), 291.0527 (16.8%), 289.0547 (16.2%), 292.0560 (1.4%)

c. Synthesis of 5-diaoxaborolane-1,1,2,2-tetramethyl-1,2-dihydroacenaphthlyene (8)

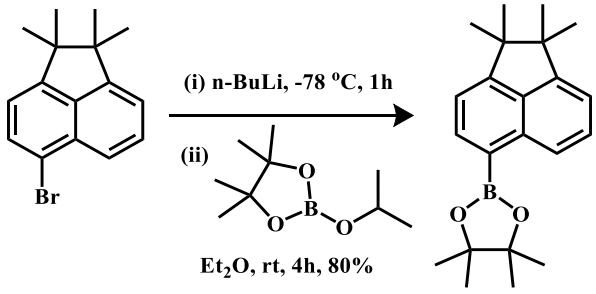

In an RB flask, 5-bromo-1,1,2,2-tetramethyl-1,2-dihydroacenaphthlyene (500 mg, 1.72 mmol, 1.0 eq.) was dissolved in 20 mL of dry diethyl ether. The reaction mixture was cooled to −78 °C, and 2.6 M nBuLi in hexane (0.72 ml, 1.81 mmol, 1.05 eq.) was added dropwise. The reaction mixture was stirred at -78 °C for 1h. In reaction mixture, 2-isopropoxy-4,4,5,5-tetramethyl-1,3,2-dioxaborolane (0.385 mL, 1.89 mmol, 1.1 eq.) was added dropwise and reaction mixture was stirred for 4 h and quenched with 20 mL of brine. The organic phase was separated, and the aqueous layer was extracted with DCM three times. The combined organic layers were washed three times with water and dried over $MgSO_4$. The solvent was removed under a vacuum. The residue is purified over column chromatography on silica gel using heptane to afford 465 mg yellowish white solid product with 80% yield.

^{1}H NMR (400 MHz, $CDCl_3$) δ 8.39 (d, *J* = 7.9 Hz, 1H), 8.10 (d, *J* = 6.9 Hz, 1H), 7.53 (dd, *J* = 8.4, 6.9 Hz, 1H), 7.25 – 7.16 (m, 2H), 1.40 (s, 12H), 1.27 (s, 6H), 1.27 (s, 6H). .

^{13}C NMR (101 MHz, $CDCl_3$) δ 157.72, 153.66, 137.92, 135.26, 134.62, 128.53, 124.19, 117.49, 117.15, 83.48, 49.91, 49.72, 26.06, 25.87, 25.07.

HRMS (MALDI) - calcd for $C_{22}H_{29}BO_2$ 336.2261 found 336.2260

d. Synthesis of 2,2-dimethyl-1-(1,1,2,2-tetramethyl-1,2-dihydroacenaphthylen-5-yl)propan-1-one (6)

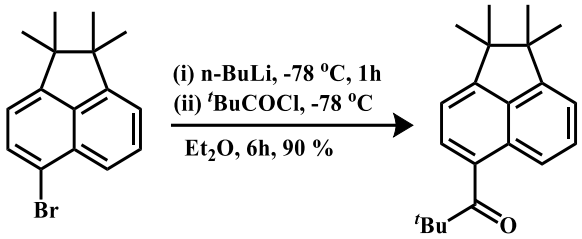

An oven dried RB flask with magnetic stir bar is charged with 5-bromo-1,1,2,2-tetramethyl-1,2-dihydroacenaphthlyene (500mg, 1.72 mmol, 1.0 eq.) and freshly distilled THF under inert atmosphere. 2.6M of ^{n}BuLi in hexane (0,730 ml, 1.90 mmol, 1.1 eq.) is added dropwise to the reaction solution at −78 °C, and then the reaction mixture was stirred to room temperature. Cooled again to −78 °C and ^{t}BuCOCl (0.231 ml, 1.89 mmol, 1.1 eq.) is added dropwise to the reaction mixture, warmed, and stirred at room temperature for 6 h. Finally, the reaction mixture is quenched with NH_4Cl (aq.), diluted with Et_2O, and washed with brine, the organic layer is dried and concentrated, the residue is purified by column chromatography on silica gel (PE/EA = 60/1, v/v) to get 458 mg product as a white solid with 90% yield.

^{1}H NMR (400 MHz, $CDCl_3$) δ 7.50 (s, 1H), 7.49 (d, *J* = 1.0 Hz, 1H), 7.47 (d, *J* = 7.0 Hz, 1H), 7.20 (t, *J* = 4.2, 3.4 Hz, 1H), 7.13 (d, *J* = 7.1 Hz, 1H), 1.34 (s, 9H), 1.27 (d, *J* = 1.1 Hz, 12H).

^{13}C NMR (101 MHz, $CDCl_3$) δ 213.43, 155.30, 153.76, 135.05, 134.21, 129.06, 128.77, 125.42, 121.37, 118.13, 115.97, 77.11, 49.87, 45.38, 27.62, 26.06.

GC-MS (EI): Calcd for $C_{21}H_{26}O$ 294.2 found 294.2

e. Synthesis of 3,3-dimethyl-2-(1,1,2,2-tetramethyl-1,2-dihydroacenaphthylen-5-yl)butan-2-ol (7)

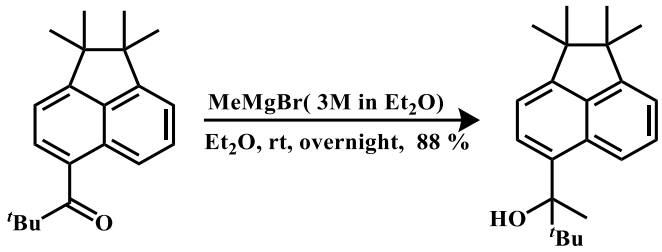

In an oven dried RB flask, 2,2-dimethyl-1-(1,1,2,2-tetramethyl-1,2-dihydroacenaphthylen-5-yl)propan-1-one (500 mg, 1.69 mmol, 1 eq.) is dissolved in diethyl ether and stirred for 20 minutes at 0 ^{o}C. Now, 3M MeMgBr in diethyl ether (0.67 ml, 2.03 mmol, 1.2 equiv.) is added to solution drop wise. After addition, reaction mixture left to stir at room temperature for the desired time and later on quench with aq. NH_4Cl solution. The product is extracted with diethyl ether and the combined organic phases were washed with water, dried over anhydrous $MgSO_4$ and the solvent was evaporated to get crude mixture. The residue was purified by flash column chromatography (basic alumina, DCM/P.E, 2:8) to afford 463 mg white solid powder with 88% yield.

^{1}H NMR – surprisingly, it was impossible to get a clear NMR

^{13}C NMR (101 MHz, $CDCl_3$) 153.05, 135.71, 129.22, 126.96, 116.73, 116.22, 49.39, 48.73, 39.71, 26.73, 26.37, 26.23, 25.98, 25.88.

GC-MS (EI) calcd for $C_{22}H_{30}O$ 310.23, found $C_{22}H_{30}O - H_2O$ 292.2

f. Synthesis of 1,1,2,2,5,5,6,6-octamethyl-1,2,5,6-tetrahydropyracene (OMPy)

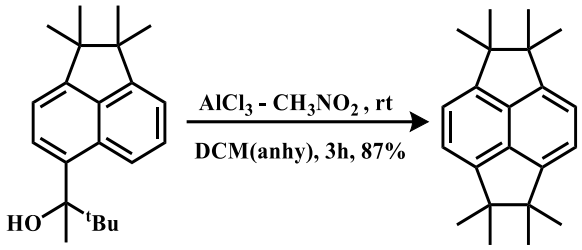

In an oven dried RB flask, anhydrous aluminum chloride (257.67 mg, 1.93 mmol 1.2 eq.) was weighed, mixed with nitromethane (1.04 ml, 19.3 mmol, 10 eq.) and anhydrous DCM. In a separate RB flask, 3,3-dimethyl-2-(1,1,2,2-tetramethyl-1,2-dihydroacenaphthylen-5-yl)butan-2-ol (500 mg, 1.610 mmol, 1 eq.) is dissolved in an equal volume of anhydrous DCM was then added drop wise to the stirred aluminum chloride suspension. This addition takes 15-20 min. After addition is complete, reaction mixture is stirred for 3h. Reaction progress checked by TLC. The reaction mixture was decomposed by pouring into ice-water and extracted with DCM (3 x 10 ml), dried over $MgSO_4$, organic layer is collected and concentrated over rotary evaporator. Residue is purified over column chromatography on silica gel, using heptane to afford 410 mg as white solid with 87% yield.

^{1}H NMR (600 MHz, $CDCl_3$) 7.14 (s, 1H), 1.31 (s, 6H).

^{13}C NMR (151 MHz, $CDCl_3$) δ 149.05, 133.58, 118.82, 52.36, 26.25.

GC-MS (EI) calcd for $C_{22}H_{28}$ 292.2 found 292.2.

g. Synthesis of 1,1,2,2-tetramethyl-5-(naphthalen-1-yl)-1,2-dihydroacenaphthene (9)

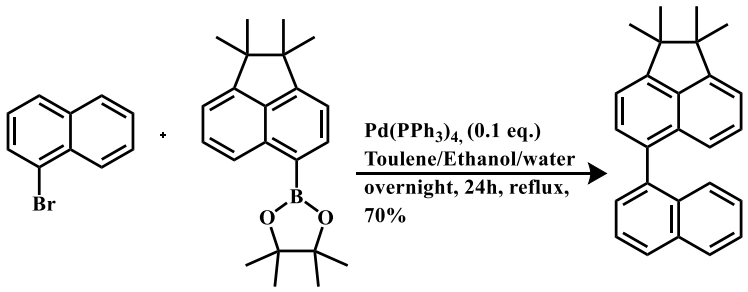

An oven dried RB flask is charged with 5-diaoxaborolane-1,1,2,2-tetramethyl-1,2-dihydroacenaphthlyene (714.56 mg, 2.12 mmol, 1.1 eq.), 1-bromonaphthalene (400 mg, 1.93 mmol, 1.0 eq.), $Pd(PPh_3)_4$ (0.2 eq., 0.0968 mmol) in Toulene (5ml) and stirred for 15 minutes at room temperature. After that, 0.5 ml of 2M aqueous K_2CO_3 solution is added into the mixture. The homogeneous mixture was then refluxed with vigorous stirring for overnight. Reaction progress is monitored with TLC. After being cooled down to room temperature, mixture is passed through silica pad and the filtrate was washed with brine and $CHCl_3$. The mixture was concentrated over rotary evaporator and further purified by silica-gel column chromatography using heptane as eluent to get fine 454 mg white powder as product with 70% yield.

^{1}H NMR (400 MHz, $CDCl_3$) δ 7.92 (dd, *J* = 8.2, 3.8, 1.1 Hz, 2H), 7.59 – 7.55 (m, 2H), 7.53 – 7.49 (m, 2H), 7.48 – 7.44 (m, 1H), 7.34 – 7.28 (m, 3H), 7.21 – 7.14 (m, 2H), 1.39 (s, 3H), 1.37 (d, *J* = 2.2 Hz, 6H), 1.34 (s, 3H).

^{13}C NMR (101 MHz, $CDCl_3$) δ 153.71, 153.36, 138.44, 135.00, 134.23, 133.73, 132.91, 130.97, 129.81, 128.20, 128.07, 128.02, 127.70, 126.82, 125.83, 125.78, 125.48, 121.89, 117.59, 117.30, 50.02, 49.70, 26.33, 26.15, 26.08.

HRMS (MALDI) – calcd for $C_{26}H_{24}$ 336.1878 found 336.1888.

h. Synthesis of 1,1,2,2-tetramethyl-1,2-dihydrocyclopenta[cd]perylene (TMP)

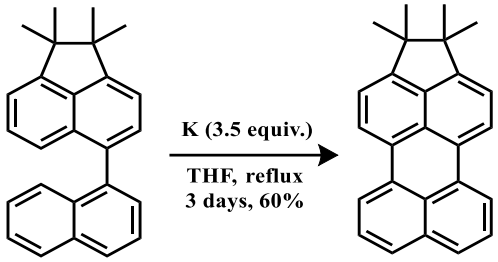

To a flame-dried seal tube was added 1,1,2,2-tetramethyl-5-(naphthalen-1-yl)-1,2-dihydroacenaphthylene (400 mg, 1.18 mmol, 1.0 eq.) and a freshly cut piece of potassium metal (136 mg, 3.5 mmol, 3.5 eq.) rinsed with hexanes and THF added to it. The seal tube was closed, and nitrogen was purged. Solvent was degassed via pump thaw freeze method in a separate Schlenk tube and later added to the reaction mixture. Solution is sealed, stirred and heated of 3 days.

After completion reaction mixture is cool down to room temperature, and the solution was removed from the remaining potassium by vacuum cannulation into a flame-dried flask under a nitrogen atmosphere. The reaction vessel was washed with some dry THF, and the solution again was removed by vacuum cannulation. The dark purple to blue solution was quenched by adding a solution of iodine (898 mg, 3.5 mmol) in ~6 mL of dry THF over a period of 15 min, which caused the solution to turn yellow. To the solution was then added slowly ethanol (5 mL) followed by sodium thiosulfate (10% in water, ~50 mL) until the colour no longer changed typically a yellow solution. The reaction was then exposed to air, and the organic solvents were removed on a rotary evaporator.

To the remaining aqueous solution containing precipitates was added dichloromethane (DCM, 100 mL), and the aqueous layer was extracted three times. The combined organic layers were washed with brine and dried over $MgSO_4$, and the solvent was removed on a rotary evaporator. The residue was adsorbed onto silica, and the mixture was subjected to flash column chromatography (SiO_2, 1:15 DCM/hexanes) to provide 238 mg of a yellow solid in 60% yield.

^{1}H NMR (400 MHz, $CDCl_3$) δ 8.12 – 8.07 (m, 4H), 7.60 (d, *J* = 7.5 Hz, 2H), 7.41 (t, *J* = 8.1, 7.4 Hz, 2H), 7.20 (d, *J* = 7.4 Hz, 2H), 1.31 (s, 12H).

^{13}C NMR (101 MHz, $CDCl_3$) δ 153.22, 135.87, 135.48, 131.67, 129.68, 128.50, 127.44, 126.82, 126.43, 121.40, 119.30, 119.27, 118.89, 50.41, 25.84.

HRMS (MALDI) – calcd for 334.1722 found 334.1733.

i. Synthesis of 1,1,1',1',2,2,2',2'-octamethyl-1,1',2,2'-tetrahydro-5,5'-biacenaphthylene (10)

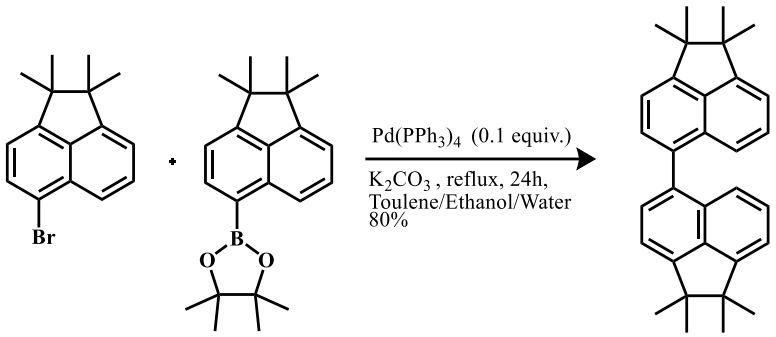

This compound was synthesized according to a protocol described.[3,4]

An oven dried RB flask is charged with 5-diaoxaborolane-1,1,2,2-tetramethyl-1,2-dihydroacenaphthlyene (639.15 mg, 1.90 mmol, 1.1 eq.), 5-bromo-1,1,2,2-tetramethyl-1,2-dihydroacenaphthlyene (500 mg, 1.72 mmol, 1.0 eq.), $Pd(PPh_3)_4$ (199.58 mg, 0.17 mmol, 0.1 eq.) in Toulene/ethanol/H_2O and stirred for 15 minutes at room temperature. After that, 0.5 ml of 2M aqueous K_2CO_3 solution is added into the mixture. The homogeneous mixture was then refluxed with vigorous stirring for 24h. Reaction progress is monitored with TLC. After being cooled down to room temperature, mixture is passed through silica pad and the filtrate was washed with brine and $CHCl_3$. The mixture was concentrated over rotary evaporator and further purified by silica-gel column chromatography using heptane as eluent to get fine 578 mg white powder as product with 80% yield.
^{1}H NMR (400 MHz, $CDCl_3$) δ 7.53 (d, *J* = 7.0 Hz, 2H), 7.35 (d, *J* = 0.7 Hz,2), 7.34 (s, 2H), 7.28 (d, *J* = 6.9 Hz, 2H), 7.19 – 7.17 (m, 2H), 1.38 – 1.33 (m, 24H).

^{13}C NMR (101 MHz, $CDCl_3$) δ 153.69, 153.03, 135.22, 134.18, 130.94, 129.91, 127.89, 122.21, 117.52, 117.39, 50.03, 49.68, 26.38, 26.28, 26.22.
HRMS (MALDI) calcd for $C_{32}H_{34}$ 418.2661 found 418.2656

j. Synthesis of 1,1,2,2,7,7,8,8-octamethyl-1,2,7,8 tetrahydrodicyclopenta[cd,lm]perylene (OMP)

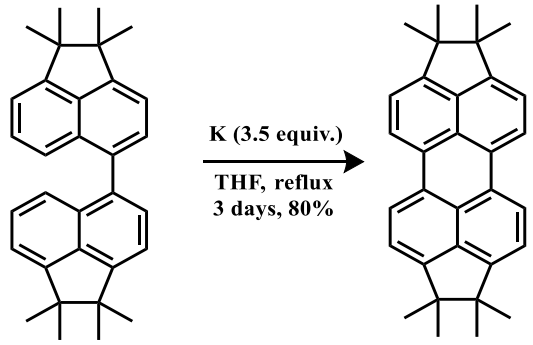

To a flame-dried seal tube was added 1,1,1',1',2,2,2',2'-octamethyl-1,1',2,2'-tetrahydro-5,5'-biacenaphthylene (400 mg, 0.95 mmol, 1.0 eq.) and a freshly cut piece of potassium metal (136 mg, 3.5 mmol, 3.5 eq.) rinsed with hexanes and THF added to it. The seal tube was closed, and nitrogen was purged. Solvent was degassed via pump thaw freeze method in a separate Schlenk tube and later added to the reaction mixture. Solution is sealed, stirred, and heated of 3 days.

After completion reaction mixture is cool down to room temperature, and the solution was removed from the remaining potassium by vacuum cannulation into a flame-dried flask under a nitrogen atmosphere. The reaction vessel was washed with some dry THF, and the solution again was removed by vacuum cannulation. The dark purple to blue solution was quenched by adding a solution of iodine (964 mg, 3.8 mmol) in ~6 mL of dry THF over a period of 15 min, which caused the solution to turn yellow. To the solution was then added slowly ethanol (5 mL) followed by sodium thiosulfate (10% in water, ~50 mL) until the colour no longer changed typically a yellow solution). The reaction was then exposed to air, and the organic solvents were removed on a rotary evaporator.

To the remaining aqueous solution containing precipitates was added dichloromethane (DCM, 100 mL), and the aqueous layer was extracted three times. The combined organic layers were washed with brine and dried over $MgSO_4$, and the solvent was removed on a rotary evaporator.

The residue was adsorbed onto silica, and the mixture was subjected to flash column chromatography heptane yielding 320 mg (80%) as a yellow solid.

^{1}H NMR (400 MHz, $CDCl_3$) δ 8.00 (d, *J* = 7.4 Hz, 1H), 7.15 (d, *J* = 7.4 Hz, 1H), 1.29 (s, 6H).

^{13}C NMR (101 MHz, $CDCl_3$) δ 152.46, 136.31, 128.91, 127.65, 120.36, 118.65, 50.18, 29.78, 25.82.

HRMS (MALDI) calcd for $C_{32}H_{32}$ 416.2504 found 416.2490

k. Synthesis of 3-(1,1,2,2-tetramethyl-1,2-dihydroacenaphthylen-5-yl)perylene (11)

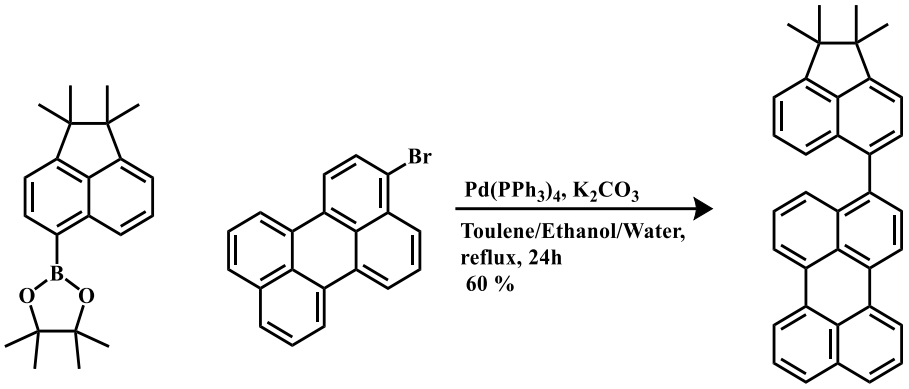

An oven-dried RB flask is charged with 5-diaoxaborolane-1,1,2,2-tetramethyl-1,2-dihydroacenaphthylene (444 mg, 1.32 mmol, 1.1 eq.), 3-bromoperylene (400 mg, 1.20 mmol, 1.0 eq.), $Pd(PPh_3)_4$ (138mg, 0.12 mmol, 0.1 eq.) and stirred for 15 minutes at room temperature. After that, 0.5 ml of 2M aqueous K_2CO_3 (1.6 g, twelve mmol, 10 eq.) solution is added into the mixture. The reaction mixture was then refluxed with vigorous stirring for overnight. Reaction progress is monitored with TLC. After cooling to room temperature, the reaction was diluted with dichloromethane (200 mL x 1), washed with water (100 mL x 2) and brine (50 mL x 1). The extract was then dried over $MgSO_4$, concentrated on rota, and purified by silica gel column chromatography (heptane) yield, 333 mg of 3-(1,1,2,2-tetramethyl-1,2-dihydroacenaphthylen-5-yl)perylene with 60 % yield as a yellow solid.

^{1}H NMR (400 MHz, $CDCl_3$) δ 8.29 (d, *J* = 7.7 Hz, 1H), 8.26 – 8.18 (m, 3H), 7.70 (d, *J* = 8.1 Hz, 2H), 7.55 – 7.49 (m, 4H), 7.43 (dd, *J* = 101.4, 8.4 Hz, 1H), 7.38 – 7.27 (m, 4H), 7.21 (d, *J* = 6.8 Hz, 1H), 1.39 (s, 3H), 1.37 (d, *J* = 1.8 Hz, 6H), 1.34 (s, 3H).

^{13}C NMR (101 MHz, $CDCl_3$) δ 153.80, 153.54, 138.32, 135.08, 134.86, 134.22, 134.19, 131.62, 131.50, 131.39, 130.86, 130.78, 129.74, 129.03, 128.85, 128.83, 128.20, 127.84, 127.81, 126.95, 126.73, 126.71, 126.41, 121.87, 120.39, 120.36, 120.18, 120.02, 117.69, 117.42, 50.05, 49.74, 26.33, 26.15, 26.08.

HRMS (MALDI) calcd for $C_{36}H_{28}$ 460.2191 found 460.2192

l. Synthesis of 1,1,2,2-tetramethyl-1,2-dihydrocyclopenta[cd]terrylene (TMT)

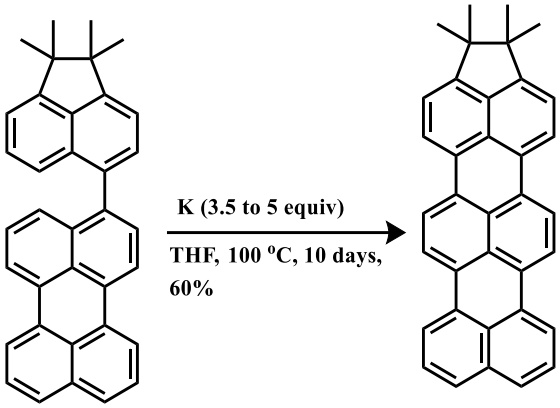

To a flame-dried seal tube was charged with 3-(1,1,2,2-tetramethyl-1,2-dihydroacenaphthylen-5-yl)perylene (400mg, 0.86 mmol, 1.0 eq.) and a freshly cut piece of potassium metal (118 mg, 3.03 mmol, 3.5 eq.) rinsed with hexanes and THF (dry) added to it. The seal tube is purged with nitrogen and closed. After half an hour of stirring, reaction mixture turns black because of the potassium. Reaction is left to stir at least 5 days to observe a considerable conversion. After completion, reaction mixture is cool down to room temperature, and the solution was removed from the remaining potassium by vacuum cannulation into a flame-dried flask under a nitrogen atmosphere. The reaction vessel was washed with some dry THF, and the solution again was removed by vacuum cannulation. The dark purple to blue solution was quenched by adding a solution of iodine (890 mg, 3.45 mmol) in ~6 mL of dry THF over a period of 15 min, which caused the solution to turn yellow. To the solution was then added slowly ethanol (5 mL) followed by sodium thiosulfate (10% in water, ~50 mL) until the colour no longer changed typically a yellow solution). The reaction was then exposed to air, and the organic solvents were removed on a rotary evaporator.

To the remaining aqueous solution containing precipitates was added dichloromethane (DCM, 100 mL), and the aqueous layer was extracted 3 times. The combined organic layers were washed with brine and dried over $MgSO_4$, and the solvent was removed on a rotary evaporator. Crude mixture result in 238 mg dark purple powder with 60% yield. The resulting product was purified further by gradient sublimation (1 x 10^{-6} Torr at 300° C) to purify further and yield 1,1,2,2-tetramethyl-1,2-dihydrodibenzo[*kl*, *rst*]indeno[1,7,6-*cde*]pentaphene as a crystalline purple powder.

^{1}H NMR (400 MHz, $CDCl_3$) δ 8.26-8.18 (m, 8H), 7.70-7.68 (m, 2H), 7.53-7.50 (m, 2H), 7.30 (d, *J* = 7.5 Hz, 2H), 1.34 (s, 12H).

^{13}C NMR – Insoluble to record carbon NMR

HRMS (MALDI) calcd for $C_{36}H_{26}$ 458,2035 found 458

m. Synthesis of 1,4-bis(1,1,2,2-tetramethyl-1,2-dihydroacenaphthylen-5-yl)naphthalene (12)

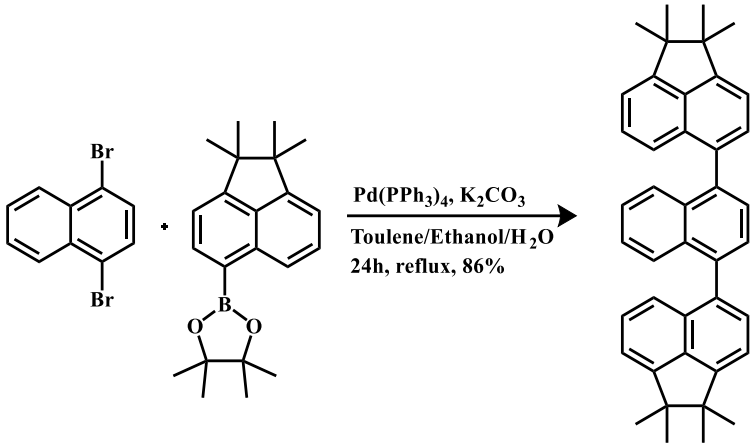

A two neck oven dried RB flask is charged with 5-diaoxaborolane-1,1,2,2-tetramethyl-1,2-dihydroacenaphthlyene (1.03 g, 3.07 mmol, 2.2 eq.), 1,4-dibromo naphthalene (400 mg, 1.39 mmol, 1.0 eq.), $Pd(PPh_3)_4$ (160.54 mg, 0.139 mmol, 0.10 eq.) in mixed solvent Toulene (35ml)/ water (7.5ml)/Ethanol (7.5 ml) and stirred for 15 minutes at room temperature. After that, 0.5 ml of 2M aqueous K_2CO_3 (1.91 g, 13.9 mmol, 10 eq.) solution is added into the mixture. The reaction mixture was then refluxed with vigorous stirring for overnight. Reaction progress is monitored with TLC. After cooling to room temperature, the reaction was diluted with dichloromethane (200 mL x 1), washed with water (100 mL x 2) and brine (50 mL x 1). The extract was then dried over $MgSO_4$, concentrated on rota, and purified by silica gel column chromatography (heptane) yield, 609 mg of 1,4-bis(1,1,2,2-tetramethyl-1,2-dihydroacenaphthylen-5-yl)naphthalene with 86% yield as a white solid.

^{1}H NMR (400 MHz, Benzene-d_6) δ 7.93 – 7.88 (m, 2H), 7.71 (d, J = 7.0 Hz, 1H), 7.65 – 7.62 (m, 2H), 7.57 (d, J = 1.3 Hz, 2H), 7.50 (d, J = 8.4 Hz, 1H), 7.33 (dd, J = 8.4, 6.8 Hz, 1H), 7.28 (dd, J = 8.4, 6.8 Hz, 1H), 7.21 – 7.17 (m, 2H), 7.10 (t, J = 7.0 Hz, 2H), 7.04 – 7.00 (m, 2H), 1.32 (s, 3H), 1.27 (d, J = 5.4 Hz, 12H), 1.23 (s, 3H).

^{13}C NMR (101 MHz, $C_2D_2Cl_4$) δ 196.43, 153.93, 153.50, 138.12, 135.33, 134.54, 133.35, 131.36, 130.17, 128.20, 127.69, 127.07, 125.56, 122.07, 117.59, 117.34, 73.84, 50.20, 49.87, 26.32, 26.20, 26.12.

HRMS (MALDI) calcd for $C_{42}H_{40}$ 544.3130 found 544.3136, isotropic distribution 544.3 (100%), 545.3 (45.6 %), 546.3 (10.1 %)

n. Synthesis of 1,1,2,2,9,9,10,10-octamethyl-1,2,9,10-tetrahydrodicyclopenta[cd,lm]terrylene (OMT)

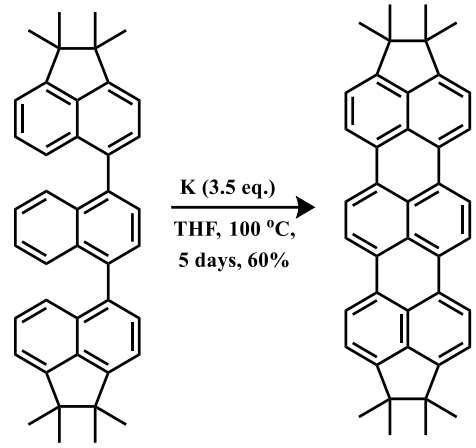

To a flame-dried seal tube was added 1,4-bis(1,1,2,2-tetramethyl-1,2-dihydroacenaphthylen-5-yl)naphthalene (400 mg, 0.734 mmol, 1.0 eq.) and a freshly cut piece of potassium metal (136 mg, 3.5 mmol, 3.5 eq.) rinsed with hexanes and THF added to it. The seal tube was closed and nitrogen is purged. Solvent was degassed via pump thaw freeze method in a separate Schlenk tube and later added to the reaction mixture. Solution is sealed, stirred and heated of 10 days.

After completion reaction mixture is cool down to room temperature, and the solution was removed from the remaining potassium by vacuum cannulation into a flame-dried flask under a nitrogen atmosphere. The reaction vessel was washed with some dry THF, and the solution again was removed by vacuum cannulation. The dark purple to blue solution was quenched by adding a solution of iodine (760 mg, 2,9 mmol) in ~6 mL of dry THF over a period of 15 min, which caused the solution to turn yellow. To the solution was then added slowly ethanol (5 mL) followed by sodium thiosulfate (10% in water, ~50 mL) until the colour no longer changed typically a yellow solution). The reaction was then exposed to air, and the organic solvents were removed on a rotary evaporator.

To the remaining aqueous solution containing precipitates was added dichloromethane (DCM, 100 mL), and the aqueous layer was extracted 3 times. The combined organic layers were washed with brine and dried over $MgSO_4$, and the solvent was removed on a rotary evaporator. Crude mixture result in 238 mg dark purple powder with 60% yield. The resulting product was purified further by gradient sublimation (1×10^{-6} Torr at 300° C) to purify further and yield 1,1,2,2,9,9,10,10-octamethyl-1,2,9,10-tetrahydrobenzo[*rst*]diindeno [1,7,6-*cde*:6',7',1' klm]pentaphene as a crystalline purple powder.

^{1}H NMR (400 MHz, $CDCl_3$) δ 8.15 (s, 4H), 8.10 (d, *J* = 7.5 Hz, 4H), 7.22 (d, *J* = 7.5 Hz, 4H), 1.31 (s, 24H).

^{13}C NMR – Insoluble to record carbon NMR

HRMS (MALDI) calcd for $C_{42}H_{36}$ 540.2817 found 540.2809

1.1.3 ^{1}H and ^{13}C NMR Spectra recorded in $CDCl_3$

1.1.3.1. ^{1}H and ^{13}C spectra of 1,2-Dihydro-1,1-dimethyl-2,2-diphenylacenaphthylene

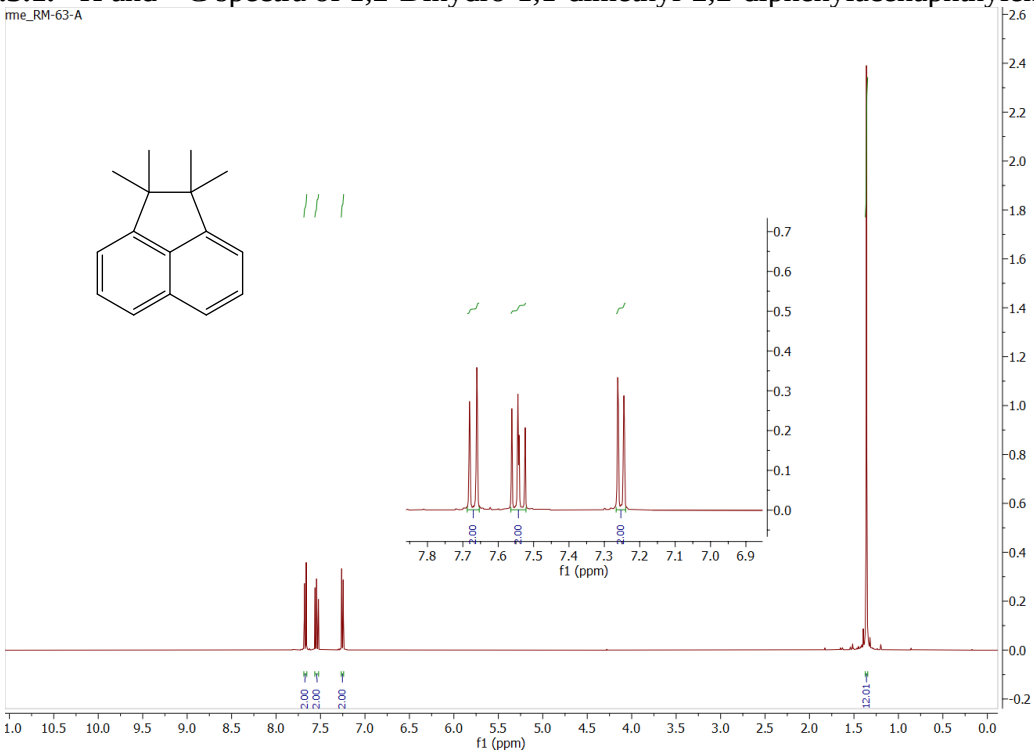

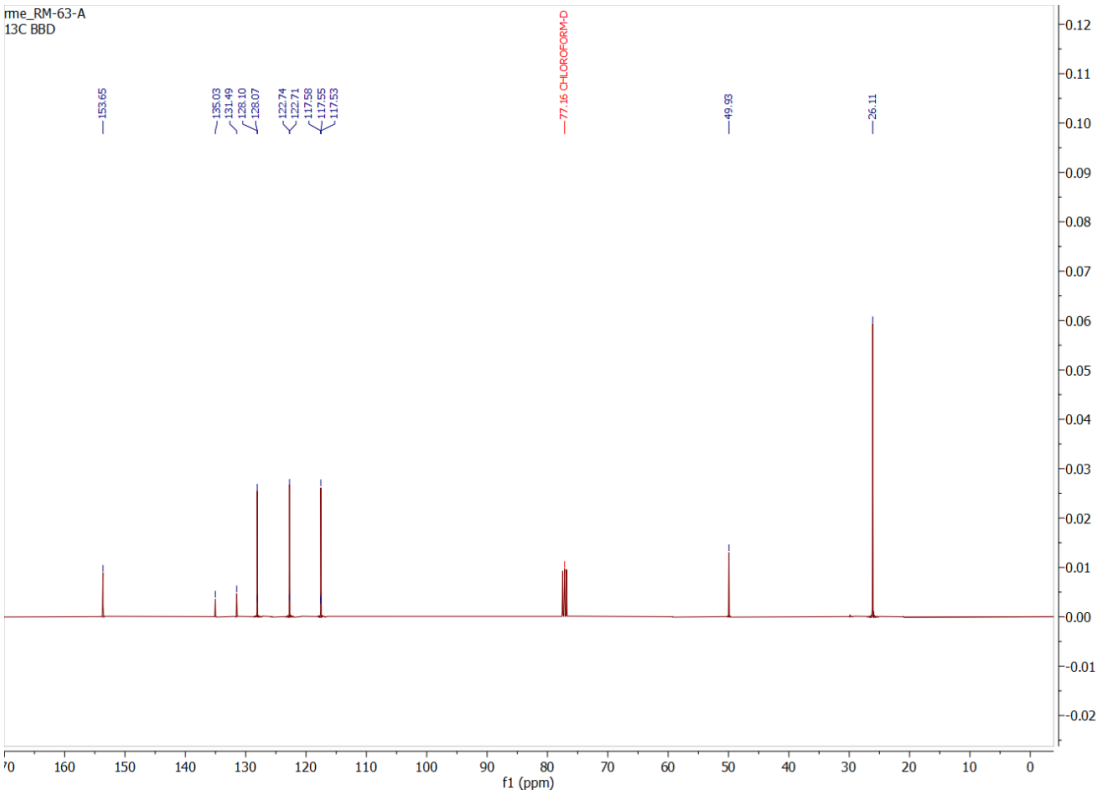

1.1.3.2. ^{1}H and ^{13}C spectra of 5-bromo-1,1,2,2-tetramethyl-1,2-dihydroacenaphthylene (5)

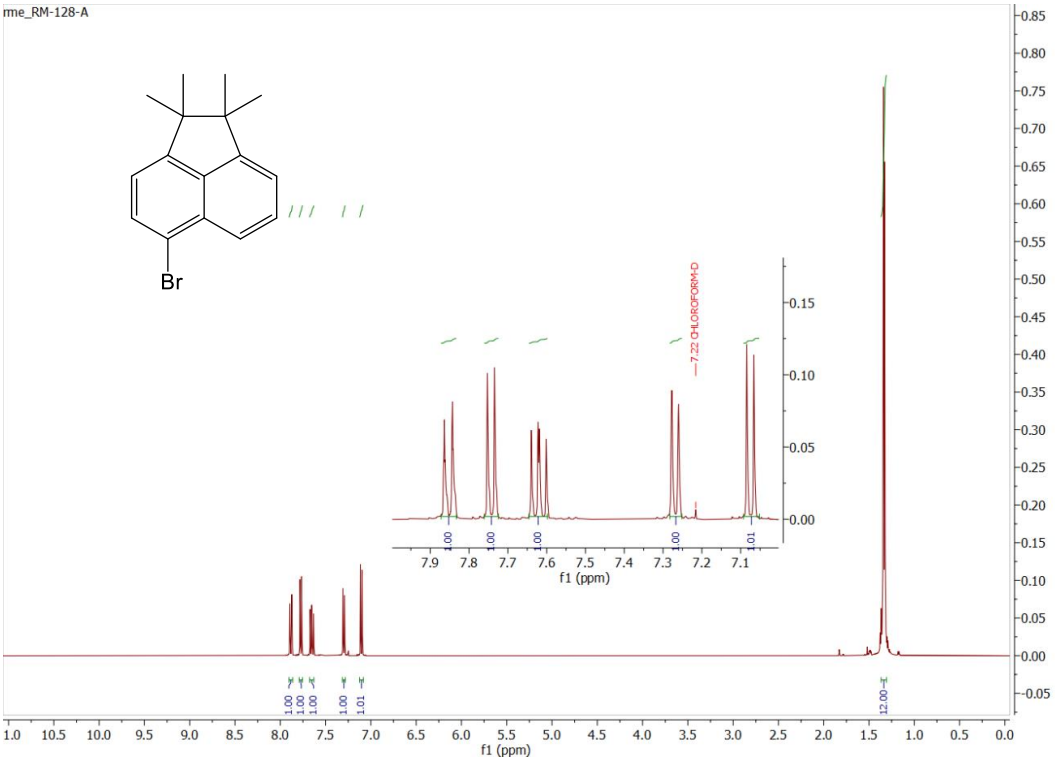

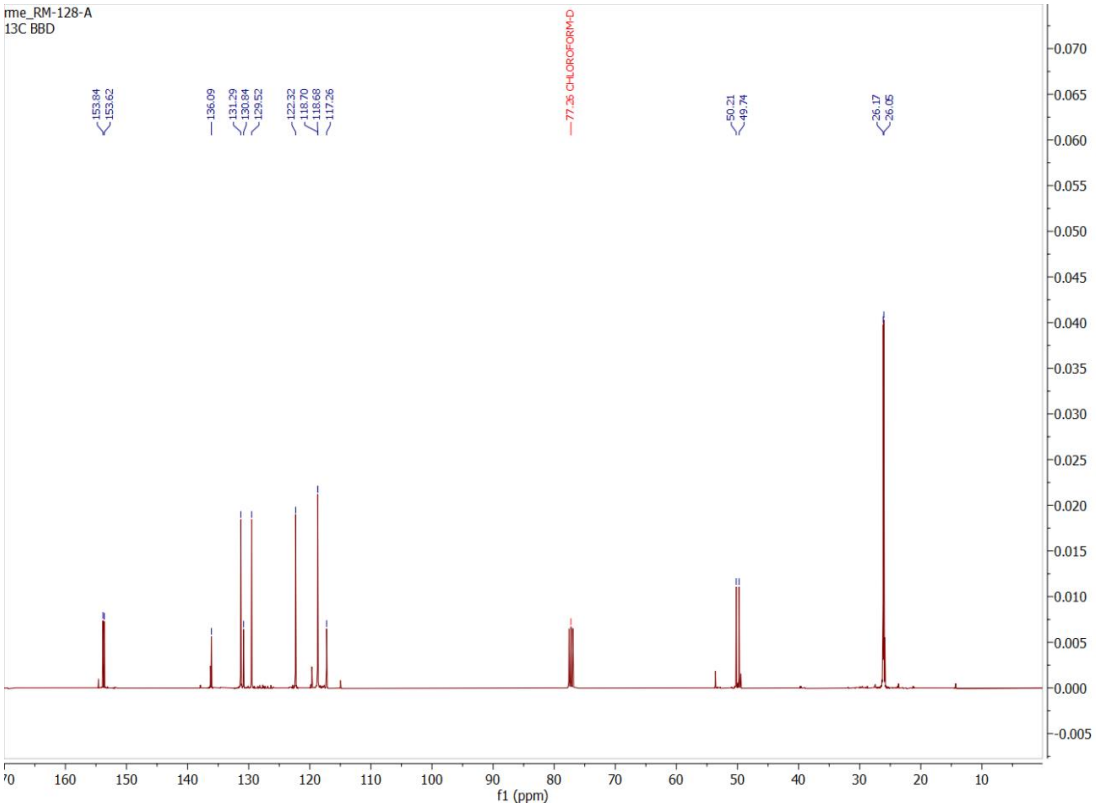

1.1.3.3. ^{1}H and ^{13}C spectra of 5-diaoxaborolane-1,1,2,2-tetramethyl-1,2-dihydroacenaphthylene (8)

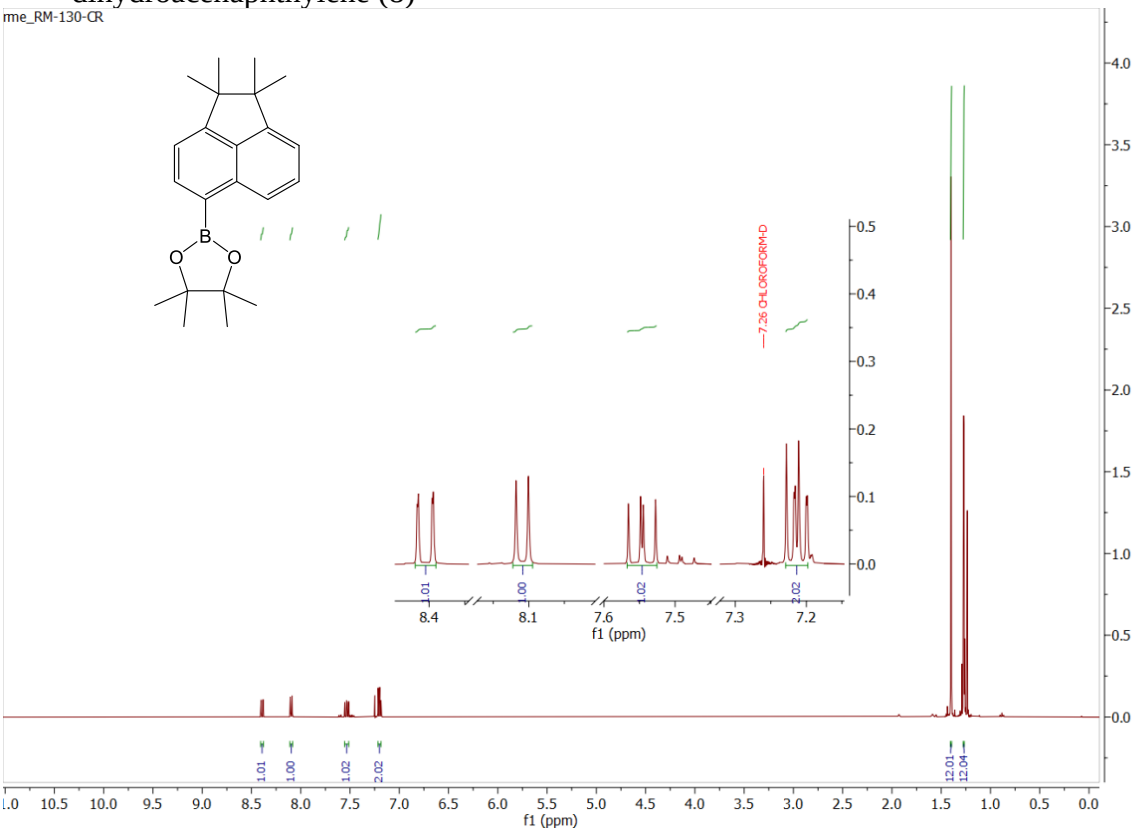

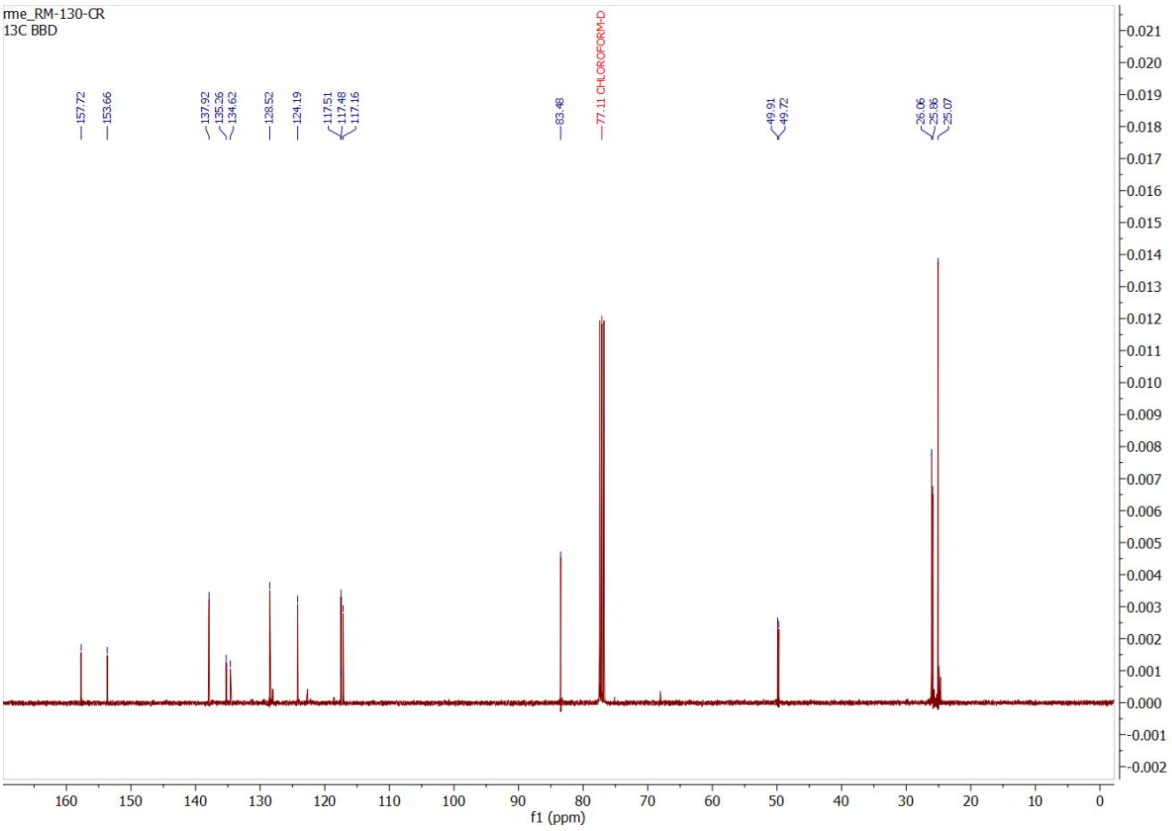
rme_RM-130-CR
13C BBD
157.72
153.66
137.92
135.26
134.62
128.52
124.19
117.51
117.48
117.16
83.48
77.11 CHLOROFORM-D
49.91
49.72
26.06
25.86
25.07
f1 (ppm)

1.1.3.4. ^{1}H and ^{13}C spectra of 2,2-dimethyl-1-(1,1,2,2-tetramethyl-1,2-dihydroacenaphthylen-5-yl)propan-1-one (6)

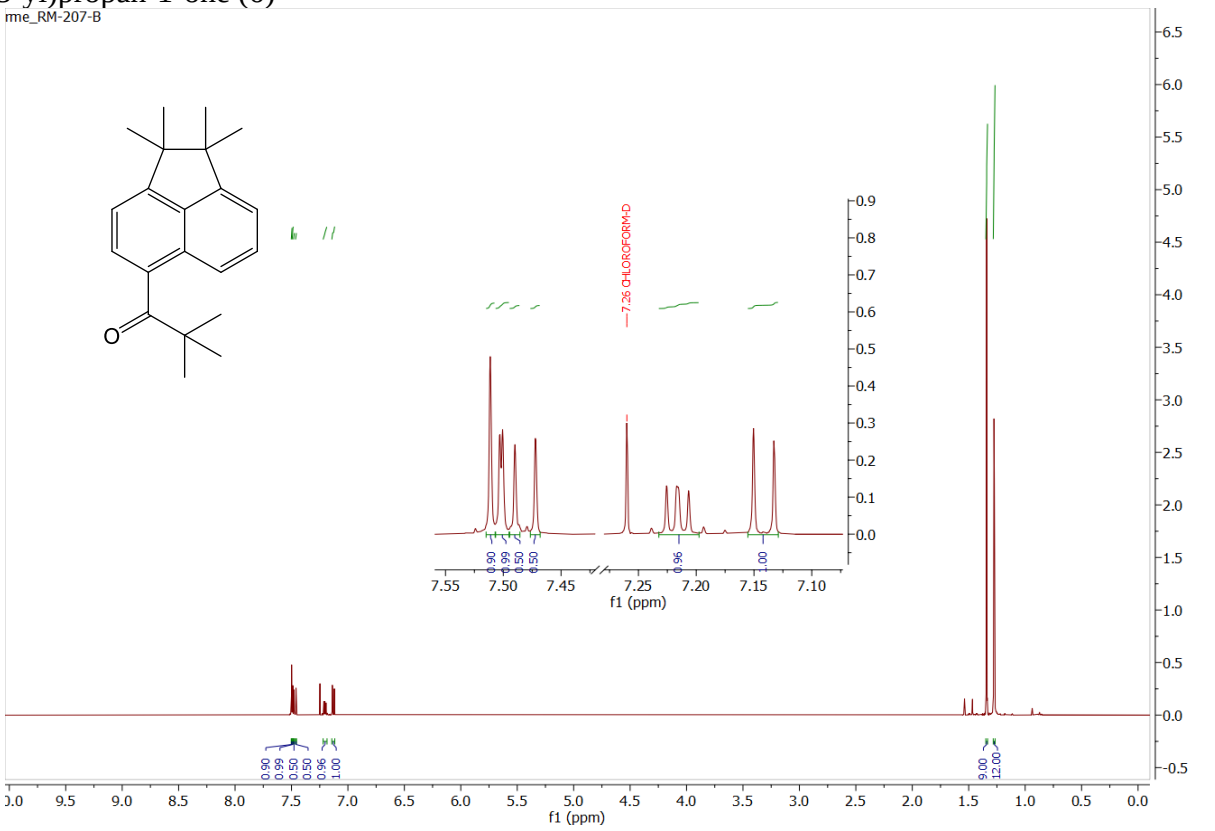

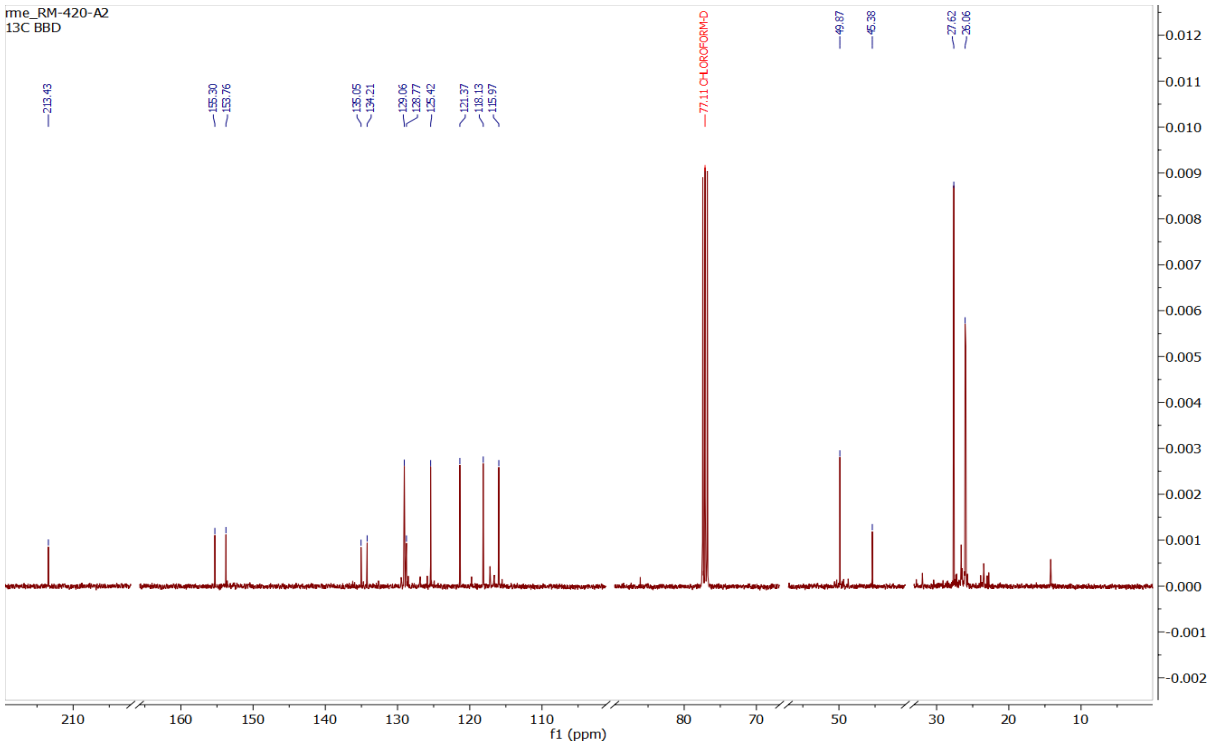

1.1.3.5. ^{1}H and ^{13}C spectra of 3,3-dimethyl-2-(1,1,2,2-tetramethyl-1,2-dihydroacenaphthylen-5-yl)butan-2-ol (7)

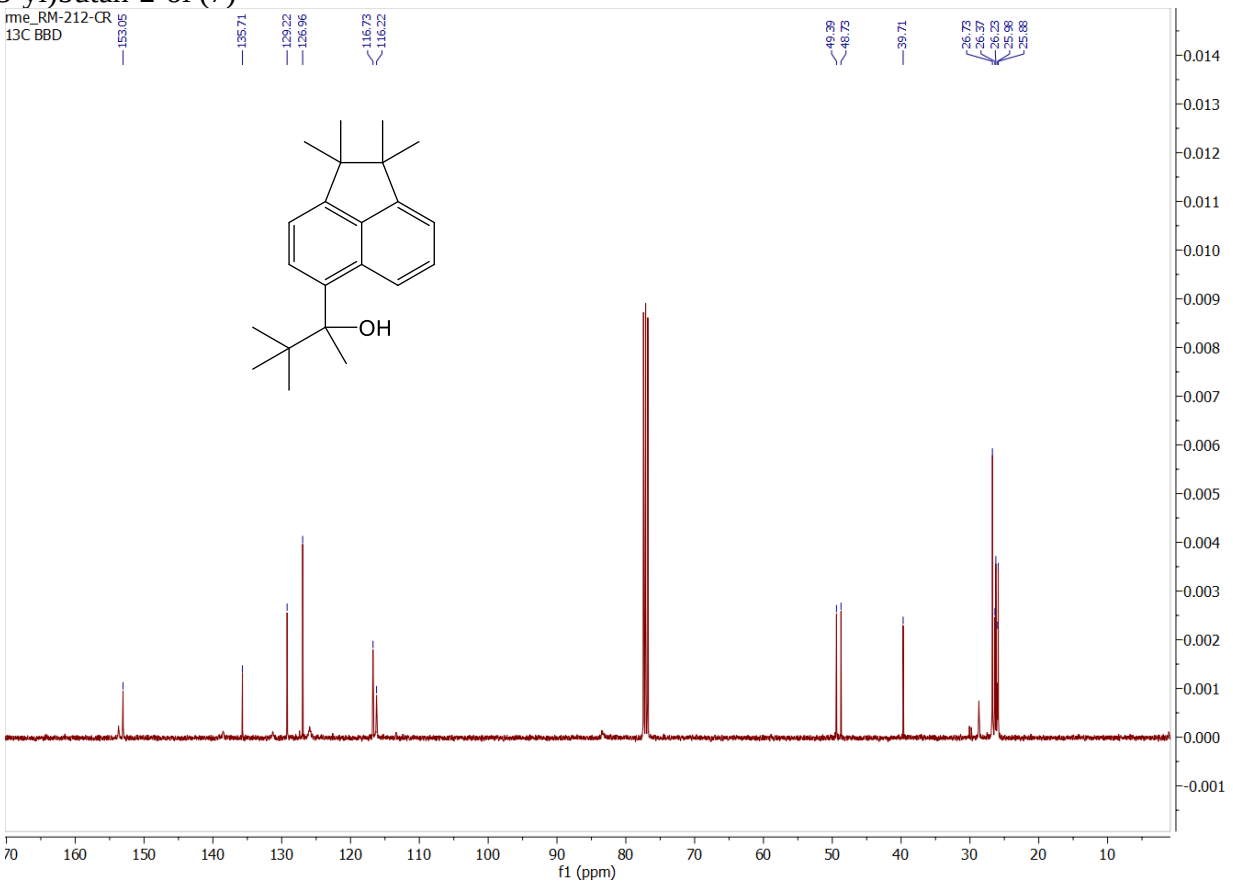

1.1.3.6. ^{1}H and ^{13}C spectra of 1,1,2,2,5,5,6,6-octamethyl-1,2,5,6-tetrahydrocyclopenta[fg]acenaphthylene (OMN)

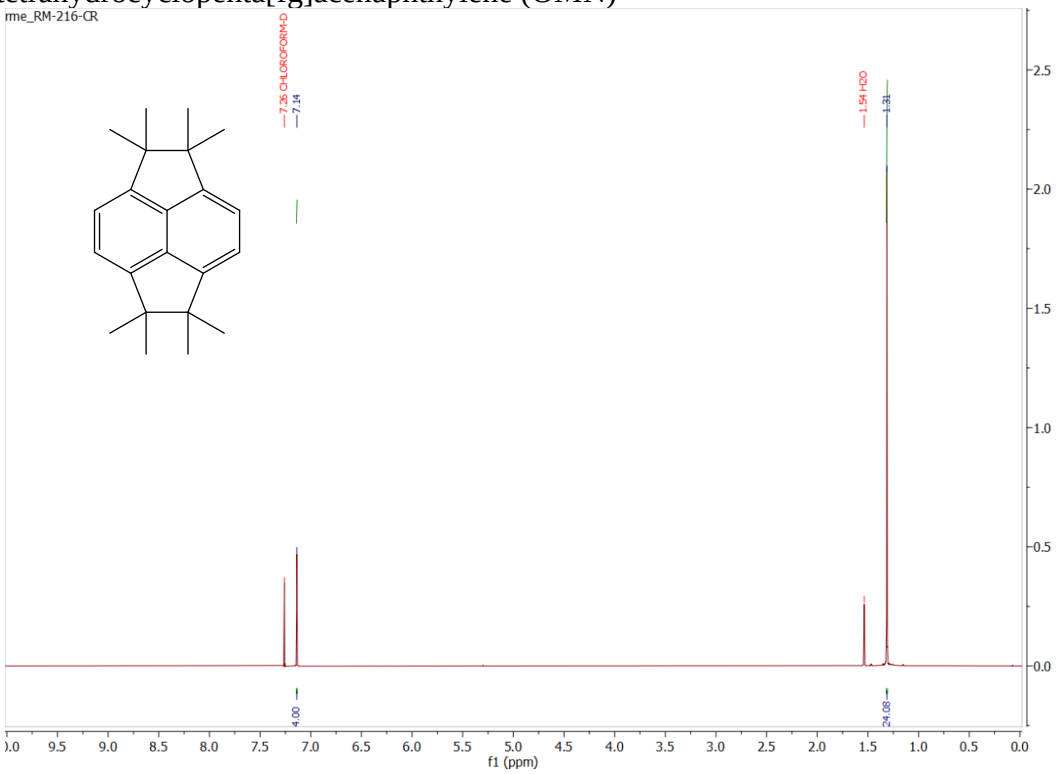

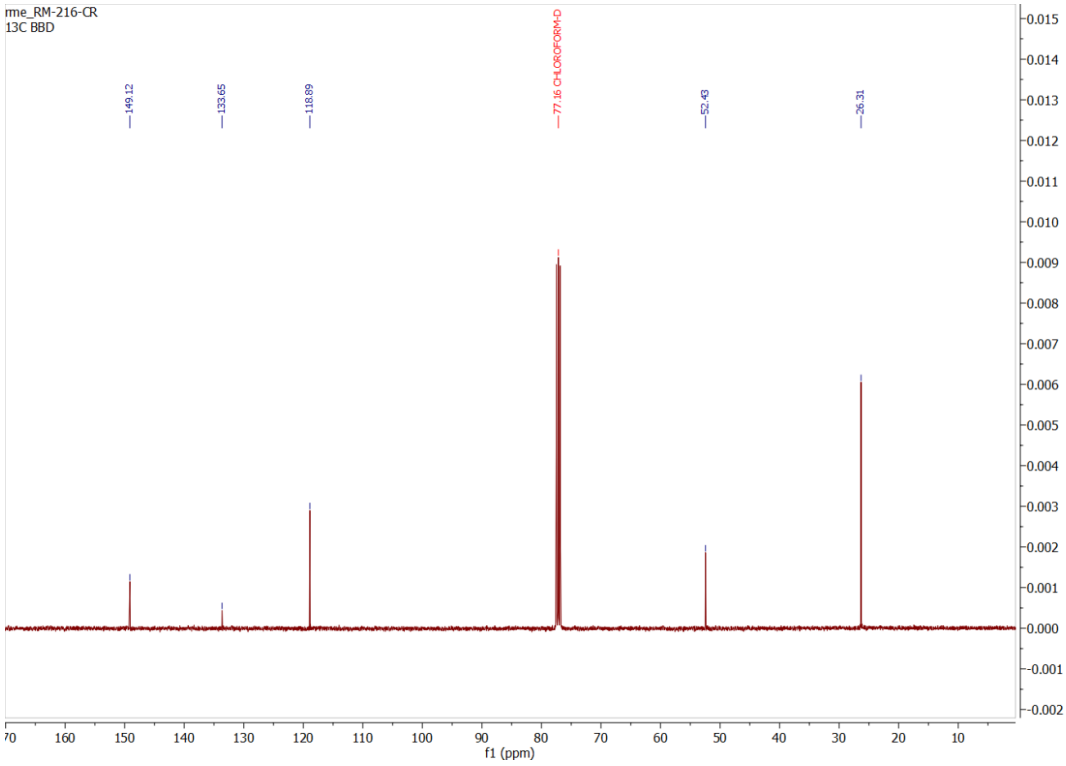

1.1.3.7. ^{1}H and ^{13}C spectra of 1,1,2,2-tetramethyl-5-(naphthalen-1-yl)-1,2-dihydroacenaphthylene (9)

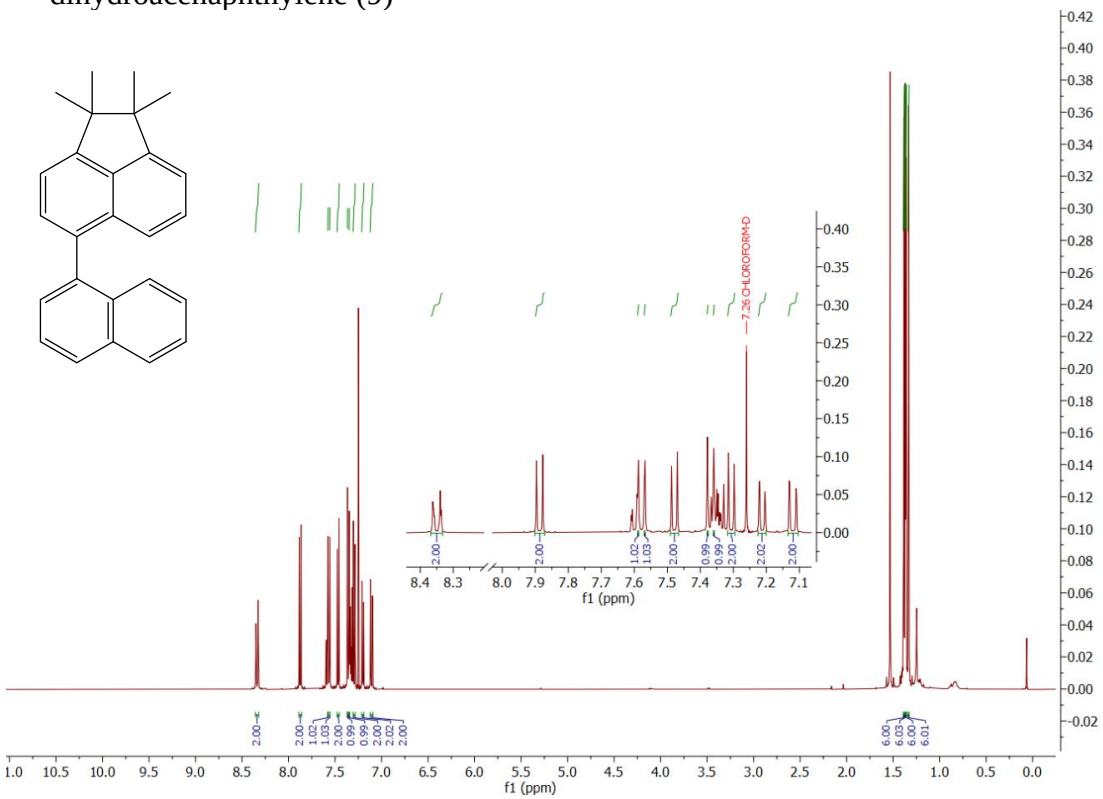

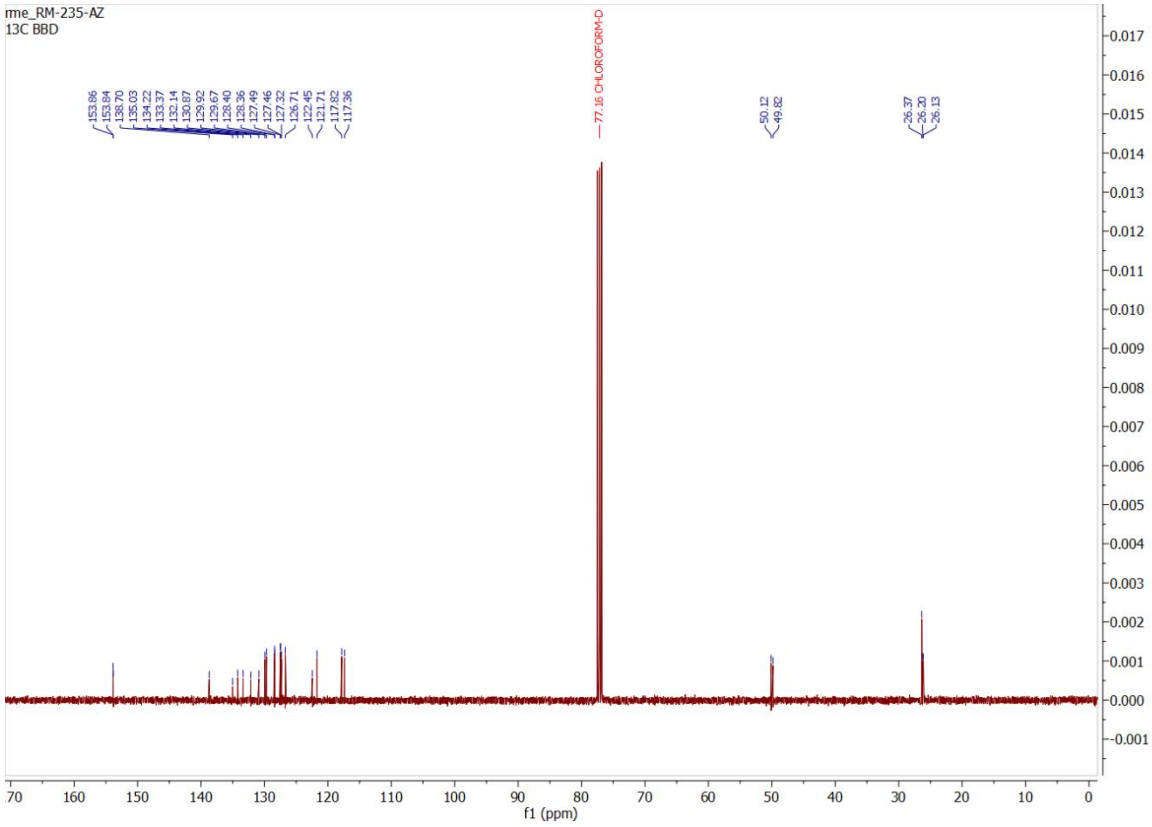

1.1.3.8. ^{1}H and ^{13}C spectra of spectra 1,1,2,2-tetramethyl-1,2-dihydrocyclopenta[cd]perylene (TMP)

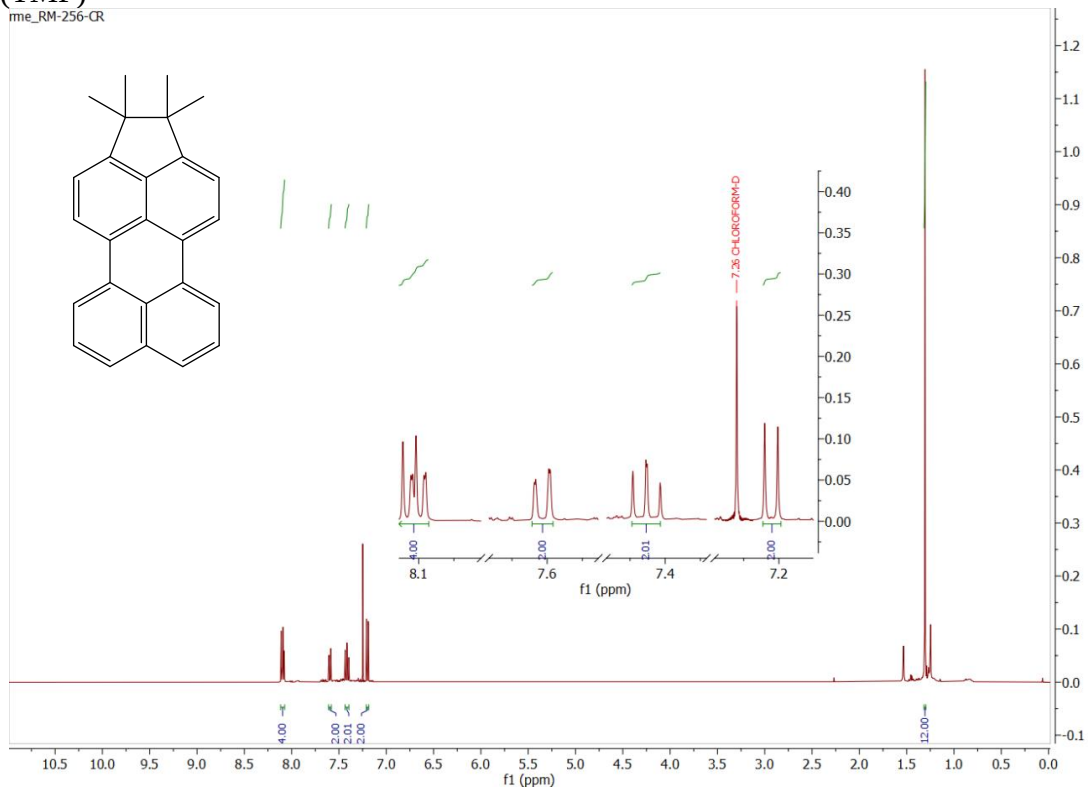

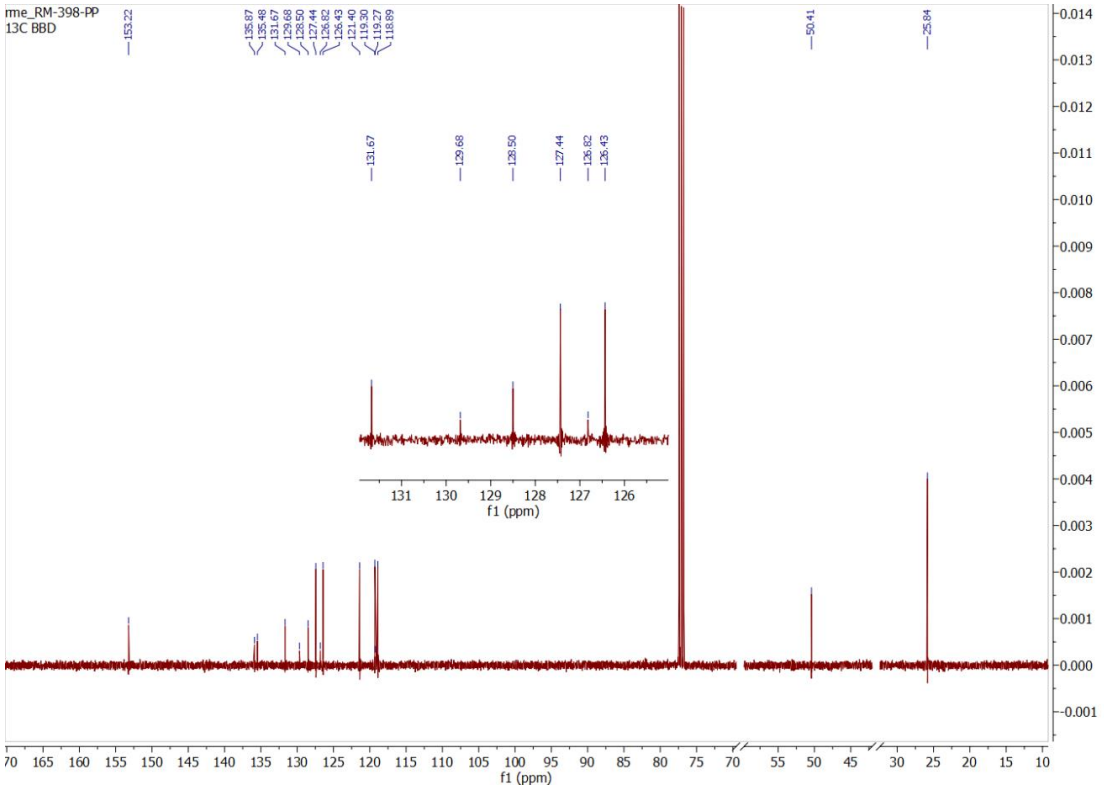

1.1.3.9. ^{1}H and ^{13}C spectra of spectra 1,1,1',1',2,2,2',2'-octamethyl-1,1',2,2'-tetrahydro-5,5'-biacenaphthylene (10)

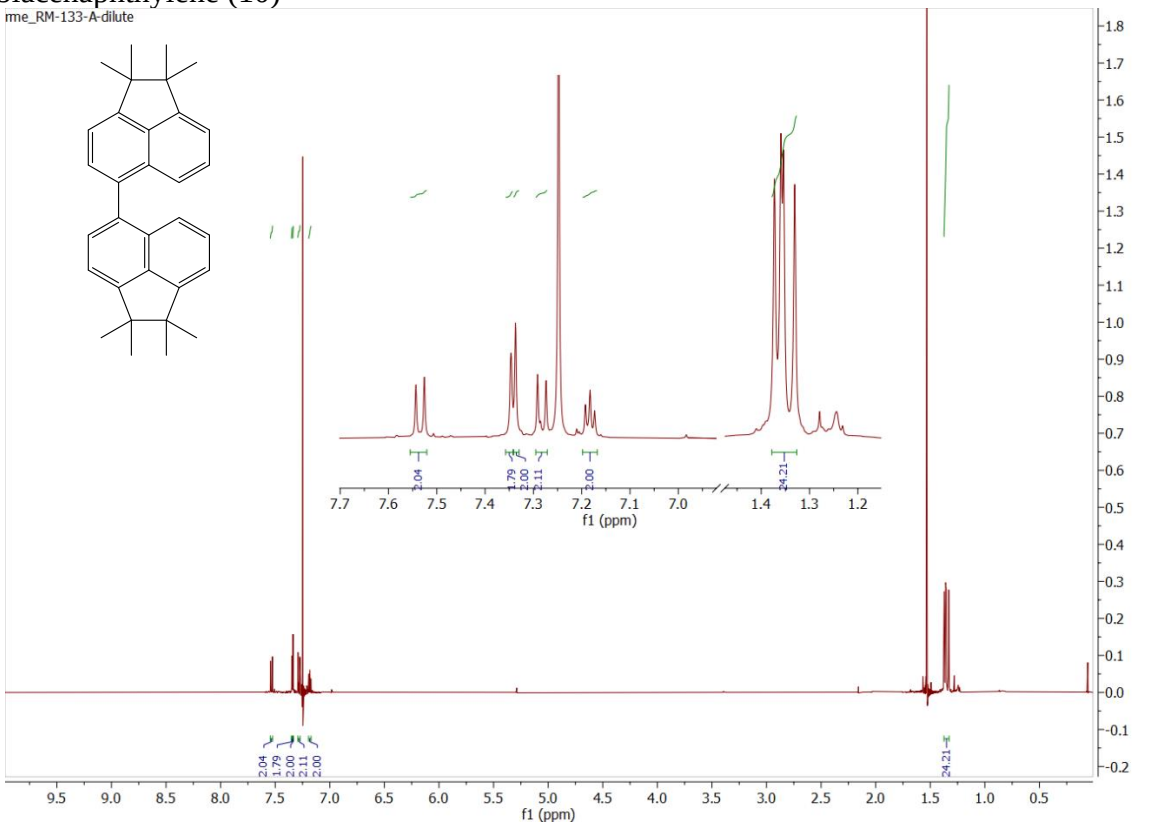

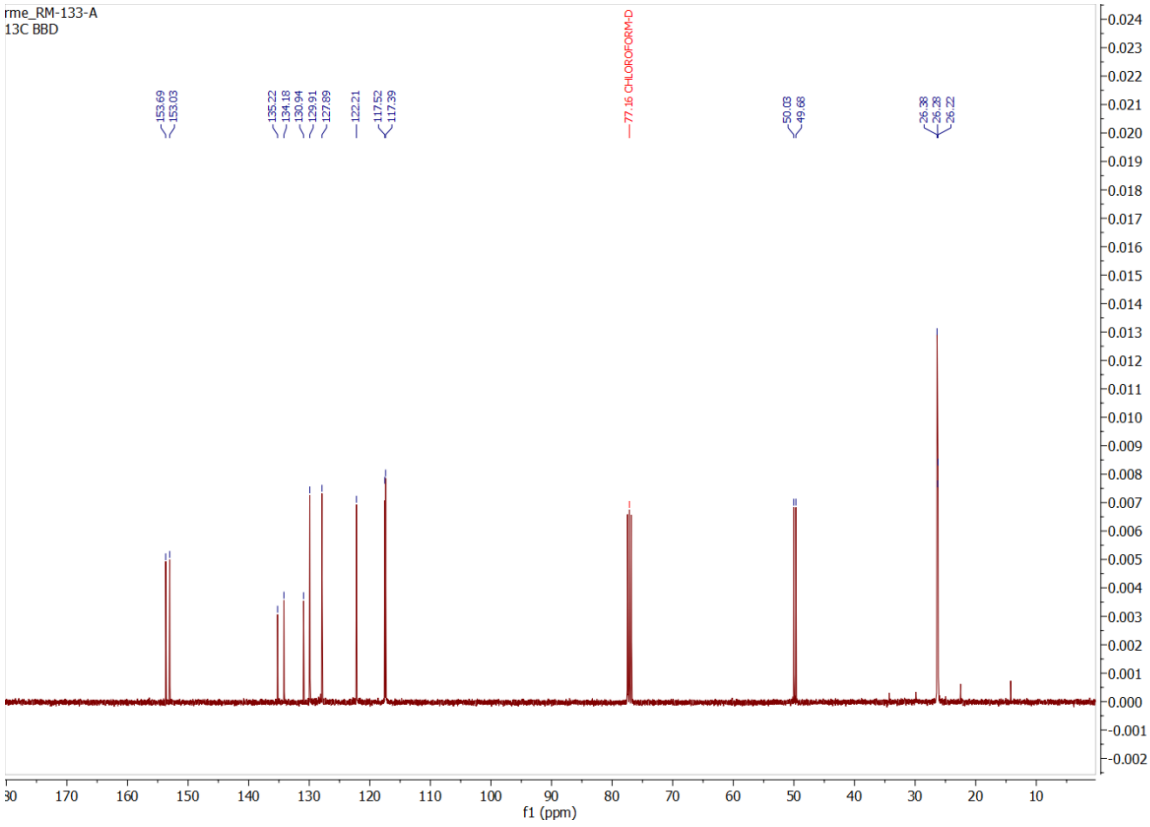

1.1.3.10. ^{1}H and ^{13}C spectra of spectra 1,1,1',1',2,2,2',2'-octamethyl-1,1',2,2'-tetrahydro-5,5'-biacenaphthylene (OMP)

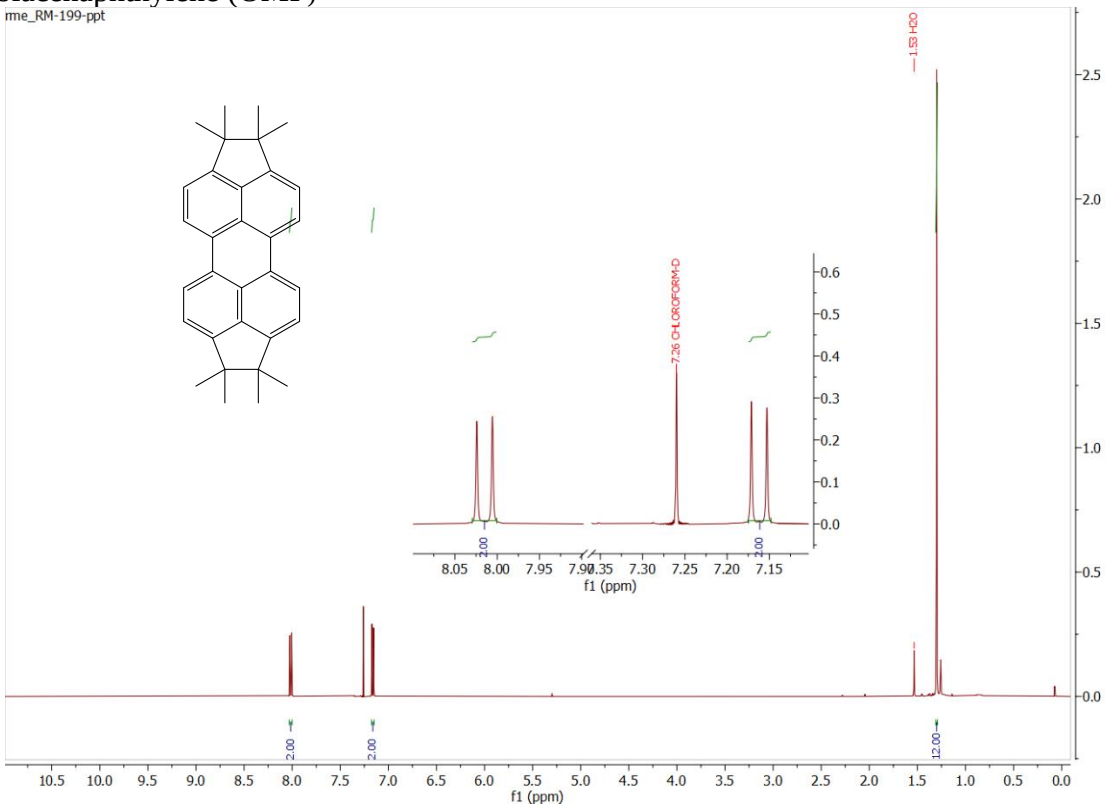

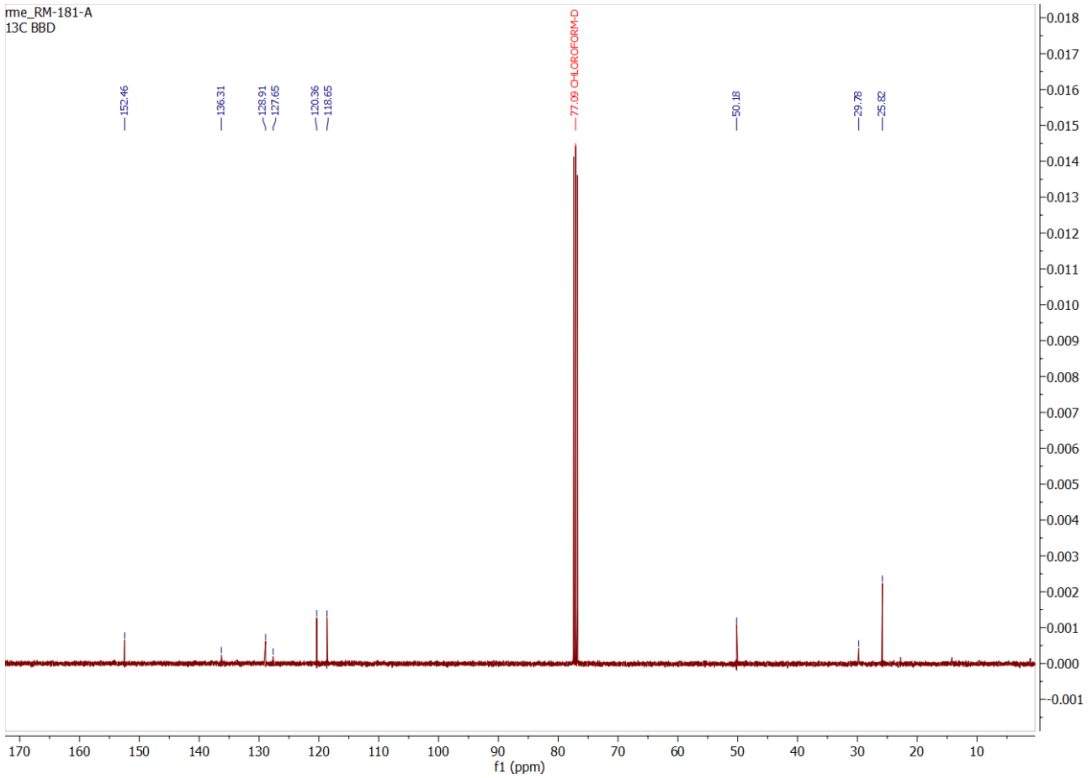

1.1.3.11. ^{1}H and ^{13}C spectra of spectra 3-(1,1,2,2-tetramethyl-1,2-dihydroacenaphthylen-5-yl)perylene (11)

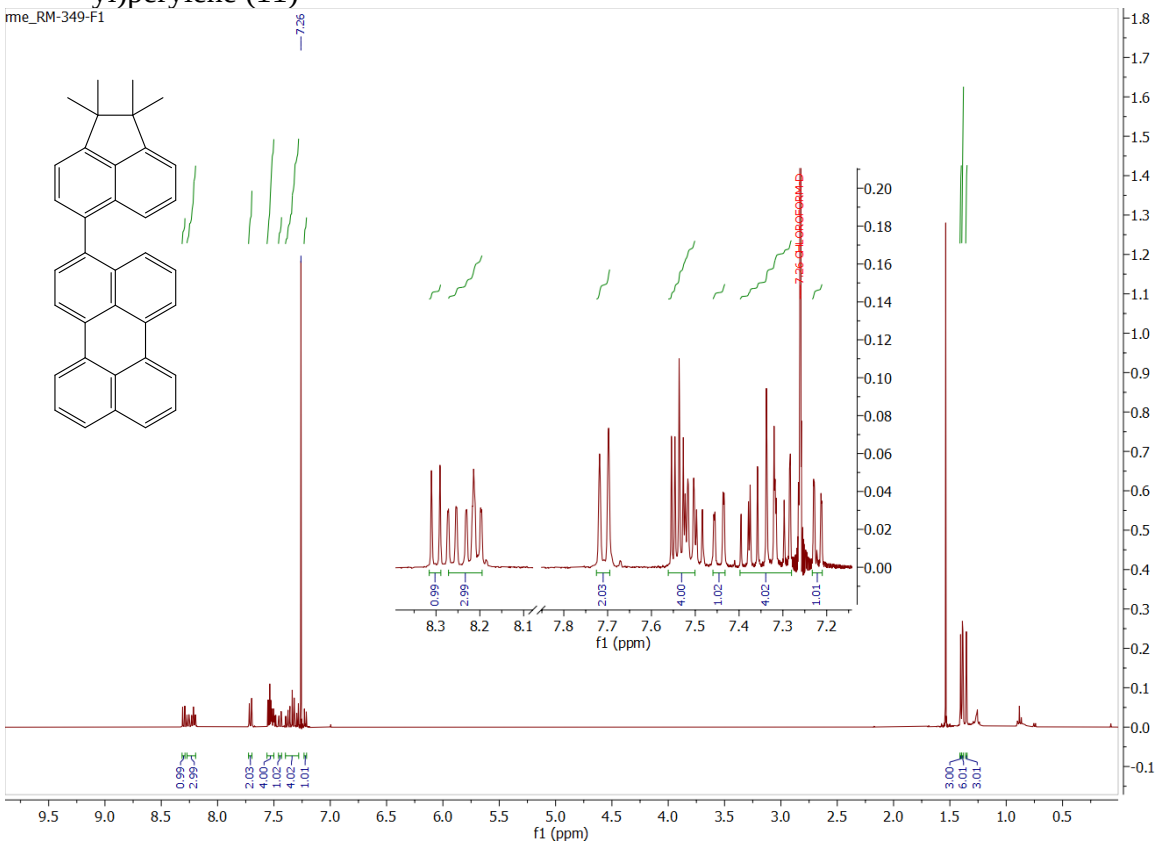

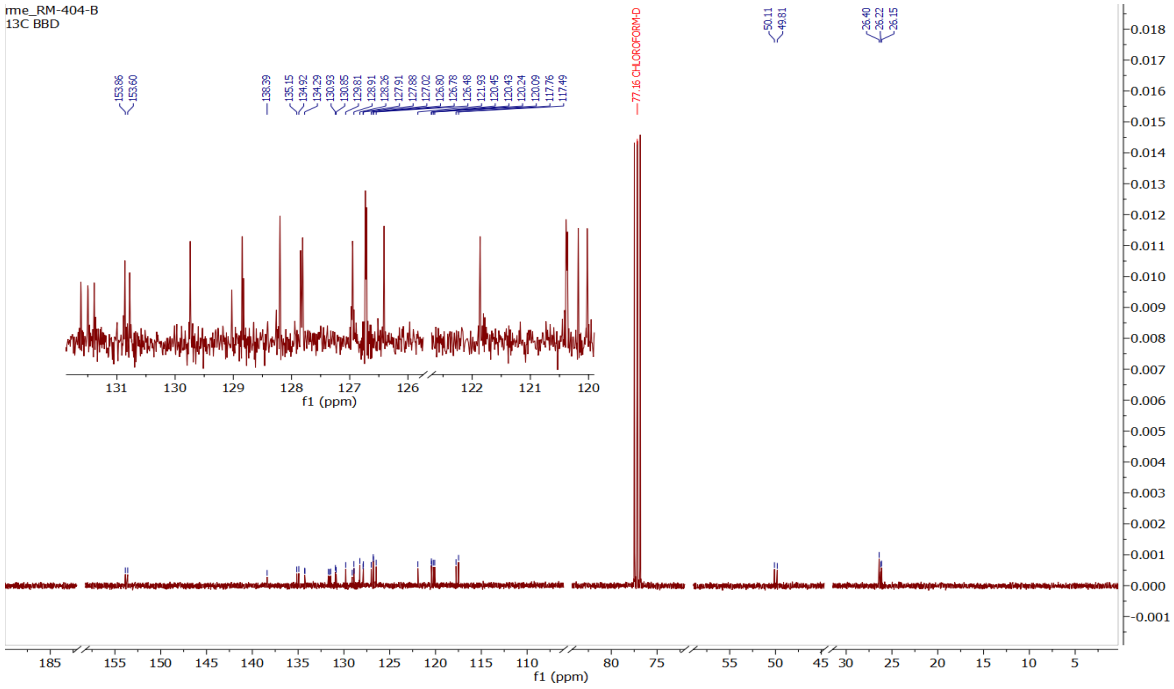

1.1.3.12. ^{1}H and ^{13}C spectra of spectra TMT

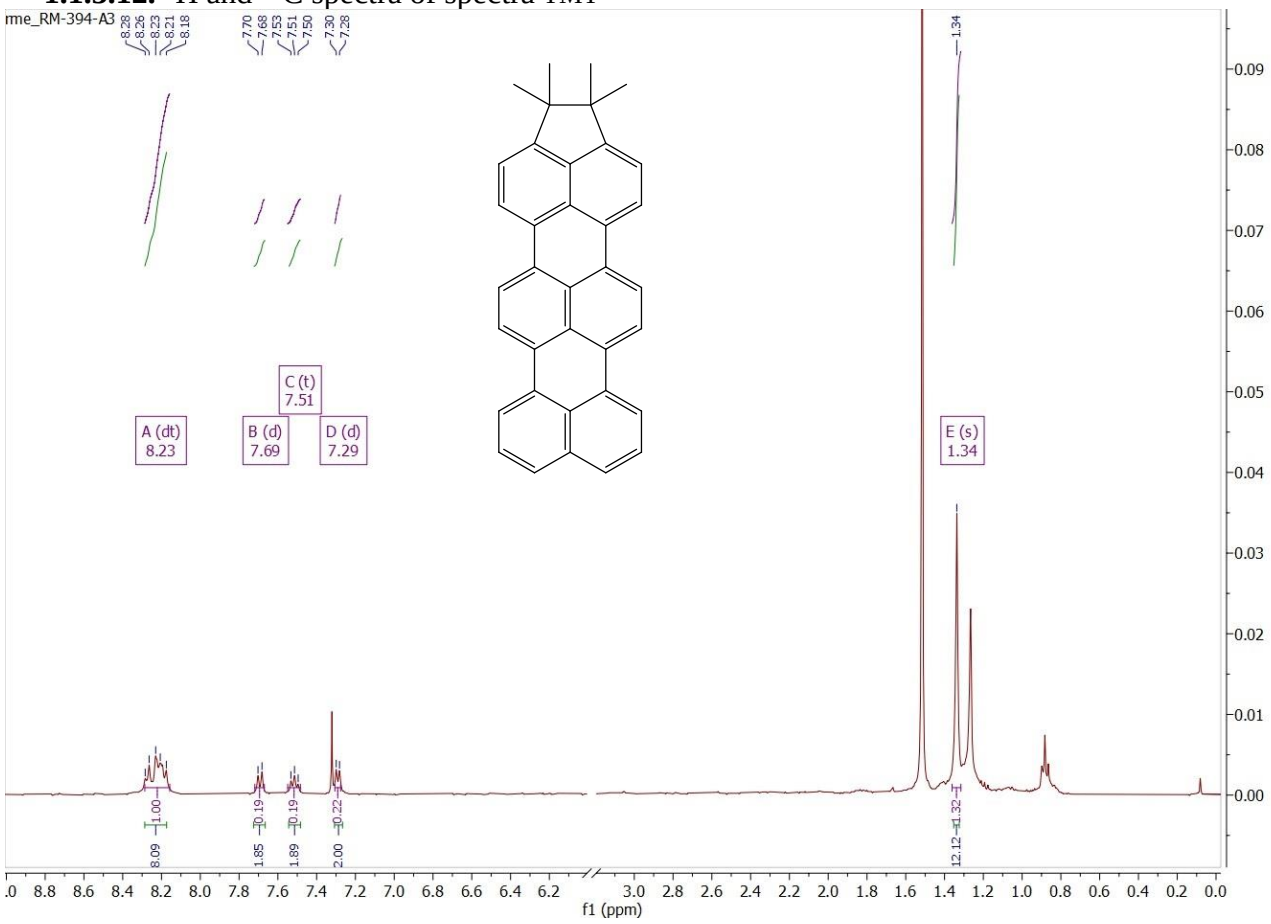

1.1.3.13. ^{1}H and ^{13}C spectra of 1,4-bis(1,1,2,2-tetramethyl-1,2-dihydroacenaphthylen-5-yl)naphthalene (12)

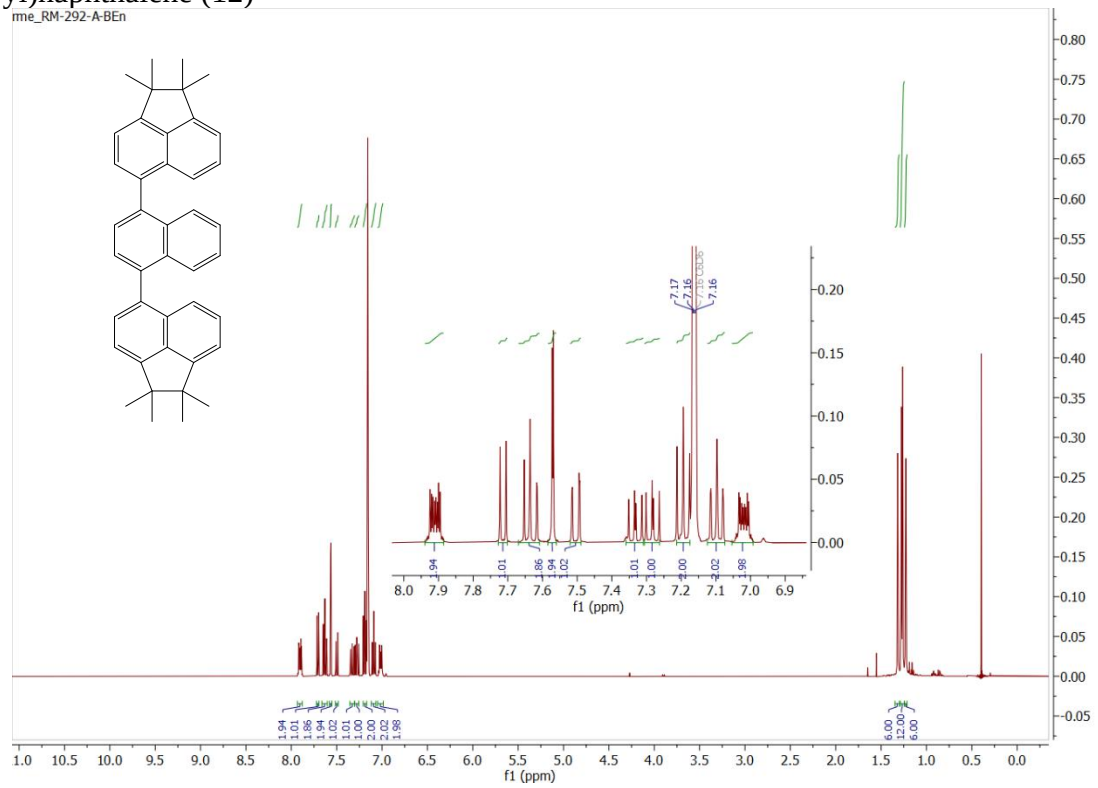

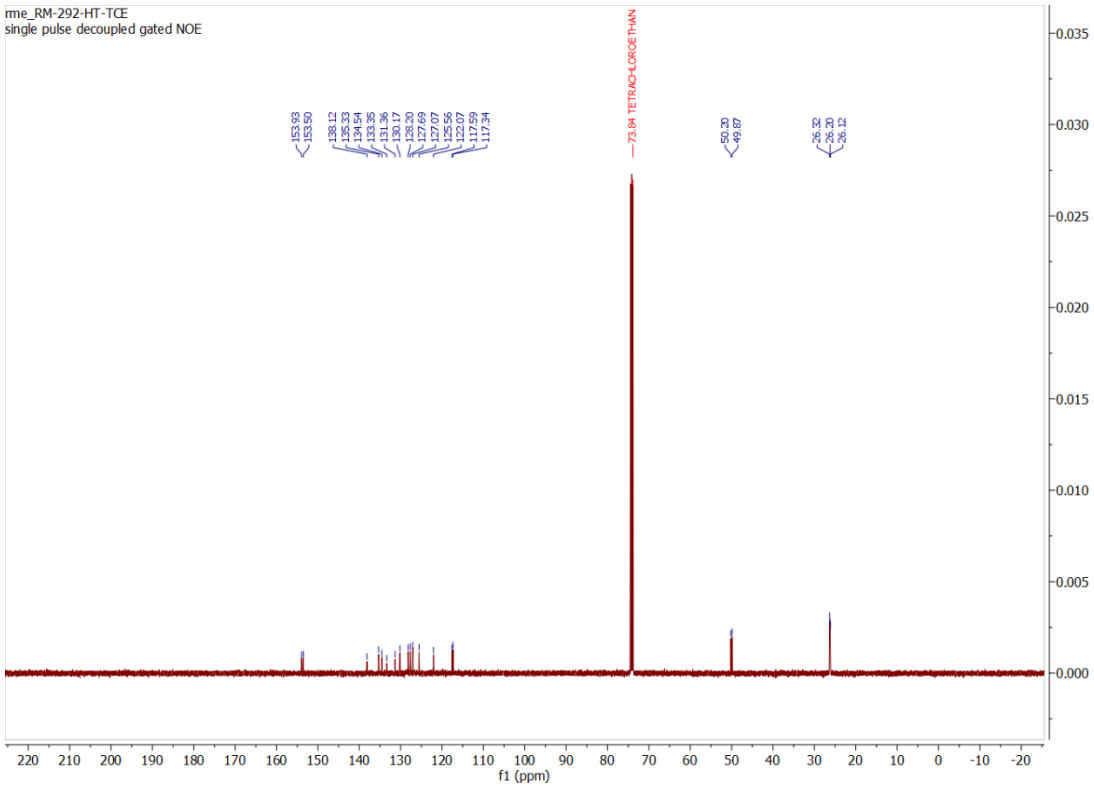

1.1.3.14. ^{1}H spectrum of of 1,1,2,2,9,9,10,10-octamethyl-1,2,9,10-tetrahydrobenzo[rst]diindeno[1,7,6-cde:6',7',1'-klm]pentaphene (OMT)

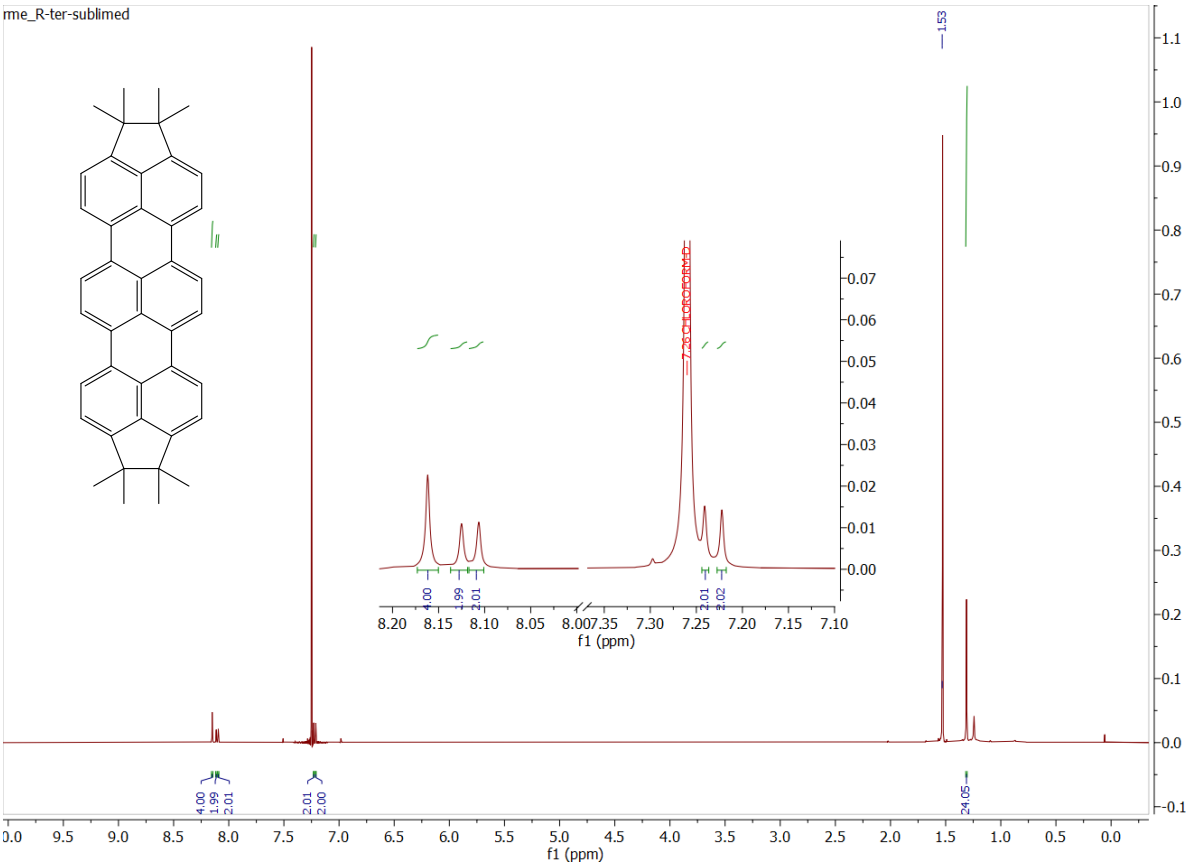

1.2 MS Spectra of all products

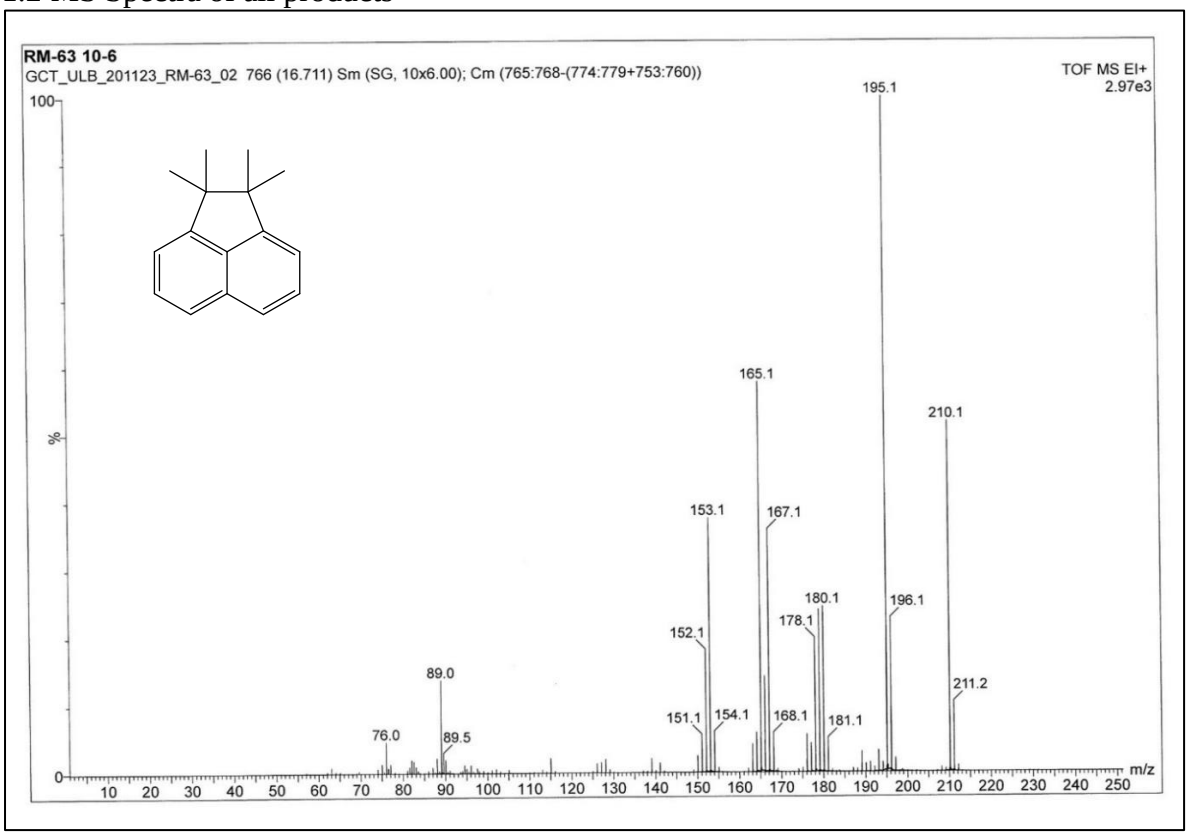

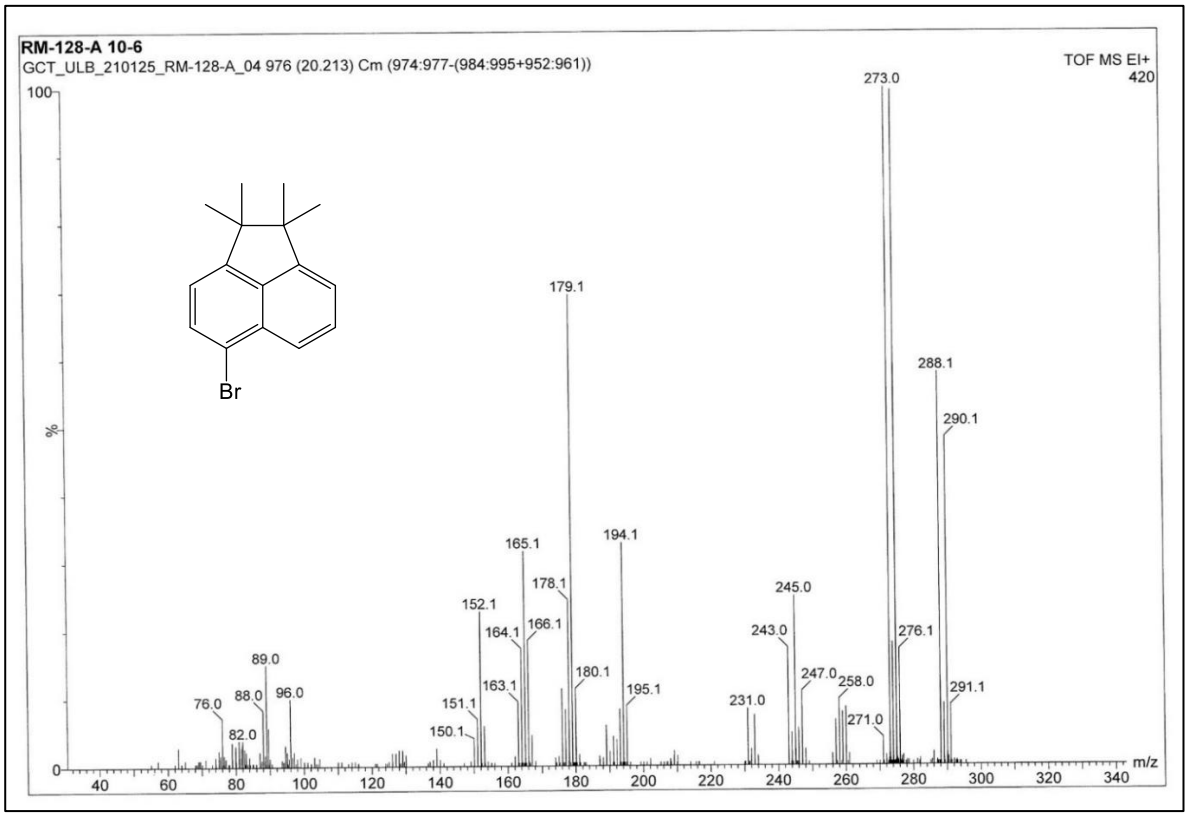

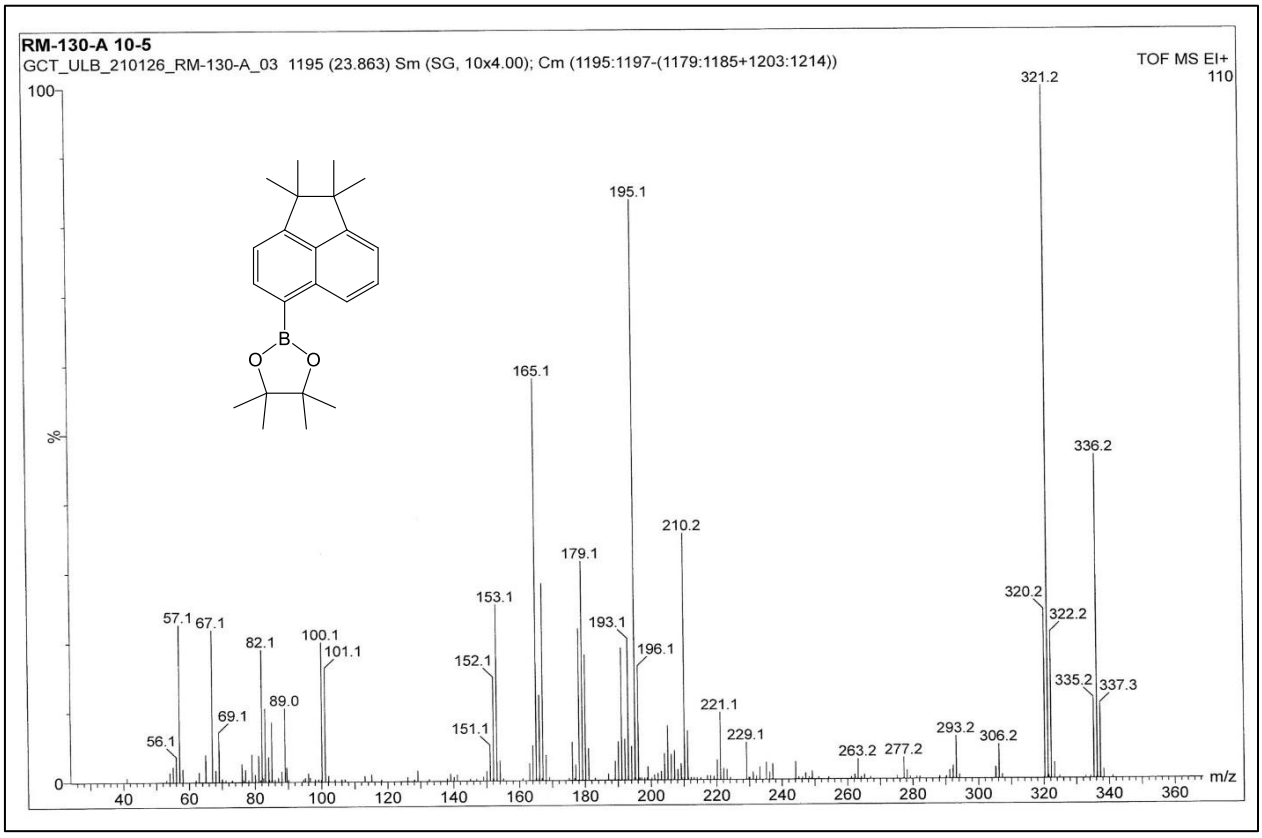
RM-130-A 10-5
GCT_ULB_210126_RM-130-A_03 1195 (23.863) Sm (SG, 10x4.00); Cm (1195:1197-(1179:1185+1203:1214))
TOF MS EI+
110
100
%
0
321.2
195.1
165.1
336.2
210.2
179.1
153.1
320.2
322.2
57.1
67.1
82.1
100.1
101.1
193.1
196.1
152.1
335.2
337.3
89.0
221.1
69.1
151.1
293.2
306.2
56.1
229.1
263.2
277.2
m/z
40
60
80
100
120
140
160
180
200
220
240
260
280
300
320
340
360

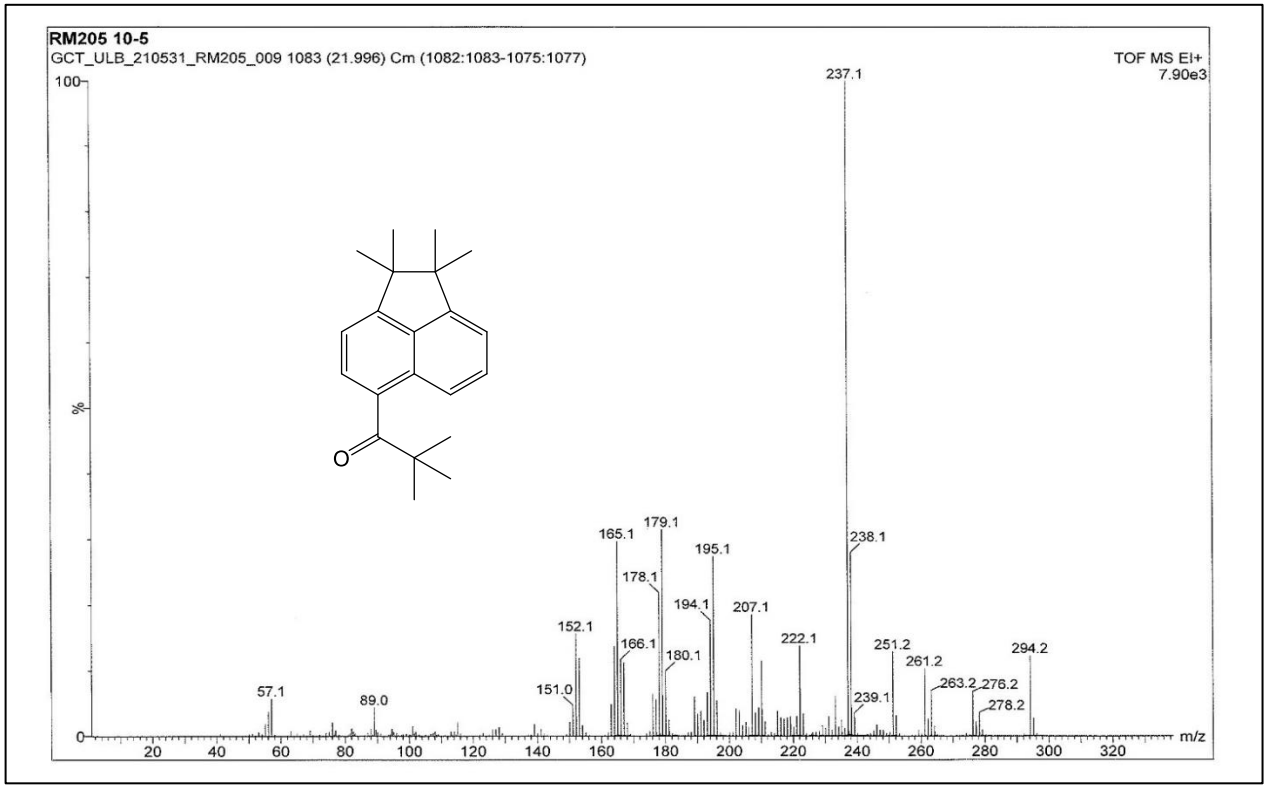
RM205 10-5
GCT_ULB_210531_RM205_009 1083 (21.996) Cm (1082:1083-1075:1077)
TOF MS EI+
7.90e3
100
%
0
237.1
238.1
179.1
165.1
195.1
178.1
194.1
207.1
152.1
166.1
222.1
180.1
251.2
294.2
261.2
263.2
276.2
278.2
57.1
89.0
151.0
239.1
m/z
20
40
60
80
100
120
140
160
180
200
220
240
260
280
300
320

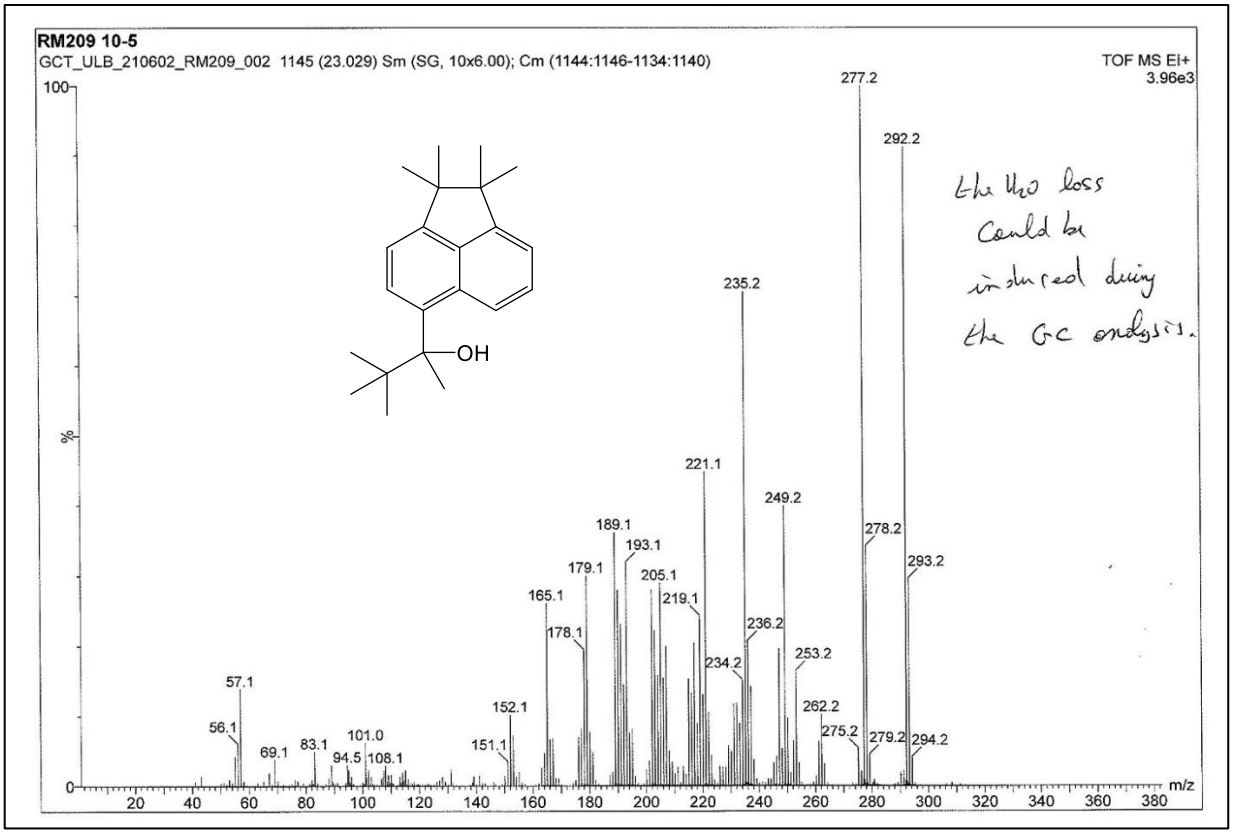
RM209 10-5
GCT_ULB_210602_RM209_002 1145 (23.029) Sm (SG, 10x6.00); Cm (1144:1146-1134:1140)
TOF MS EI+
3.96e3
OH
the H2O loss could be instead during the GC analysis.
277.2
292.2
235.2
221.1
249.2
189.1
193.1
278.2
293.2
179.1
205.1
165.1
219.1
236.2
178.1
253.2
234.2
57.1
152.1
262.2
56.1
275.2
279.2
294.2
69.1
83.1
101.0
151.1
94.5
108.1
%
m/z

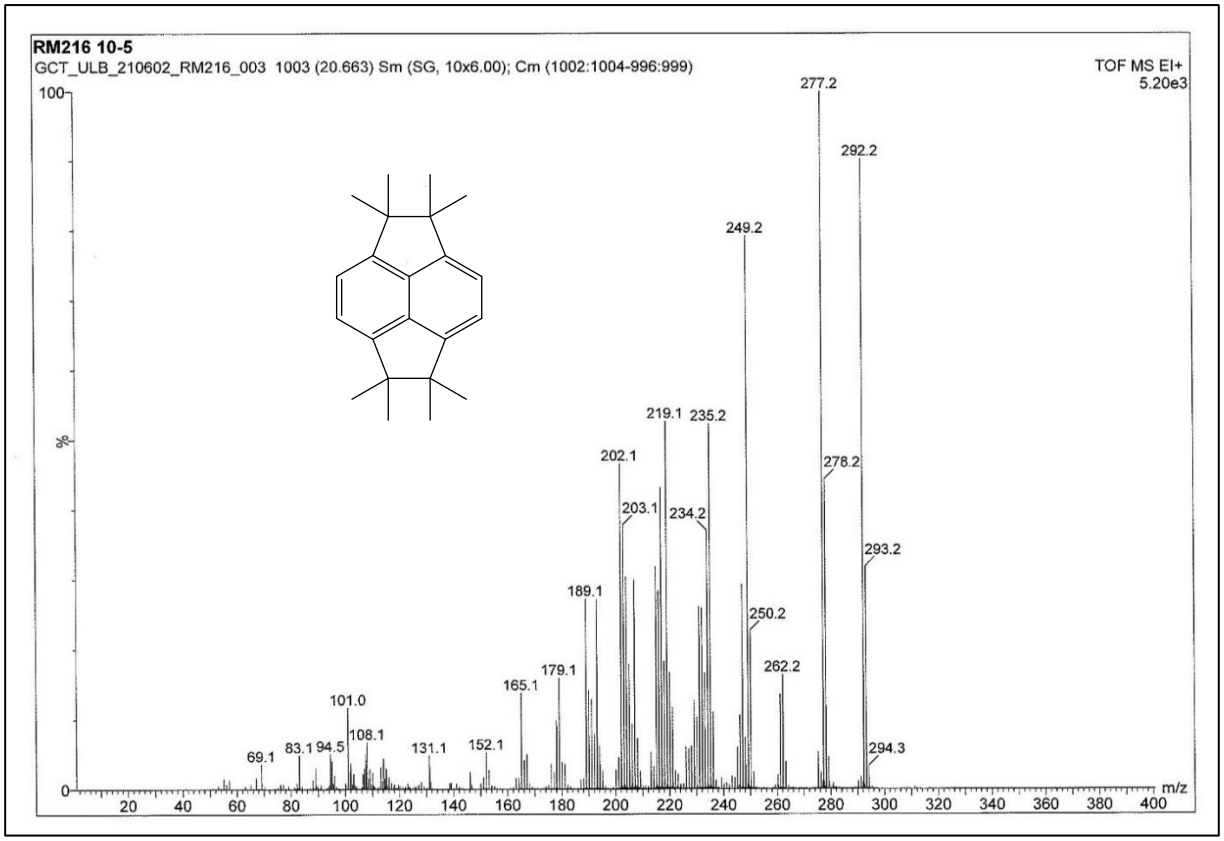
RM216 10-5
GCT_ULB_210602_RM216_003 1003 (20.663) Sm (SG, 10x6.00); Cm (1002:1004-996:999)
TOF MS EI+
5.20e3
277.2
292.2
249.2
219.1
235.2
202.1
278.2
203.1
234.2
293.2
189.1
250.2
262.2
179.1
165.1
101.0
108.1
69.1
83.1
94.5
131.1
152.1
294.3
%
m/z

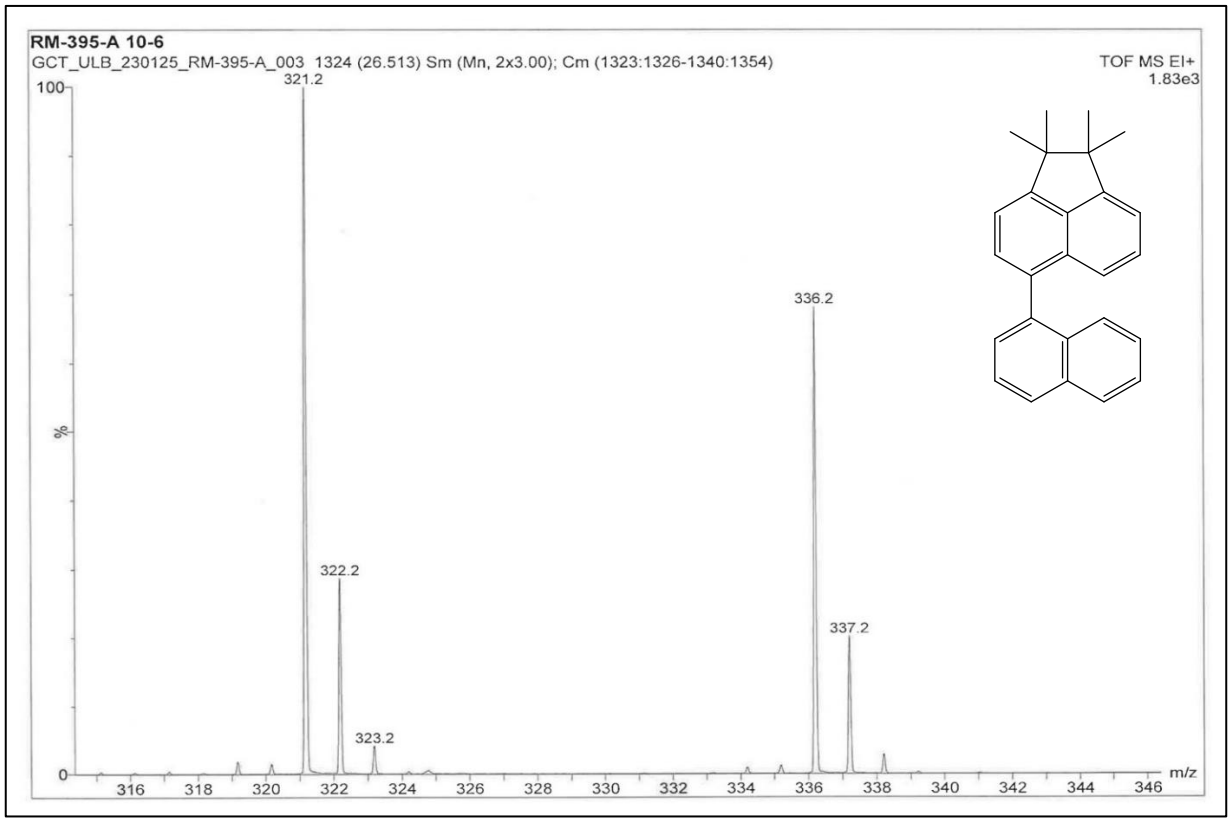
RM-395-A 10-6
GCT_ULB_230125_RM-395-A_003 1324 (26.513) Sm (Mn, 2x3.00); Cm (1323:1326-1340:1354)
TOF MS EI+
1.83e3
100
%
0
321.2
322.2
323.2
336.2
337.2
316 318 320 322 324 326 328 330 332 334 336 338 340 342 344 346
m/z

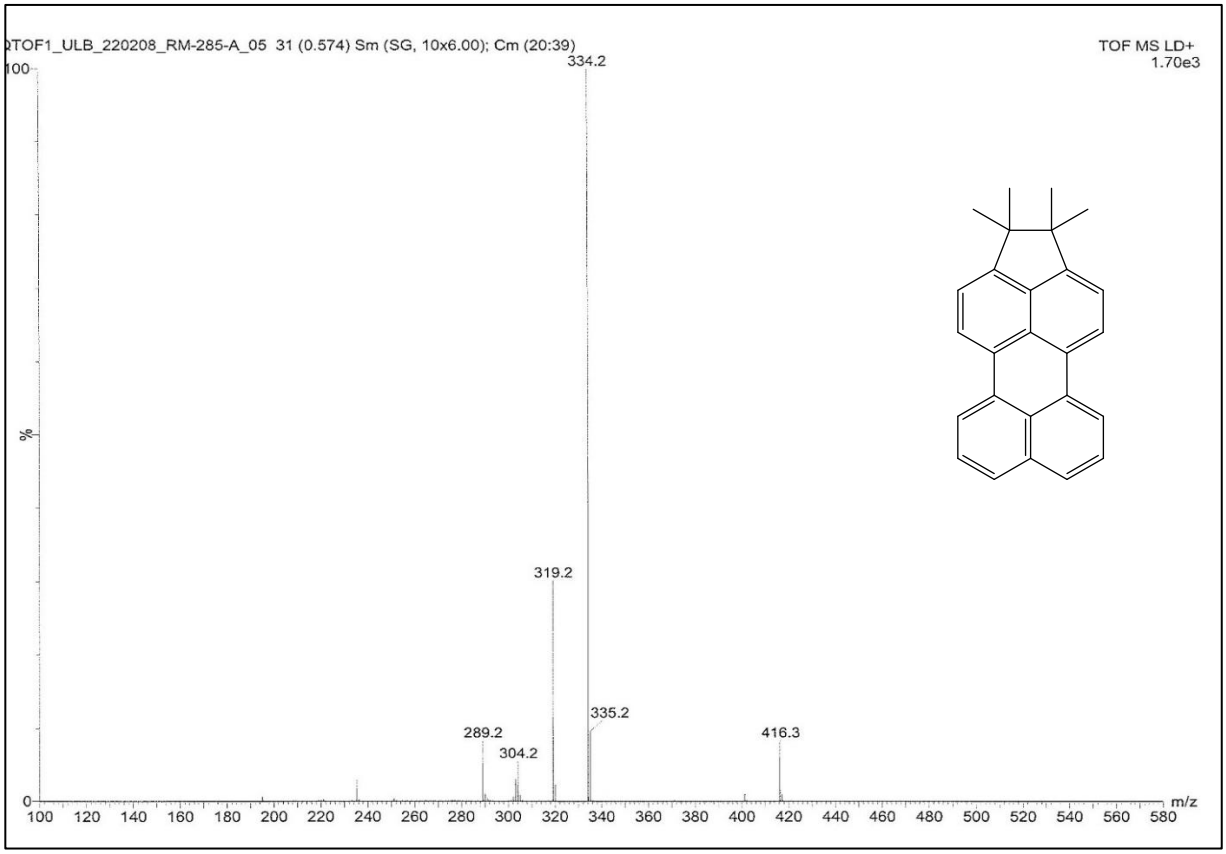
QTOF1_ULB_220208_RM-285-A_05 31 (0.574) Sm (SG, 10x6.00); Cm (20:39)
TOF MS LD+
1.70e3
100
%
0
334.2
319.2
335.2
289.2
304.2
416.3
100 120 140 160 180 200 220 240 260 280 300 320 340 360 380 400 420 440 460 480 500 520 540 560 580
m/z

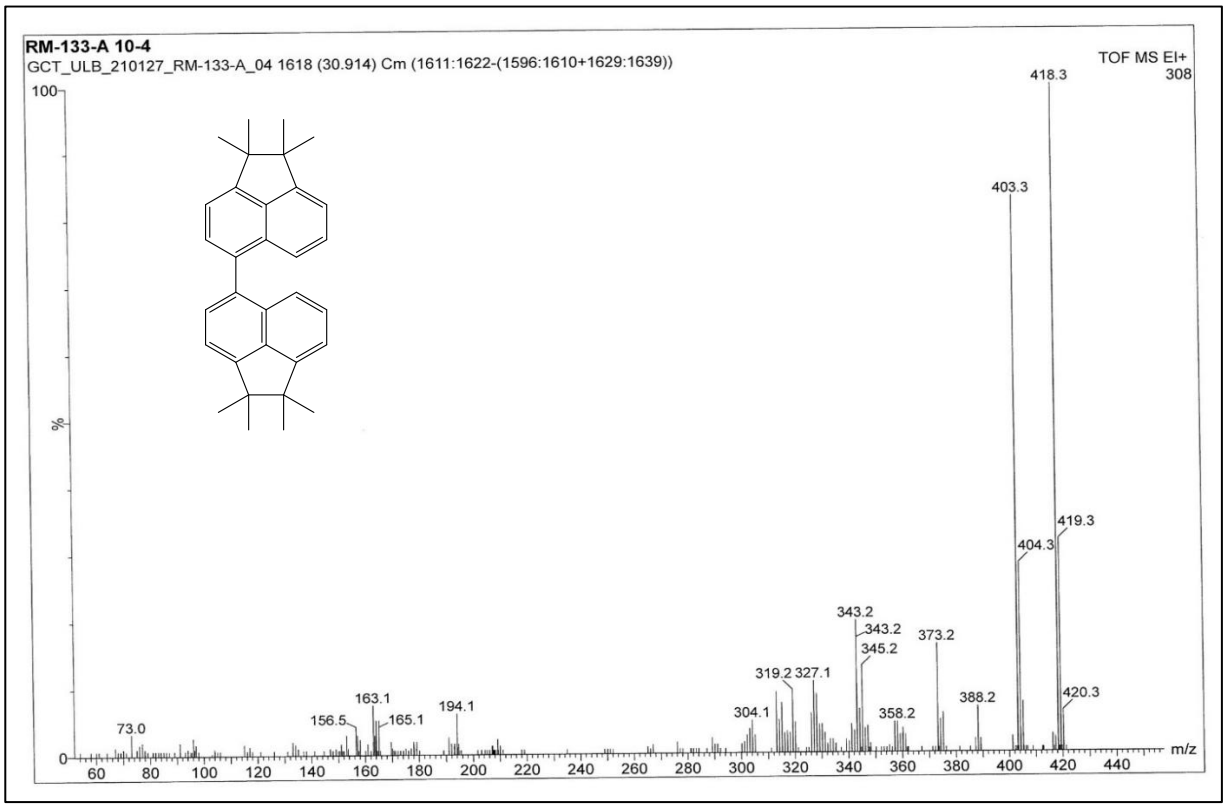
RM-133-A 10-4
GCT_ULB_210127_RM-133-A_04 1618 (30.914) Cm (1611:1622-(1596:1610+1629:1639))
TOF MS EI+
308
100
%
0
418.3
403.3
419.3
404.3
343.2
343.2
345.2
373.2
319.2
327.1
163.1
194.1
156.5
165.1
304.1
358.2
388.2
420.3
73.0
60 80 100 120 140 160 180 200 220 240 260 280 300 320 340 360 380 400 420 440
m/z

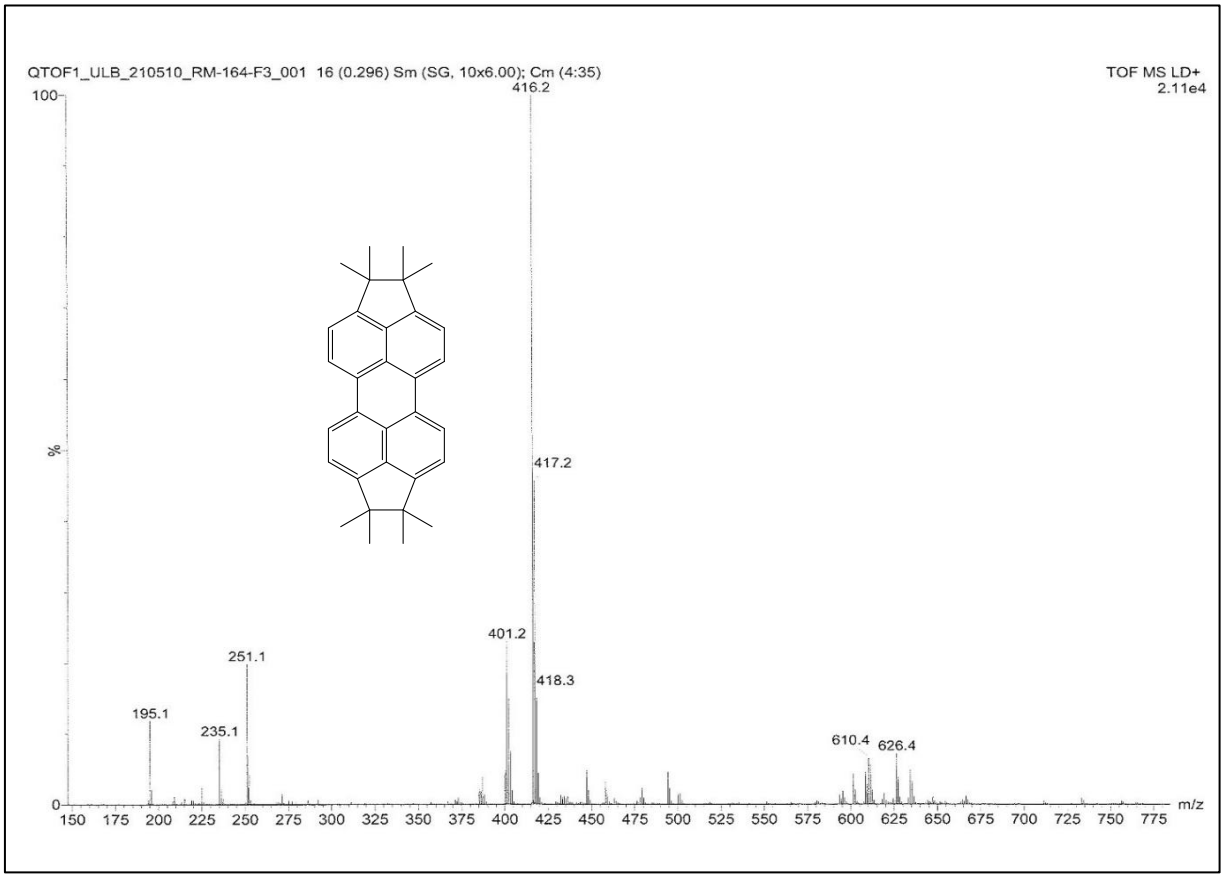
QTOF1_ULB_210510_RM-164-F3_001 16 (0.296) Sm (SG, 10x6.00); Cm (4:35)
TOF MS LD+
2.11e4
100
%
0
416.2
417.2
401.2
418.3
251.1
195.1
235.1
610.4
626.4
150 175 200 225 250 275 300 325 350 375 400 425 450 475 500 525 550 575 600 625 650 675 700 725 750 775
m/z

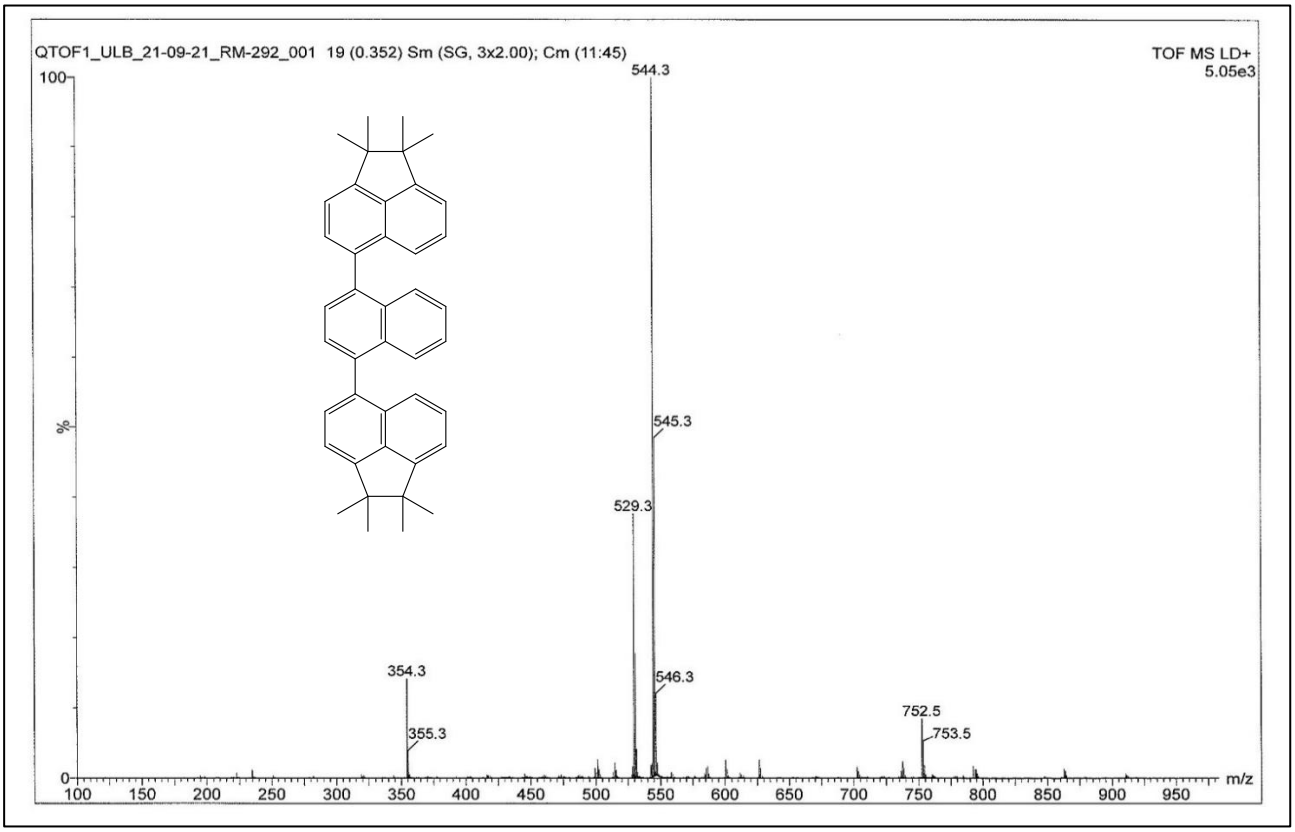
QTOF1_ULB_21-09-21_RM-292_001 19 (0.352) Sm (SG, 3x2.00); Cm (11:45)
TOF MS LD+
5.05e3
544.3
545.3
529.3
354.3
546.3
752.5
355.3
753.5
%
m/z

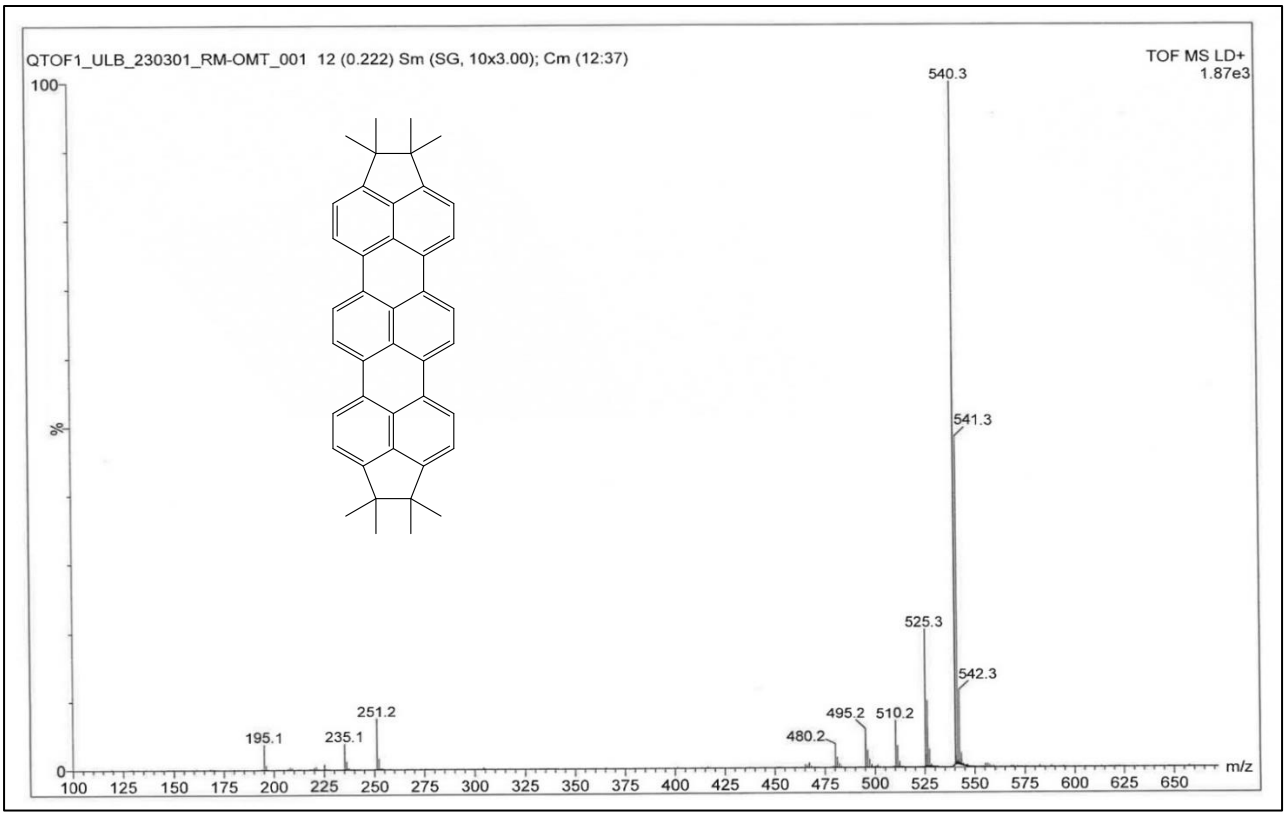
QTOF1_ULB_230301_RM-OMT_001 12 (0.222) Sm (SG, 10x3.00); Cm (12:37)
TOF MS LD+
1.87e3
540.3
541.3
525.3
542.3
251.2
495.2
510.2
195.1
235.1
480.2
%
m/z

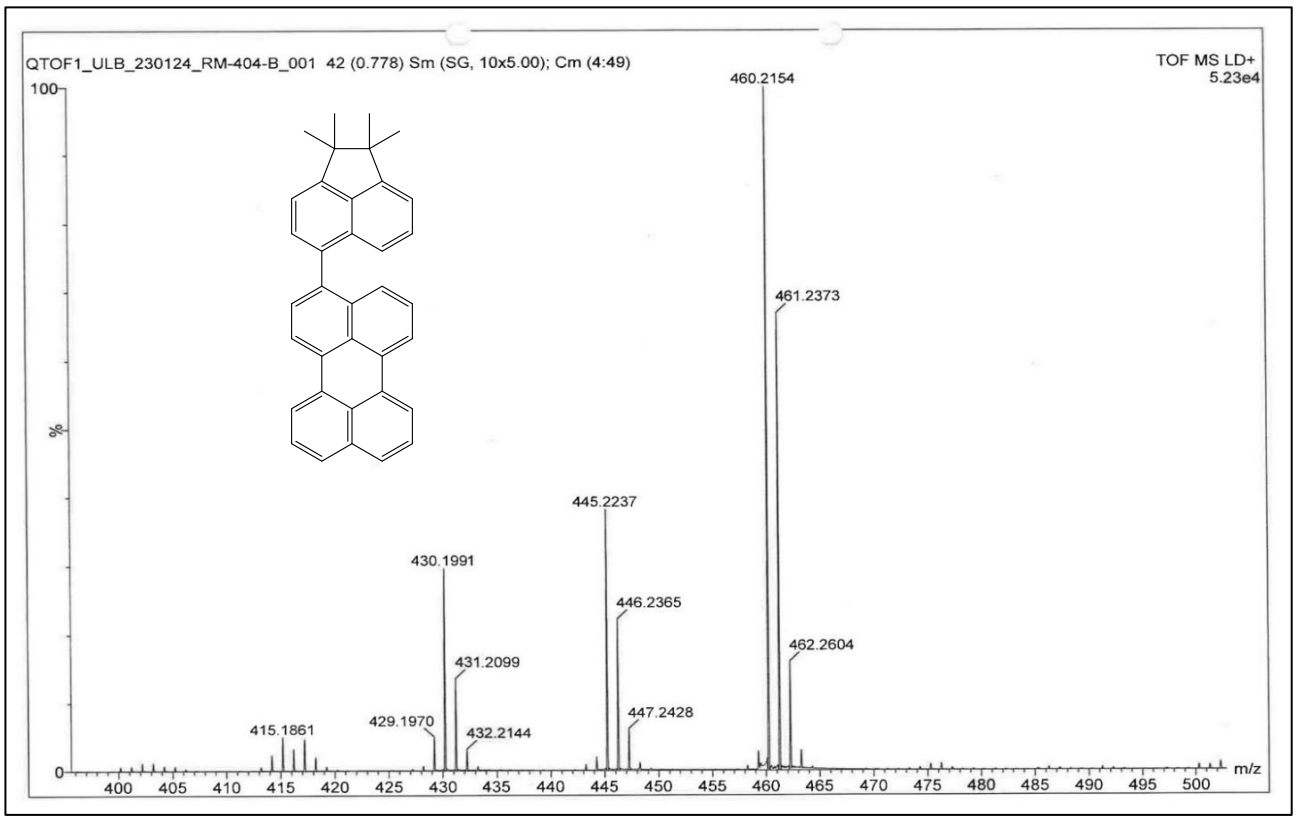
QTOF1_ULB_230124_RM-404-B_001 42 (0.778) Sm (SG, 10x5.00); Cm (4:49)
TOF MS LD+
5.23e4
100
%
0
460.2154
461.2373
445.2237
430.1991
446.2365
462.2604
431.2099
447.2428
429.1970
415.1861
432.2144
400 405 410 415 420 425 430 435 440 445 450 455 460 465 470 475 480 485 490 495 500
m/z

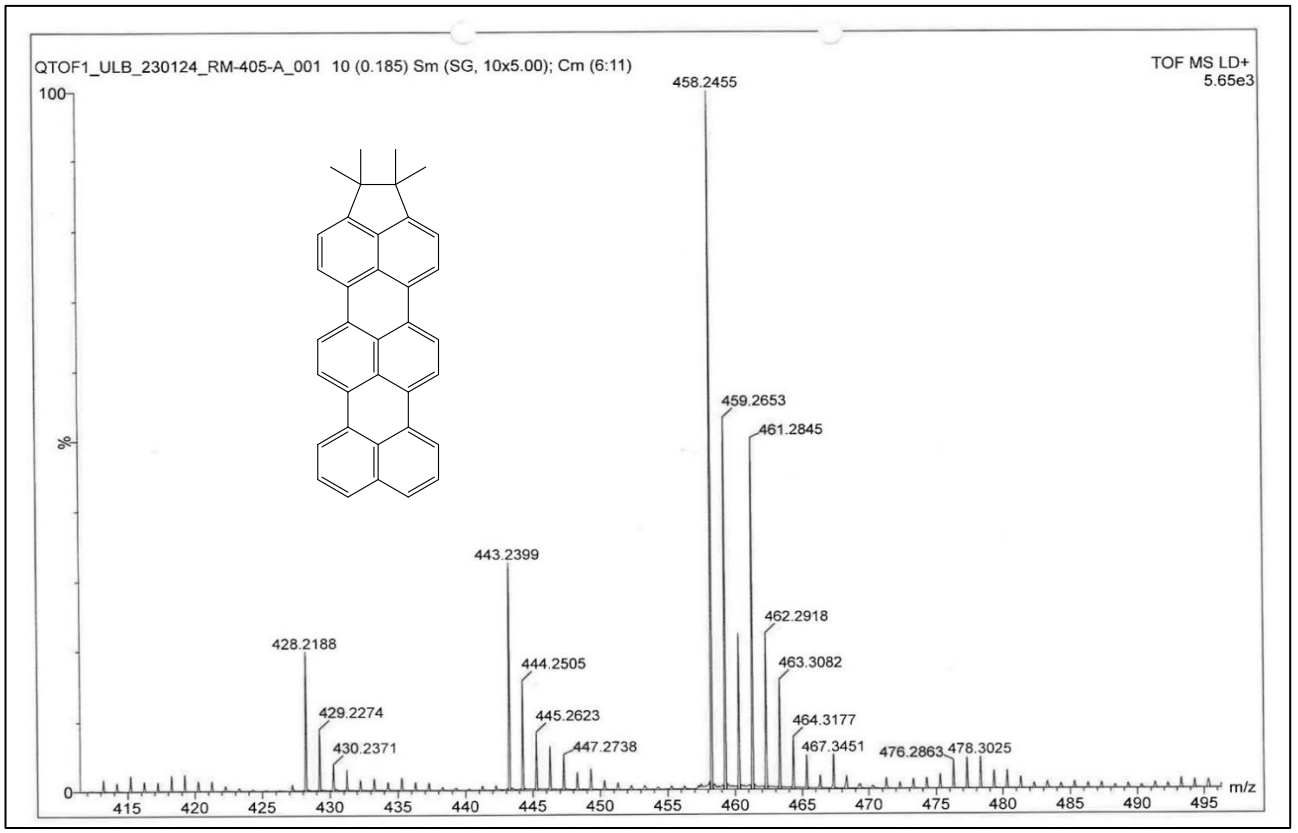
QTOF1_ULB_230124_RM-405-A_001 10 (0.185) Sm (SG, 10x5.00); Cm (6:11)
TOF MS LD+
5.65e3
100
%
0
458.2455
459.2653
461.2845
443.2399
462.2918
428.2188
444.2505
463.3082
429.2274
445.2623
464.3177
430.2371
447.2738
467.3451
476.2863
478.3025
415 420 425 430 435 440 445 450 455 460 465 470 475 480 485 490 495
m/z

1.3 Thermogravimetric analysis (TGA)

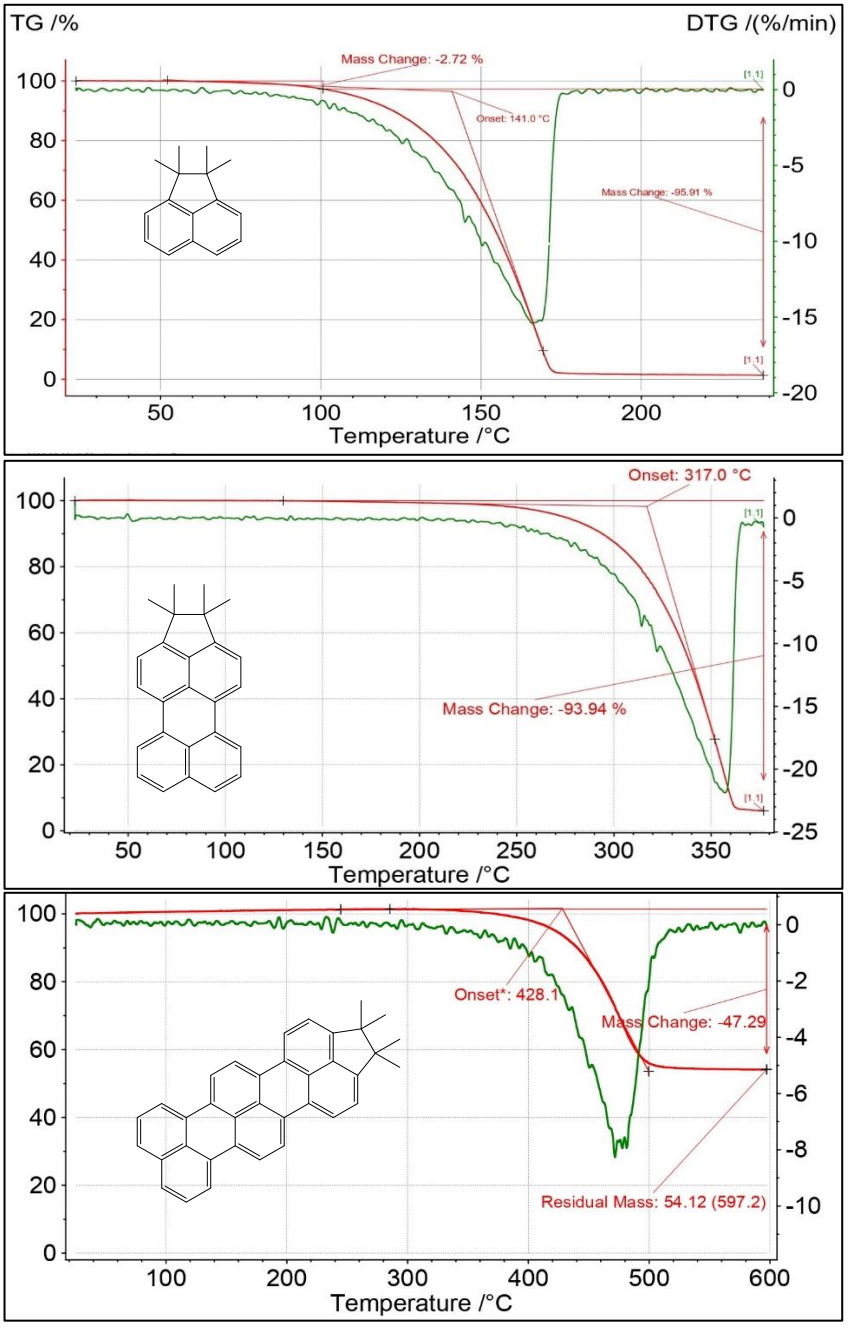

Figure S 1. TGA curves of TMN, TMP and TMT (red solid line) and first derivatives (green solid line). The data were recorded with a heating rate of 5°C/min

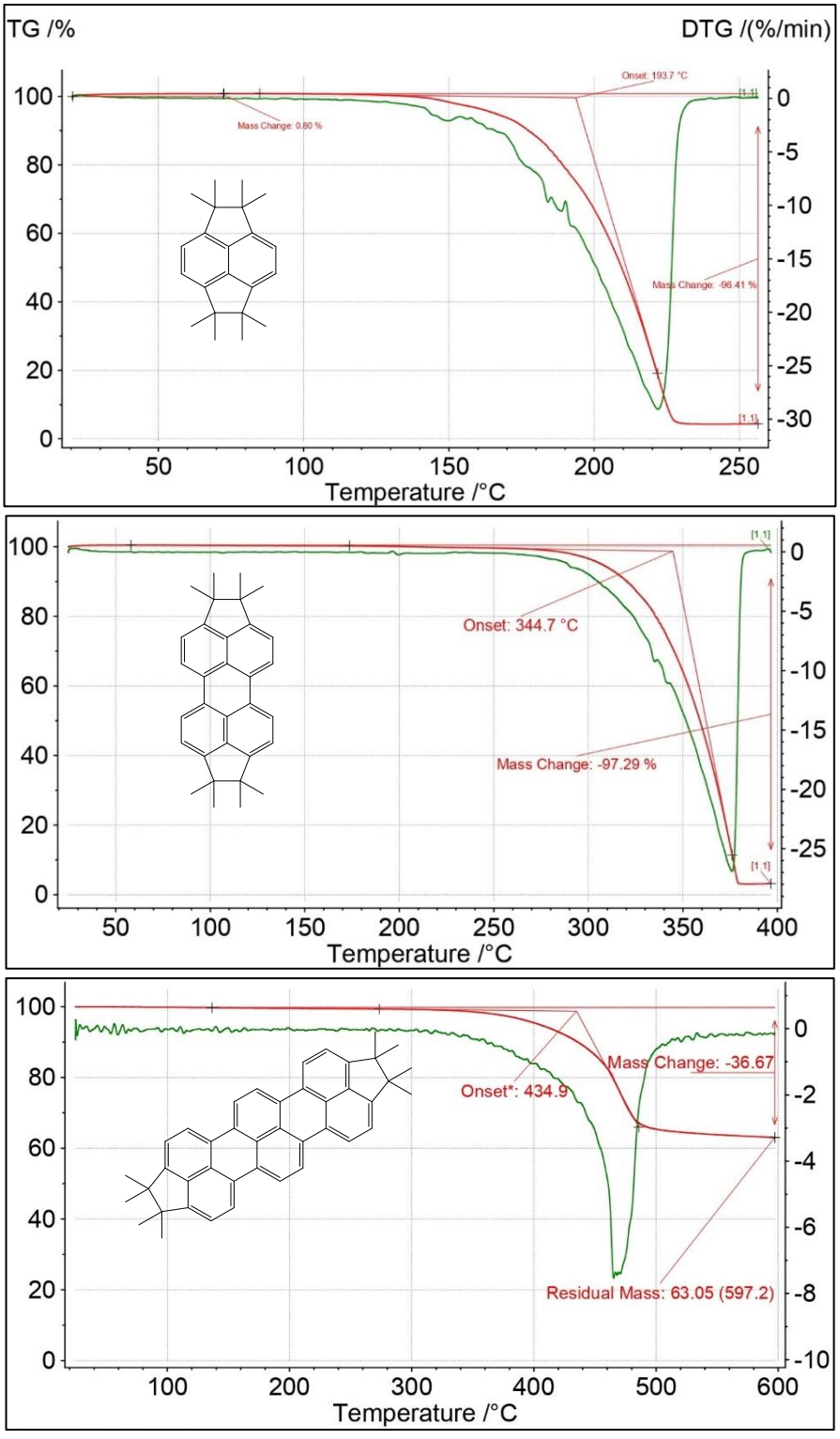

Figure S 2. TGA curves of OMN, OMP and OMT (red solid line) and first derivatives (green solid line). The data were recorded with a heating rate of 5°C/min

1.4 Differential Scanning Calorimetry (DSC)

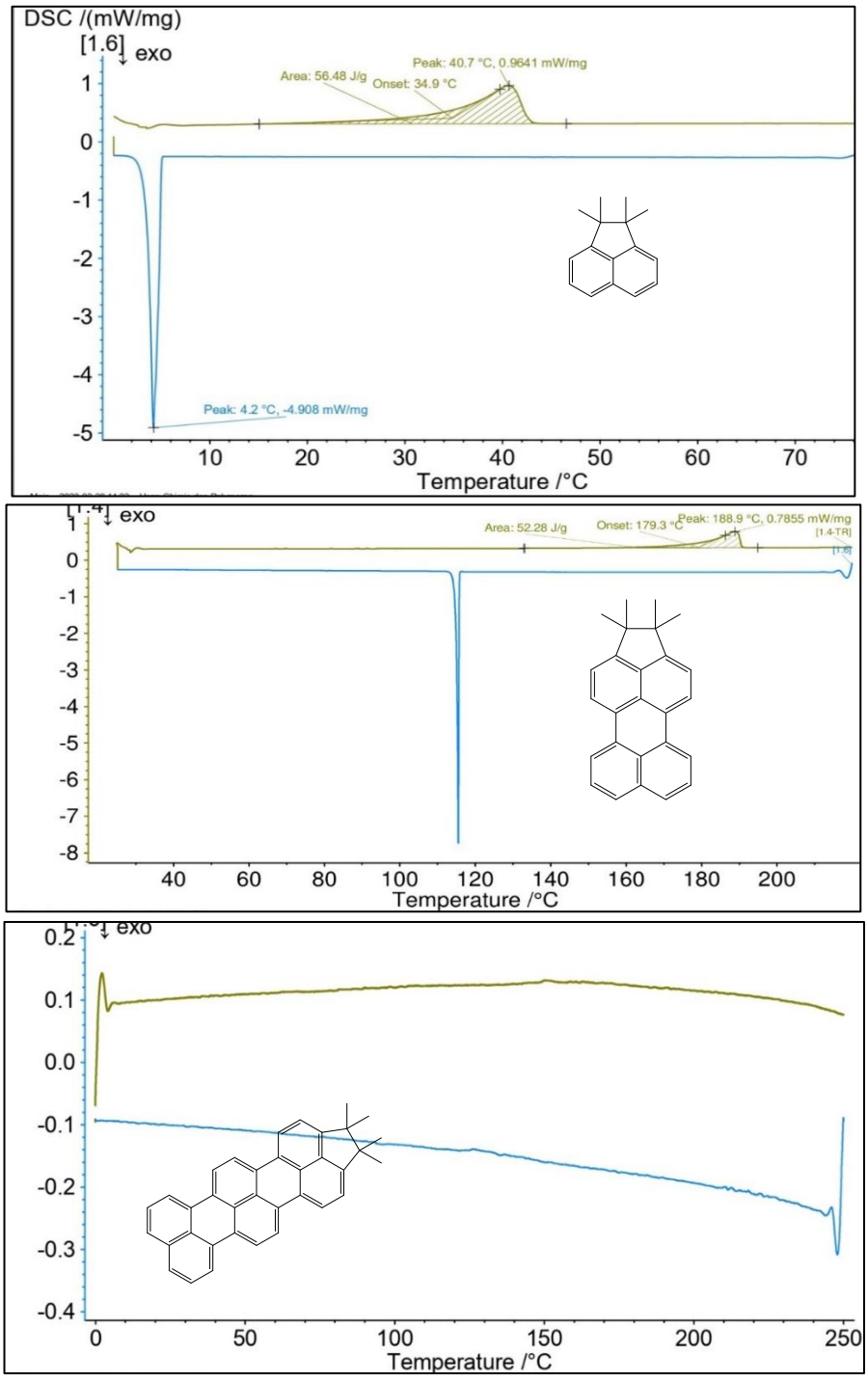

Figure S 3. DSC curves of TMN, TMP and TMT (red solid line) recorded at 10°C/min.

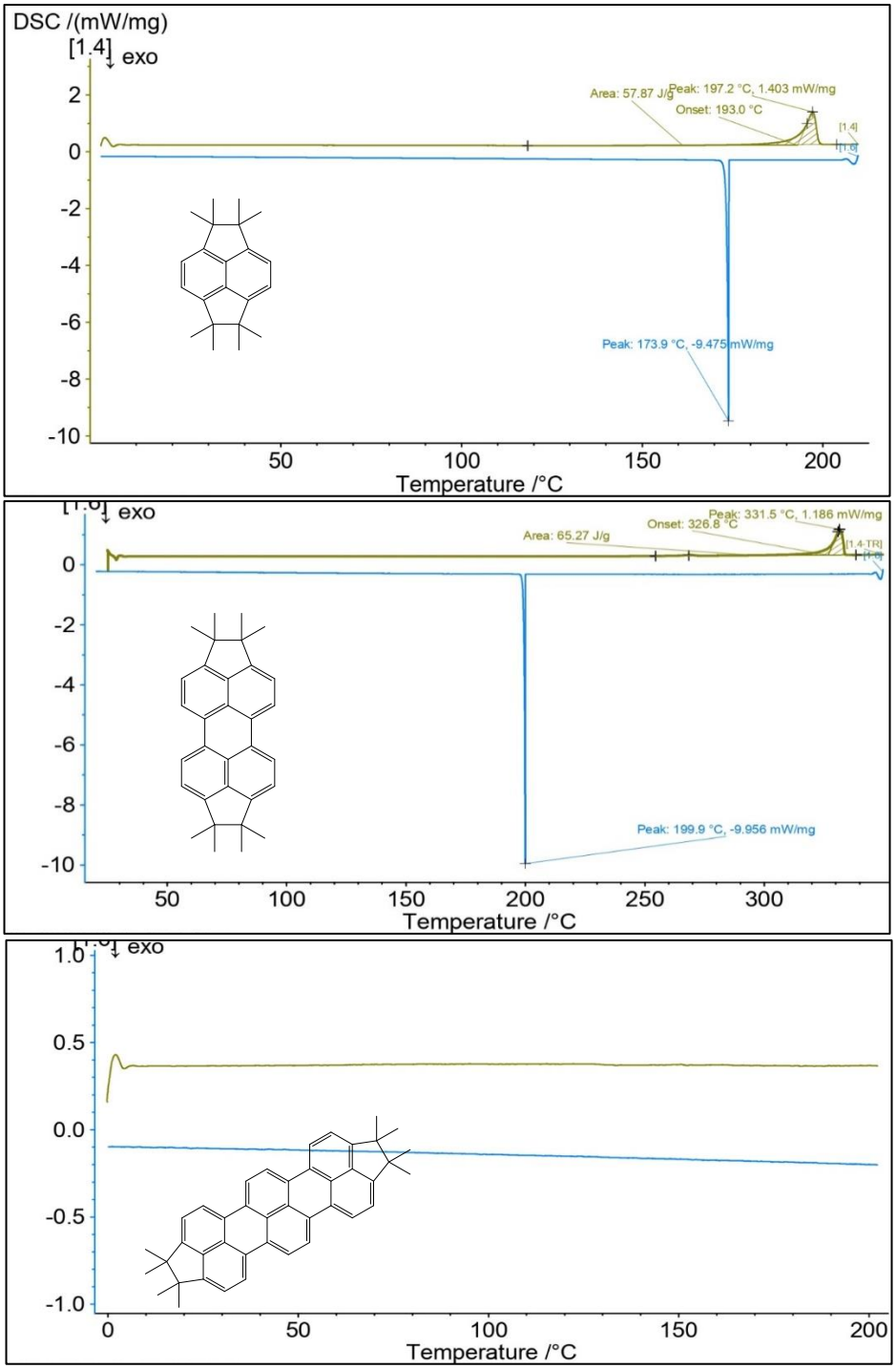

Figure S 4. DSC curves of OMN, OMP and OMT recorded at 10°C/min. For OMN, the phase transition and the TGA onset temperatures are the same, preventing to conclude on the nature of the phase transition, i.e., evaporation, sublimation, or melting. For OMP, the melting temperature occurs 18°C below the TGA onset temperature. No phase transition could be observed for before onset temperature for OMT.

1.5 Crystal Structure Data

Parameters	*Naphthalene*	*3a*[5]	*4a*[6]	*Perylene (α-form)*[7]	*Perylene (β-form)*[8]	*3b*[3]	*4b*[9]	*Terrylene*[10]
CCDC number	233928	1100613	1240682	198723	215338	2022135	1435826	2086493
Formula	$C_{10}H_8$	$C_{12}H_{10}$	$C_{14}H_{12}$	$C_{20}H_{12}$	$C_{20}H_{12}$	$C_{22}H_{14}$	$C_{24}H_{16}$	$C_{30}H_{16}$
Mol. Wt. (g.mol^{-1})	128.17	154.21	180.24	252.31	252.31	278.34	304.38	376.58
Crystal system	Monoclinic	Orthorhombic	Monoclinic	Monoclinic	Monoclinic	Monoclinic	Monoclinic	Monoclinic
Space group	*P 2$_1$/c*	*Pcm2$_1$ -C$_{2v}$*	P2$_1$/*n*	*P 2$_1$/c*	*P 2$_1$/a*	P2$_1$/*n*	*P 2$_1$*/n	*P 2$_1$/a*
a (Å)	7.8248(2)	8.290(8)	12.56(4)	10.239(1)	9.7450(10)	7.9860	7.7067(3)	11.3(2)
b (Å)	5.94349(2)	14.00(12)	5.030(1)	10.786(1)	5.823(10)	9.7282	8.2568(3)	10.4(2)
c (Å)	8.0997(10)	7.225(3)	7.320(1)	11.132(1)	10.5824(10)	17.2083	12.0508(5)	14.8(3)
β (°)	114.441(2)	90	96.14	100.92(1)	96.69	99.270	101.981(2)	96.6(5)
V (Å^3)	342.438	838.533	459.723	1207.13	596.428	1319.43	750.121	1727.77
Z/Z'	2/0.5	4/0	2/0.5	4/0	2/0.5	4/0	2/0.5	4/0
Density (g·cm^{-3})	1.248	1.19	1.302	1.388	1.405	4.18	1.348	1.4461

Table S 1. Crystal structure data of reported oligorylene structures extracted from literature.

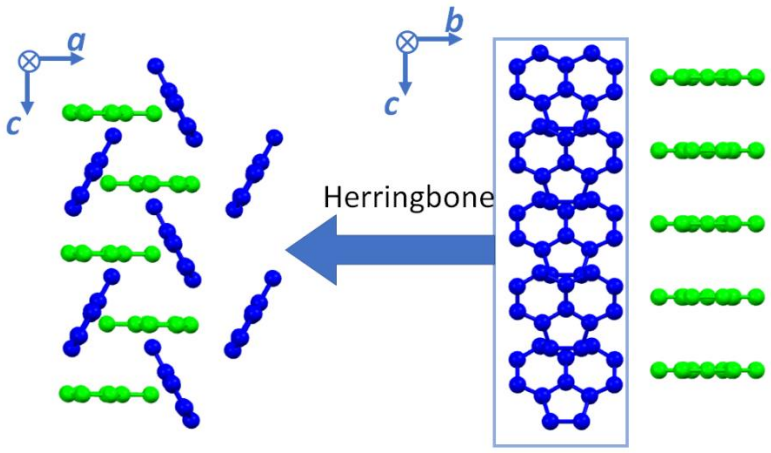

Figure S 5.Crystal packing of 3a, (left picture: view from b-axis) and (right picture: view from a-axis) blue colour molecule indicating Herringbone structure whereas, green colour indicating molecule with co-facial arrangement.

Molecules	Interplanar Distances (Å)
Naphthalene	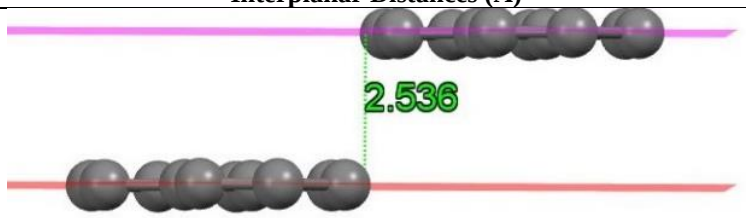
3a	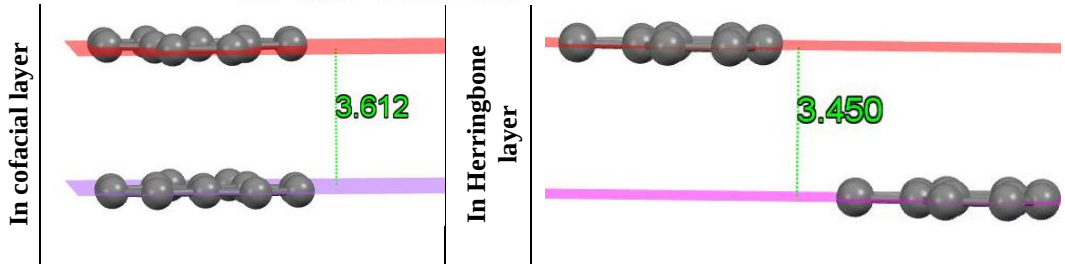
4a	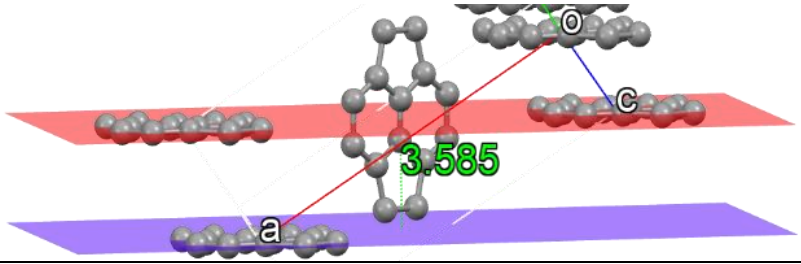

TMA **OMPy**	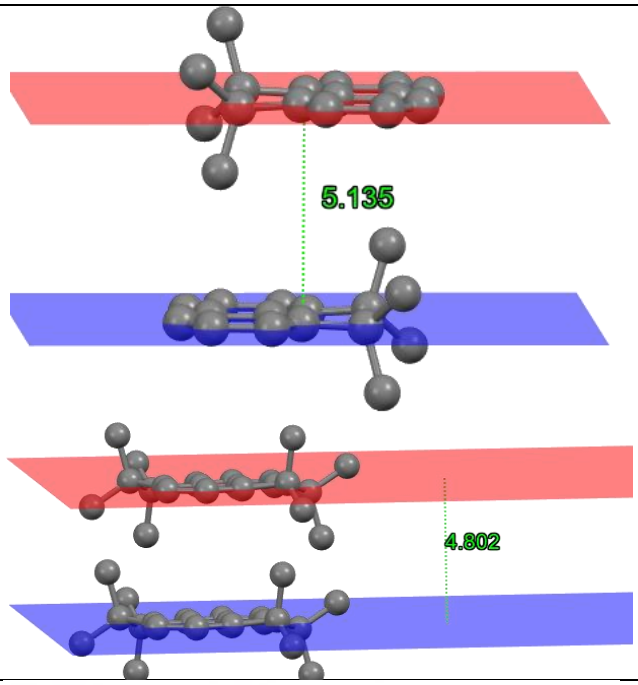
***α*-Perylene** ***β*-Perylene** **3b** **4b**	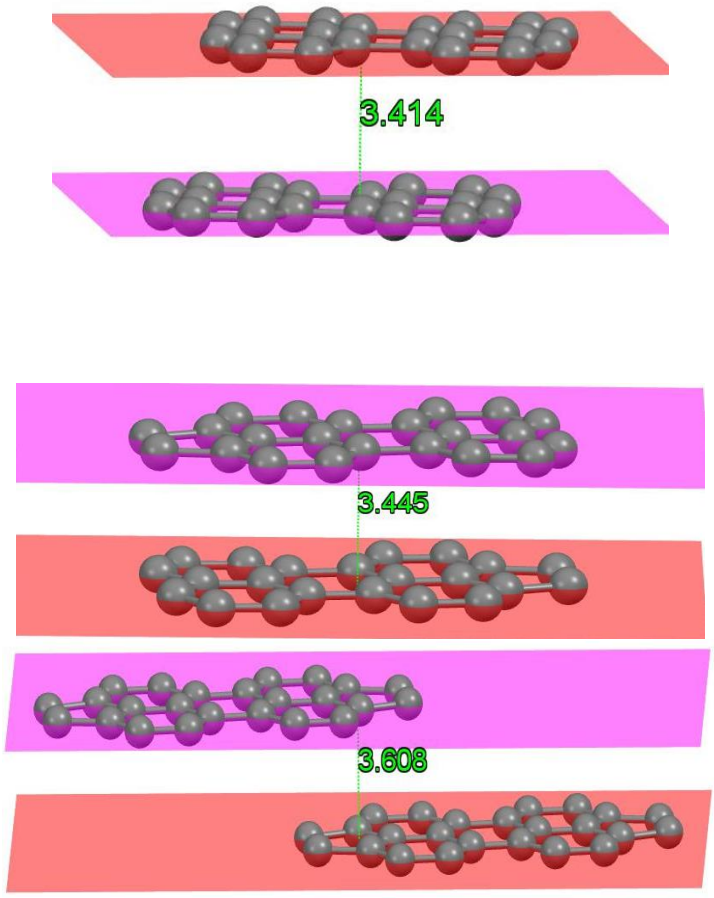

TMP **OMP**	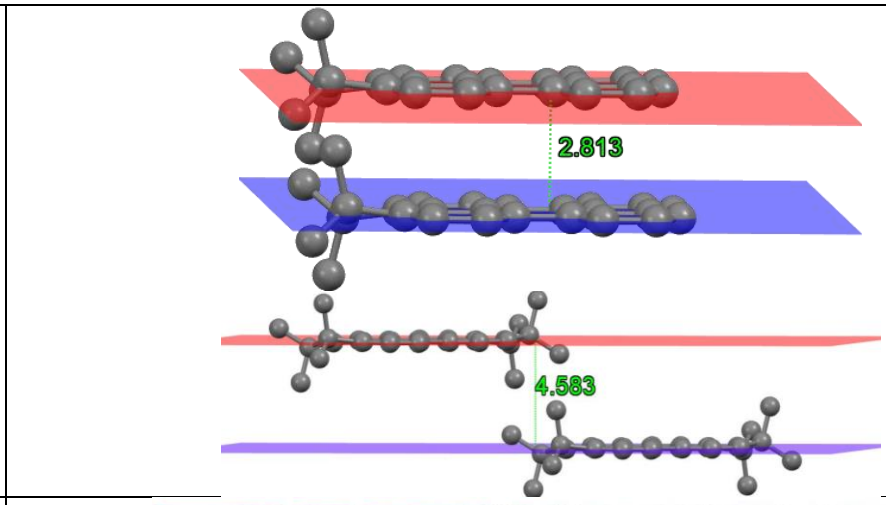
Terrylene **TMT** **OMT**	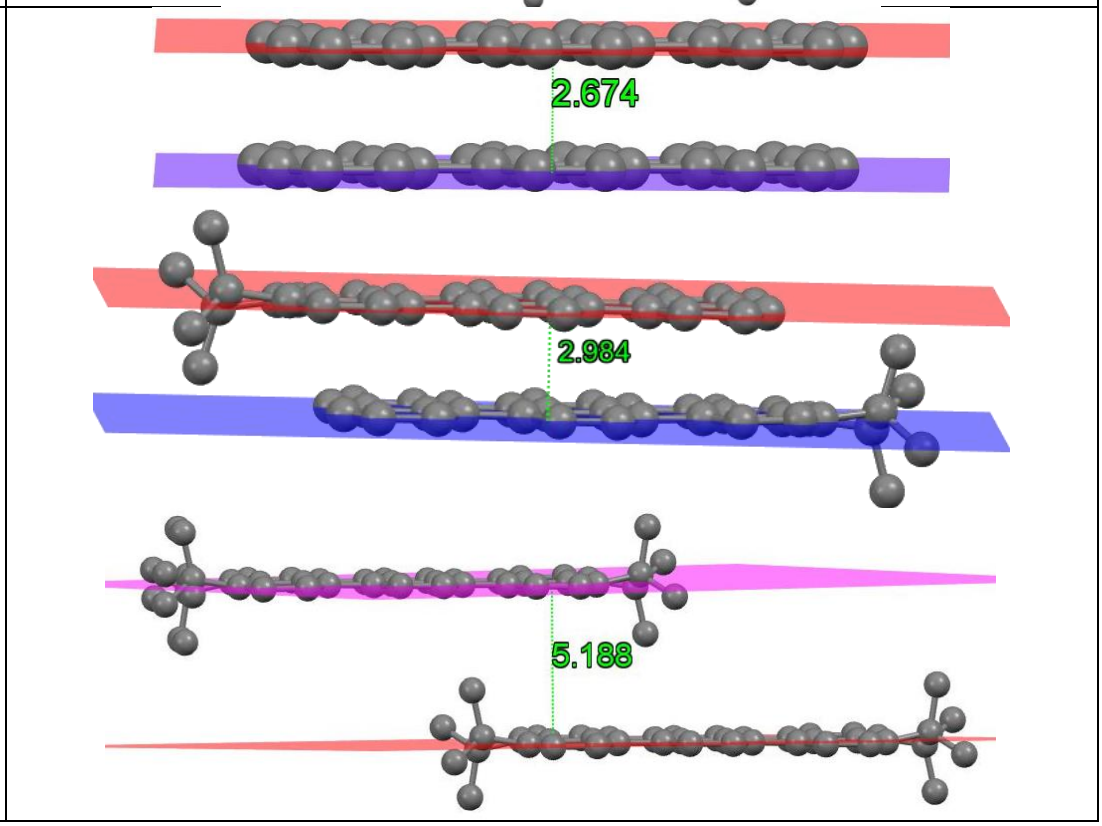

Table S 2. Interplanar distances of oligorylene derivative

Parameters	*TMA*	*TMP*	*TMT*	*OMPy*	*OMP*	*OMP-I*	*OMT*
Formula	$C_{16}H_{18}$	$C_{26}H_{22}$	$C_{36}H_{26}$	$C_{22}H_{28}$	$C_{26}H_{22}$	$C_{26}H_{22}$	$C_{42}H_{36}$
Mol. weight ($g.mol^{-1}$)	210.30	334.45	458.6	292.44	334.459	334.459	538.99
Temp (K)	293	293	150	293	293	293	150
Crystal system	Monoclinic	Orthorhombic	Monoclinic	Monoclinic	Monoclinic	Orthorhombic	Monoclinic
Space group	*P $2_1/n$*	*$P2_12_12$*	$P2_1/c$	*$P2_1/n$*	*$P2_1/c$*	*Pbca*	*$P2_1/n$*
a (Å)	7.774(7)	7.5439(8)	20.473(4)	7.604(6)	9.684(7)	14.112(2)	9.602(3)
b (Å)	11.563(7)	7.992(12)	9.438(1)	10.126(9)	11.023(7)	9.306(2)	18.736(3)
c (Å)	14.090(10)	15.094(3)	12.807(1)	11.811(9)	11.049(10)	17.683(4)	8.413(2)
β (°)	97.887(7)	90	91.80(1)	103.015(7)	90(7)	90	108.39(2)
V ($Å^3$)	1254.71(16)	910.03	2473.4	886.15	99.257(16)	2322.2	1436(1)
Z/Z'	4/1	2/0.5	4/0	2/0.5	4/0	8/0.5	2/0.5
Density ($g \cdot cm^{-3}$)	1.113	1.220	1.232	1.096	1.188	1.113	1.250
HB (°)	73.36	43.79	86.73	73.75	68.03	67.59	57.74
Core-tilt angle (°)	89.98	90	6.7	53.04	61.83	56.21	67.1
Stacking dist. (Å)	5.45	7.54	7.7	7.61	11.05	9.31	8.41
Interplanar distance, d(Å)	5.135	2.813	2.984	4.802	4.583	5.18	5.188
x (°)	73.59	90	73.4	37.31	32.31	34.73	65.79
Ψ (°)	89.57	21.71	29.5	84.41	69.72	82.29	30.61
Δ x	1.54	0.00	2.2	6.05	9.34	7.65	3.45
Δ Ψ	0.04	7.01	6.7	0.74	3.83	1.15	7.24
Pitch (°)	16.68	0.00	36.7	51.55	63.86	55.91	54.73
Roll angle (°)	0.46	68.13	66.3	8.77	39.88	12.55	71.37

Table S 3. Crystal structure data of oligorylene series present in this work

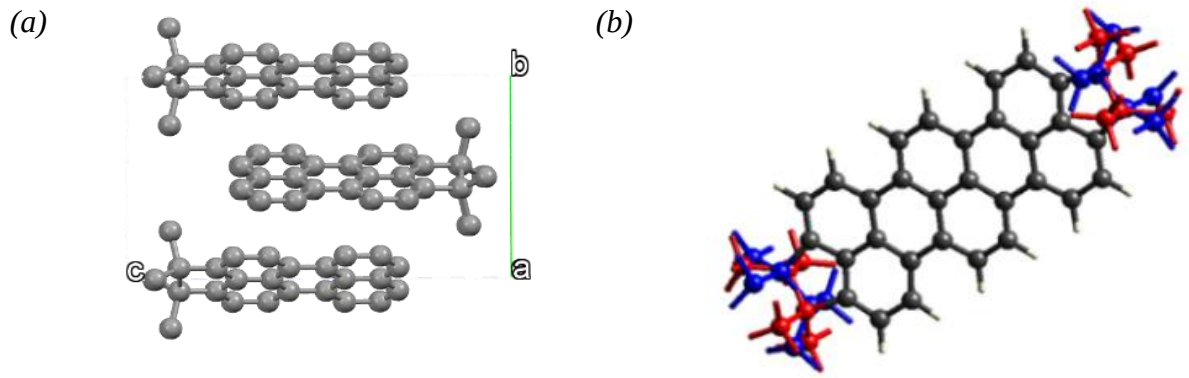

Figure S 6. (a) Anti-parallel packing of TMP (b) Disorder in terminal methyl group in OMT

1.6 Hirshfeld Surface Analysis

The Hirshfeld surfaces were generated through *CrystalExplorer17* software.[11,12] The normalized contact distance (*d*norm) based on d_e (the distance from the point on the surface to the nearest nucleus external to the surface) and d_i (the distance from 26 the point on the surface to the nearest nucleus internal to the surface) and van der Waals radii of the atom is calculated by:

$$d_{norm} = \frac{(d_i - r_i^{vdw})}{r_i^{vdw}} + \frac{(d_e - r_e^{vdw})}{r_e^{vdw}}$$

where $r_i{}^{vdw}$ and $r_e{}^{vdw}$ are the van der Waals radii of the atoms.

2D fingerprint plot derived from a Hirshfeld surface reveals visually the frequency of each combination of de and di over the molecular surface. The colour on the plot with a range from blue (relatively few points) through green (moderate fraction) to red (highest fraction) reflects the contribution from different interatomic contacts.

Curvedness surface, a measure of "how much" shape is useful to measure curvature, offers further chemical insight into molecular packing. Low values of curvedness designate essentially a flat region of the surface and may be a sign of π-π stacking in the crystal. High curvedness is highlighted as dark-blue edges and tends to divide the surface into patches. Curvedness, C, is given by:

$$C = \frac{2}{\pi} ln \sqrt{K_1{}^2 + K_2{}^2}$$

Where, k_1 and k_2 are principal curvatures.

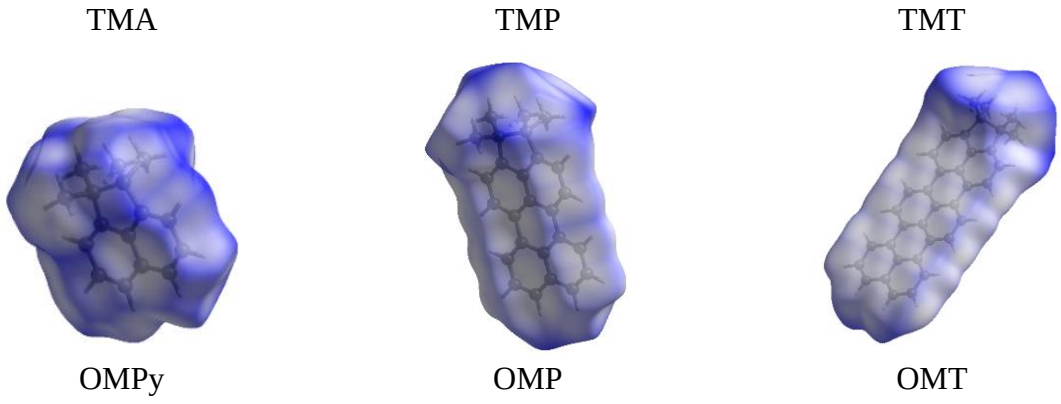

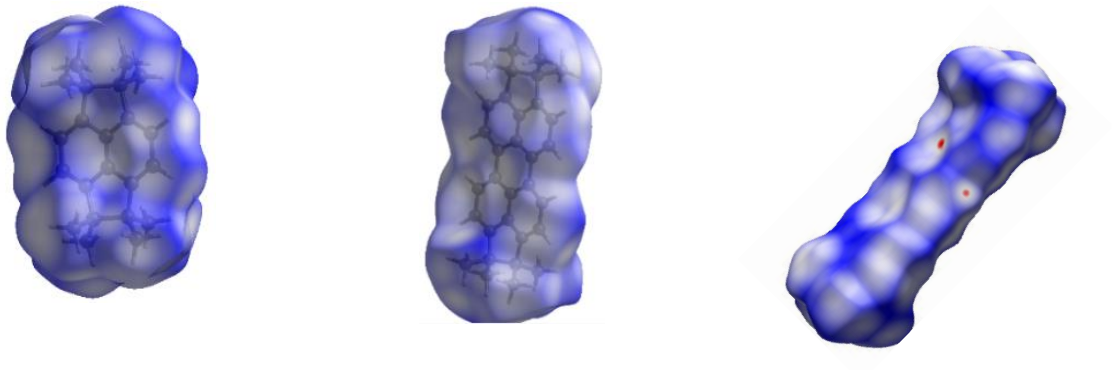

Figure S 7. Hirshfeld surface, d_{norm} of TMA, TMP, TMT, OMPy, OMP and OMT with defining short contact.

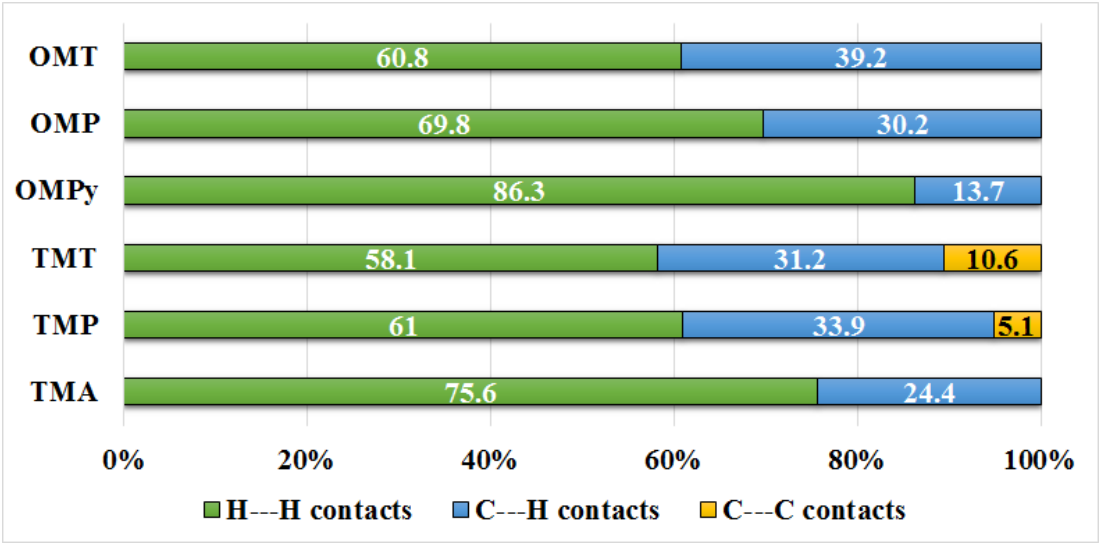

Figure S 8. Contribution of H---H, C---H and C---C contacts in crystal structure of different members of oligorylene series.

(a) Shape index of TMA (b) Shape index of OMPy

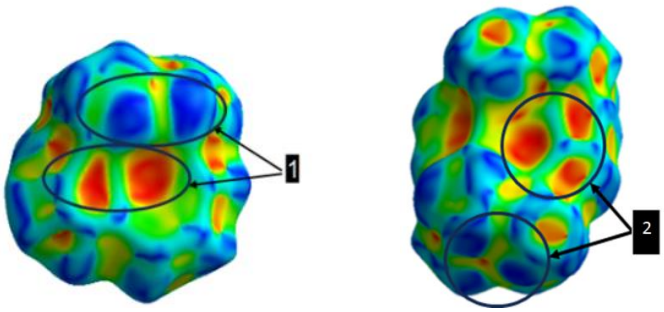

Figure S 9. (a) Shape index of TMA showcasing complementary sites involved in C-H---π interactions (blue region above methyl group) and (red-region above π-core), encircled by 1. (c) shape index of OMPy showing the complementary red-blue region (encircled by 2) for C—H_{methyl}---π interaction.

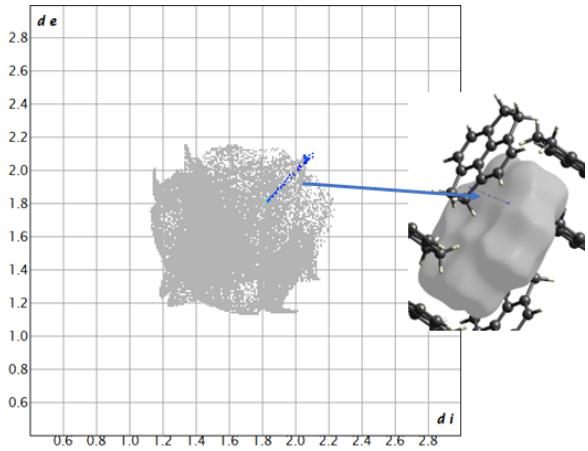

Figure S 10. C---C (0.2 %) contacts contribution in 4a

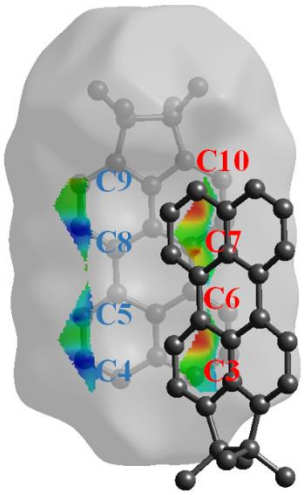

Figure S 11. Different carbon atoms in TMP molecule involved in C---C contacts or π---π interactions.

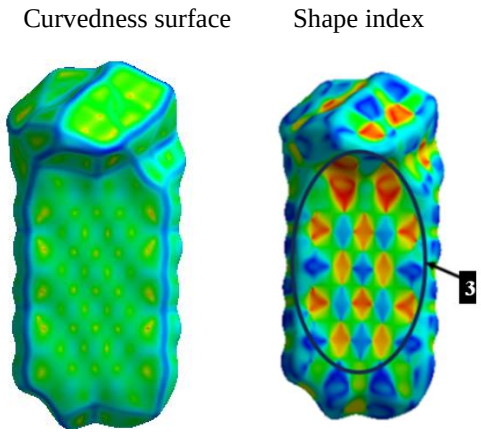

Figure S 12.(Curvedness surface and shape index map of TMT depicting regions involved in π-π interactions.

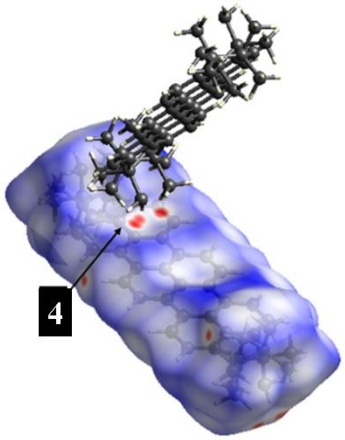

Figure S 13. OMT molecule shows close contact due to end-to-face orientation visible as two consecutive red dots illustrated by number 4 in d_{norm} *surface.*

1.7 Optical Measurements

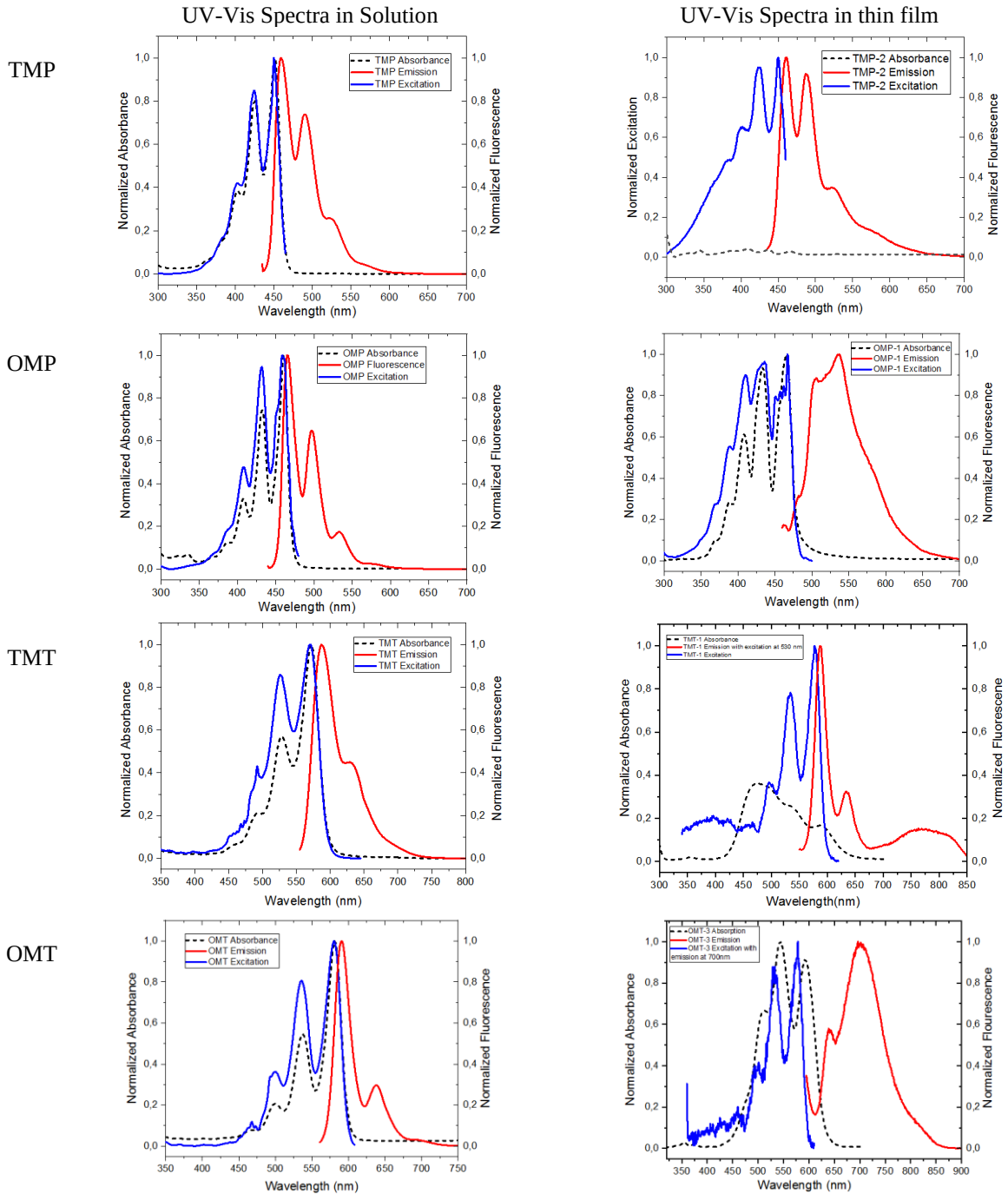

Table S 4. Comparison of Absorbance and Excitation spectra of TMP, OMP, TMT and OMT in solution and solid state. Emission spectra of TMP, OMP, TMT and OMT in solution and solid state. (Dotted black curve represent absorbance, blue curve represents excitation and red curve represent emission spectra)

1.8 XRD data of oligorylenes collected on thin film samples and powdered samples

(a)

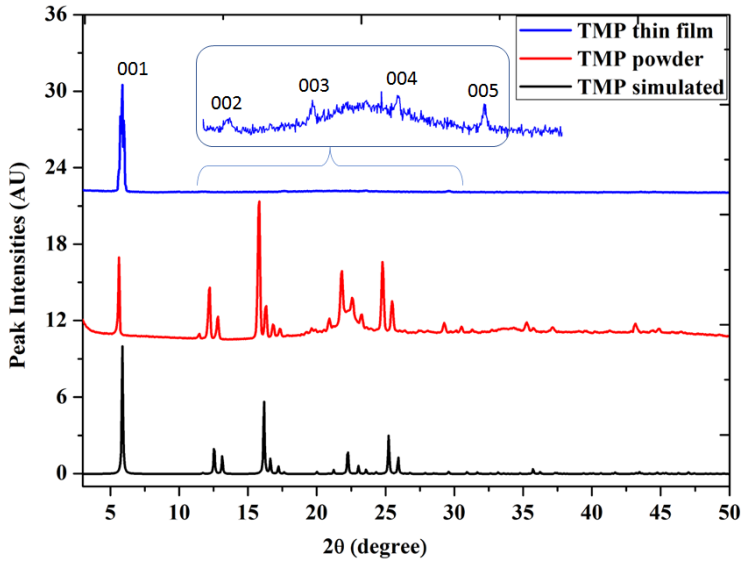

(b)

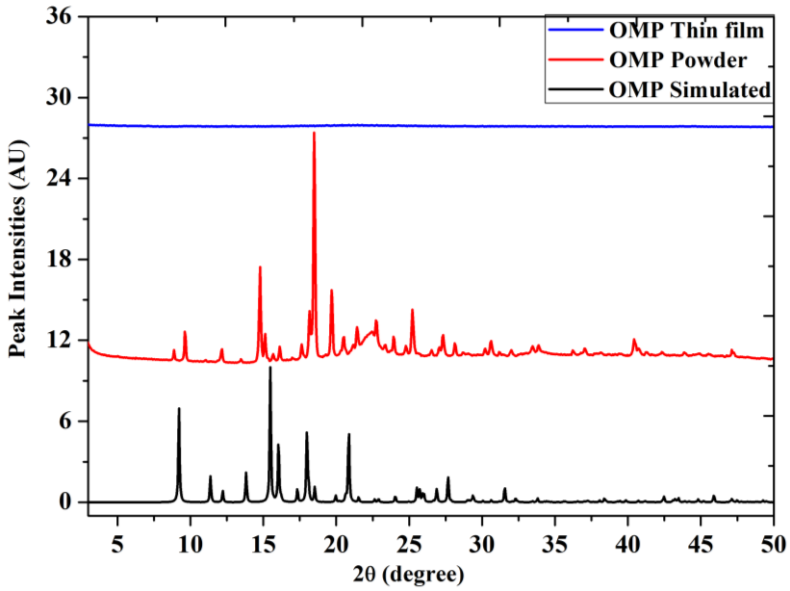

(c)

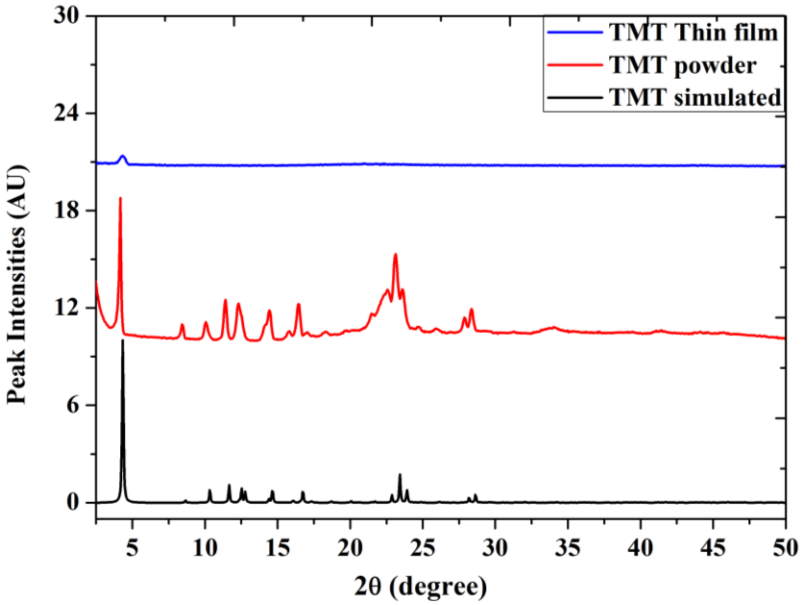

(d)

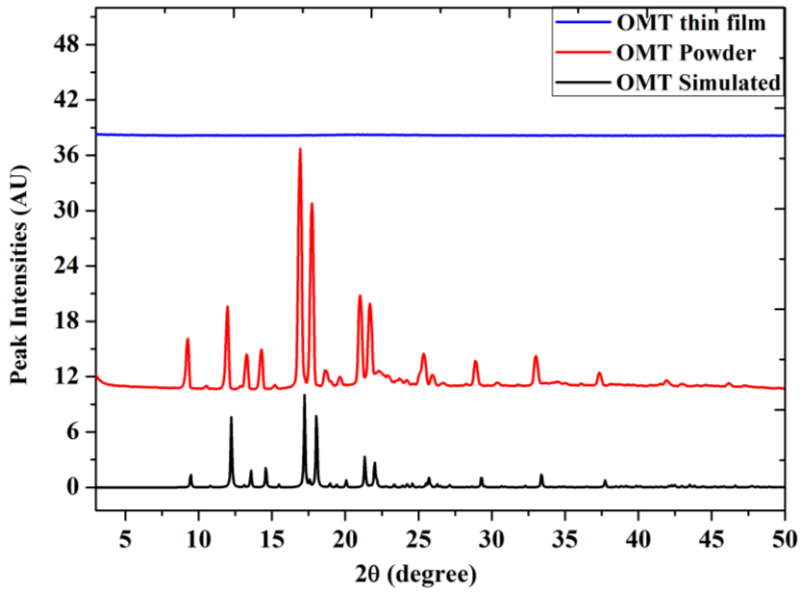

Figure S 14. Comparison of simulated powder XRD (black line) to experimental XRD on powdered (red line) and thin film (blue line) deposited on quartz substrate in oligorylene.(a) TMP; inset presents the other peaks related to 00l family of plane (b) OMP (c) TMT and (d) OMT

1.9 Quantum calculations and transfer integrals

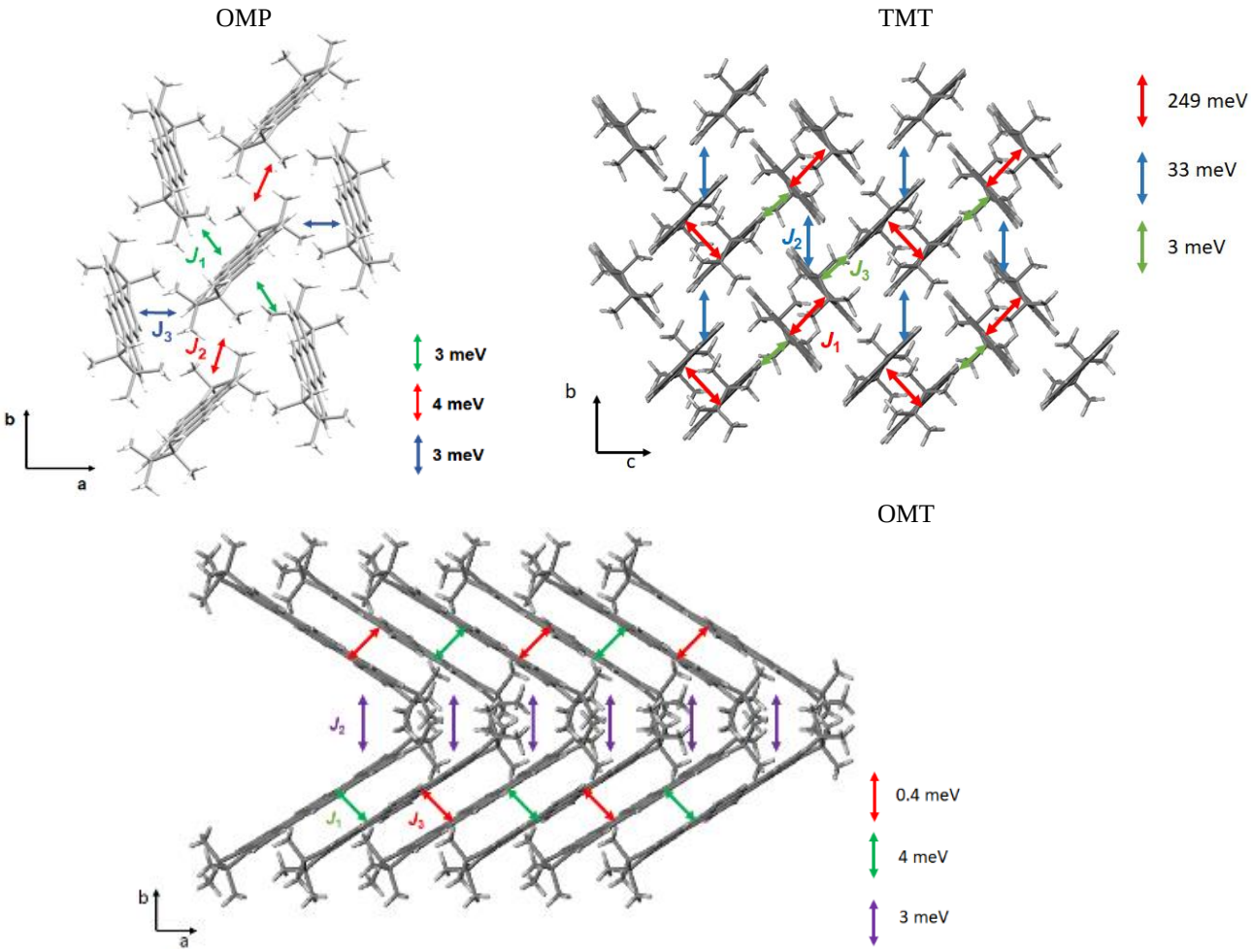

Figure S 15. Calculated Transfer Integrals of TMT, OMP and OMT

1.10 Measurement curves and thin film XRD diffractogram recorded on OFET devices.

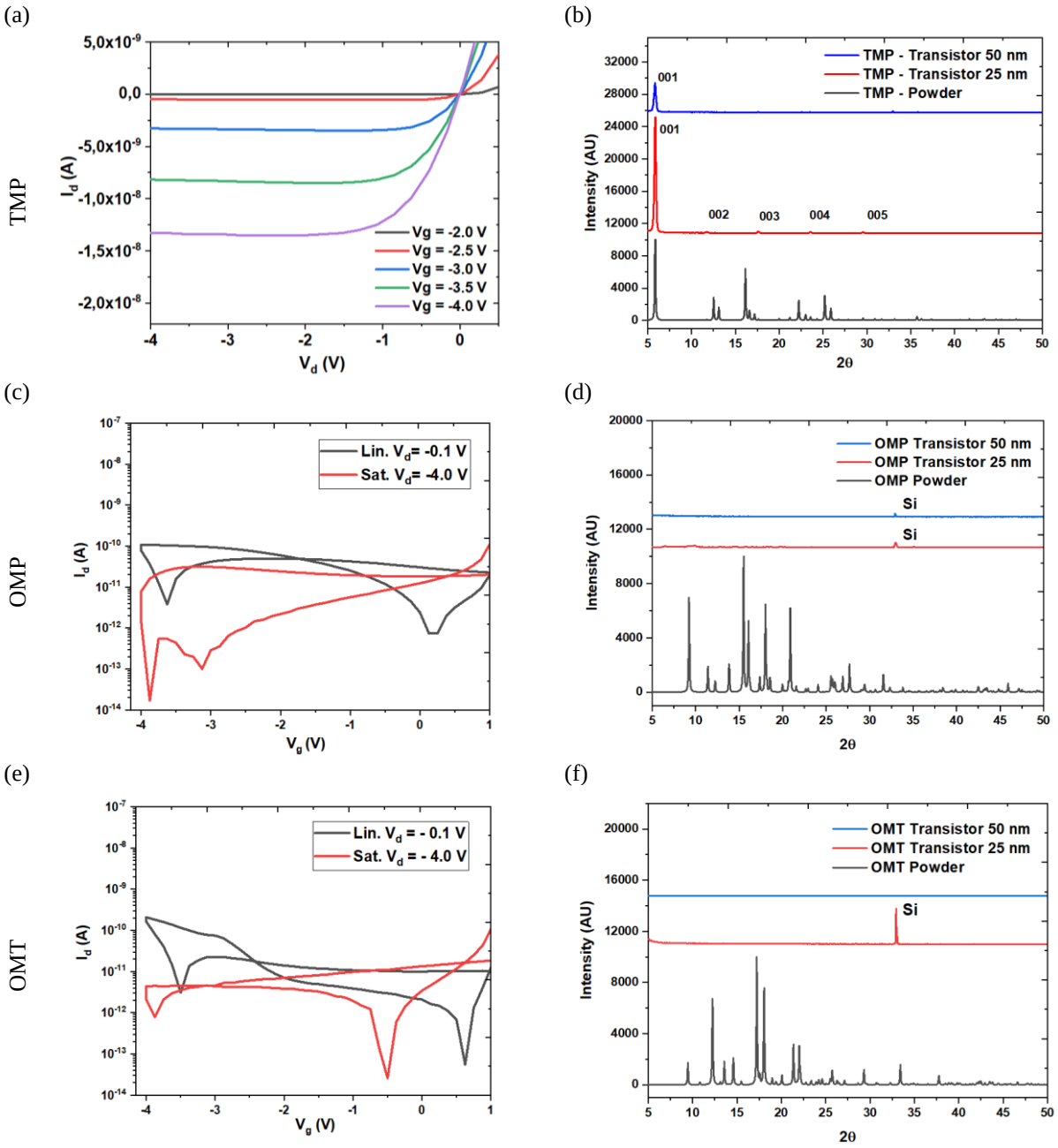

Figure S 16. (a) and (b) Output characteristic curve from OFET of TMP and thin film XRD diffractogram recorded on OFET of TMP; (c) and (d) Transfer characteristic curve from OFET of OMP and thin film XRD recorded on same OFET device; (e) and (f) Transfer characteristic curve from OFET of OMT and thin film XRD diffractogram recorded on same OFET device

1.11 Polarized Optical Microscope Images

Thickness of the OSC film in transistor

Compounds	25nm	50nm
TMP	a 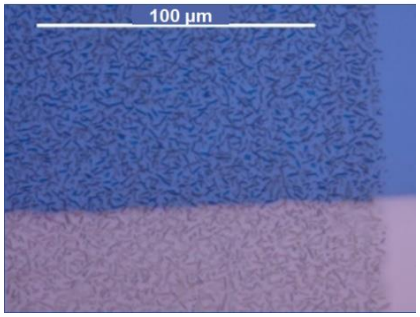	b 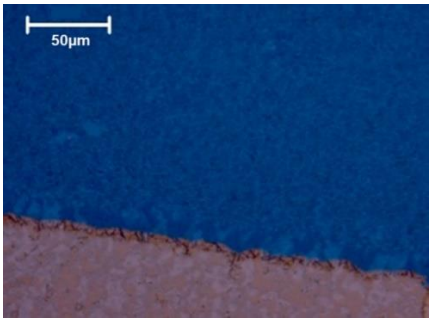
OMP	c 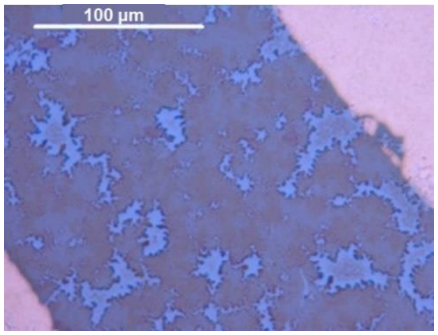	d 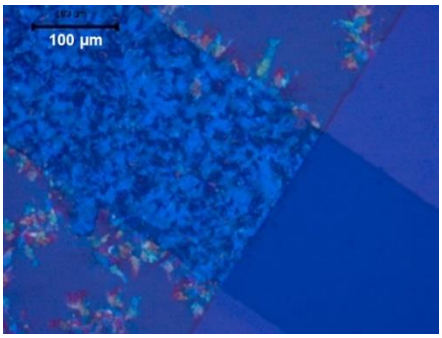
OMT	e 	f 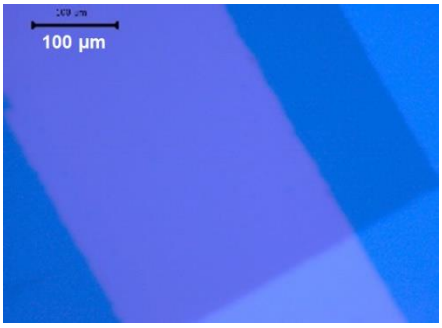

Figure S 17. Polarized optical microscope images of (a) TMP thin film thickness 25nm (b) TMP thin film thickness 50nm (c) OMP thin film thickness 25nm (d) OMP thin film thickness 50nm (e) OMT thin film thickness 25nm (f) OMT thickness thin film 50nm.

1.12 FI-TRMC results

While OFETs probe transport on macroscopic length-scale (µm) and timescales (s), microwave-based techniques operate at short length (nm) and timescales (ns).[13] These measurements are based on the absorption spectroscopy of microwaves by mobile charges and provide a contactless evaluation of intrinsic charge transport. The length-scale is much smaller than the average grain size, therefore the measurements are not affected by scattering of charges at grain boundaries or trapping at defects, contrary to OFETs. After generation of the charges in the semiconducting material, the absorption of the microwaves induces displacement of the charges and allows to probe their intrinsic mobility. In absence of mobile charges, microwaves propagate through the material without attenuation of the transmitted microwave power. In presence of mobile charges, the oscillating electric field of the microwaves induces a motion of the charges due to microwave absorption and the transmitted microwave power decreases.[14]

According to Equation 1, where K (S/cm) is a calibration factor computed experimentally, the change in microwave power $\Delta P/P$ (dimensionless) is directly proportional to the change in conductivity i.e. $\Delta\sigma$ (S/cm). However, $\Delta\sigma$ is directly related to μ through Equation 2, where e is the elementary charge (1.602×10^{-19} C) and N is the number of charge carrier generated and ΔN is the change in number of charge carrier inside the semiconductor (cm^{-3}).

Equation 1

$$\Delta\sigma = K\frac{\Delta P}{P}$$

Equation 2

$$\Delta\sigma = e\mu\Delta N$$

The measurements are performed on a metal-insulator-semiconductor (MIS) devices, fabricated using SiO_2 and poly(methyl methacrylate) (PMMA) as the dielectric, and vapor deposited films of the organic semiconductor as the active layer forming a diode type device (bottom Au/SiO_2/PMMA/OSC/top Au). Similarly, to OFETs, upon application of a bias between the two electrodes, charges are injected, and they accumulate at the interface between the semiconductor and the dielectric layer. Therefore, selective investigations at interfaces, which play a key role in the performance of FET devices, are available in FI-TRMC measurement. Due to the similarities between MIS and OFET devices, it is possible to make a direct comparison between microscopic and macroscopic charge transport.

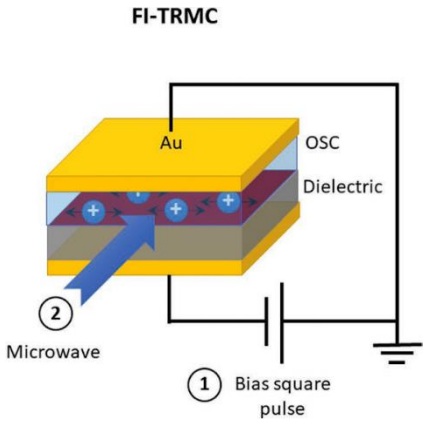

Figure S 18. Schematic representation FI-TRMC techniques.

Upon application of a gate bias in the MIS device, charges are injected in the semiconducting layer and the change in charge carrier number ΔN is proportional to the change in the applied voltage ΔV according to Equation 3, where C is the capacitance and e is the elementary charge of an electron.

Equation 3

$$\Delta N = C \Delta V e$$

Figure S 19 shows a schematic illustration of a microwave circuit for FI-TRMC. The microwave source generates microwaves with a certain frequency (~9 GHz) and power (200-300 nW) and split them in the circuit. A source meter applies a bias on the MIS device in the cavity, promoting the generation of field-induced charge carriers that interact with the microwaves. The FI-TRMC signals are picked up by a diode and finally monitored with an oscilloscope. In Figure S 19 (top right) is reported a typical FI-TRMC output of current (blue line) and power (red line) variation with time, when a square gate bias (V_g, green line) is applied. Similar plot is recorded for oligorylene TMP, OMP and OMT. The corresponding MIS devices display a time-dependent microwave power change (ΔP), as shown in Figure S 20. For TMP, when the applied gate bias voltage was decreased from -3 V to –60 V, ΔP increased proportionally, because the number of accumulated holes became large in relation to the absolute value of the gate bias. However, no change in microwave power in case of OMP and OMT represents either the absence of charge carriers (which is practically isn't possible). Hence, no response or lack of response could be attributed to lower conductivity for charge carriers.

By combination of Equation 1 and Equation 2, it is possible to directly correlate ΔP and the product $\Delta N\mu$ which results in a new Equation 4, where K' is a sensitivity factor determined experimentally.

Equation 4

$$\Delta P = K' \Delta N \mu$$

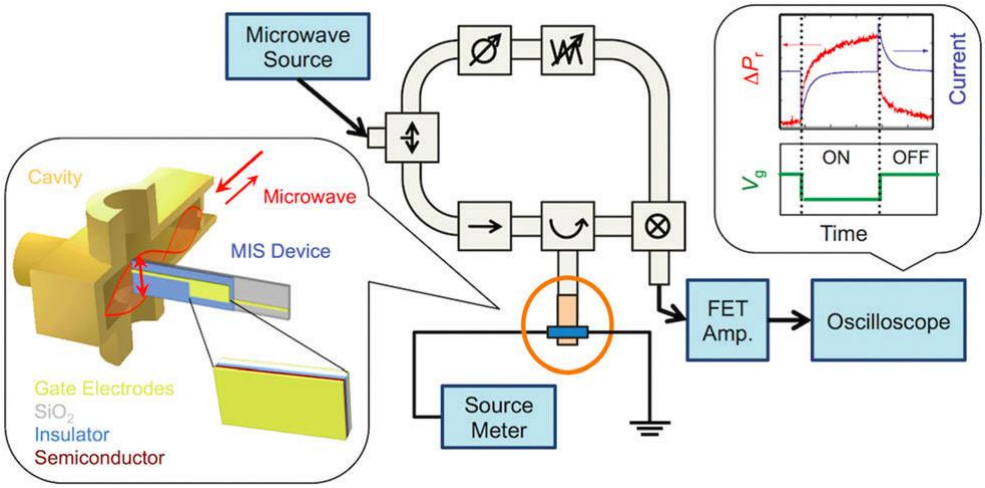

Figure S 19. Schematic diagram of the FI-TRMC measurement system. The MIS device is loaded into the microwave cavity and the transient current injected into the device is monitored by an external electric circuit.[14]

After measuring ΔP at different gate bias and capacitance and using equations (4) and (3), we can draw the ΔN–$\Delta N\mu$ plots, as shown in Fig. 6. The slope (ΔN /$\Delta N\mu$) corresponds to the value of mobility.

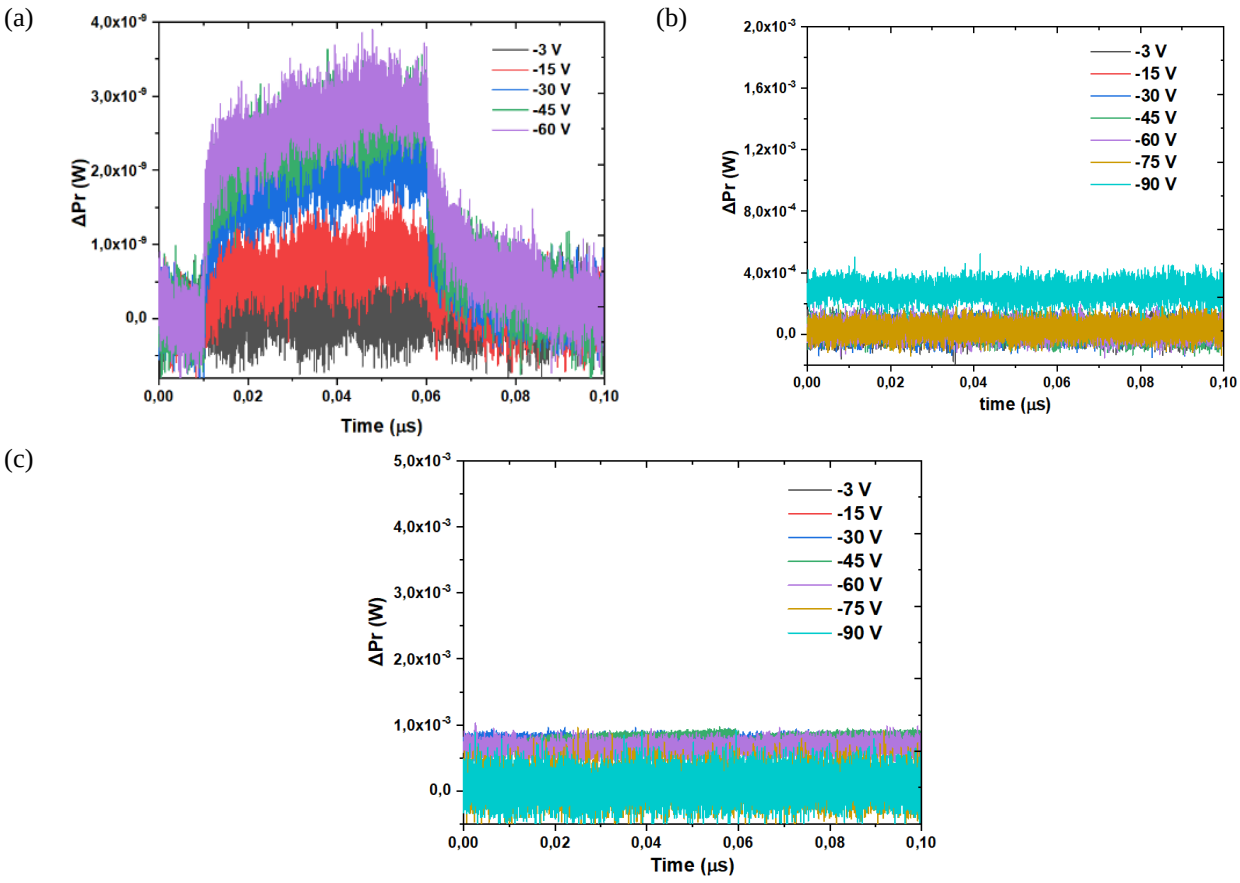

Figure S 20. Plots representing response of oligorylene molecule, (a) TMP, (b) OMP and (c) OMT measured by FI-TRMC technique.

The value of mobility measured by FI-TRMC is performed on polycrystalline samples and it is comparable with mobility measurements in OFETs made with single crystalline materials. Therefore, potentially this technique allows the determination of mobility in single crystalline states even using polycrystalline materials, because the small length-scale of the microwave's probes charge displacement in single domains and it is insensitive to grain boundaries.

1.13 References

(1) Abd El-Aal, H. A. K.; Khalaf, A. A. Modern Friedel-Crafts Chemistry. Part 38. Facile Synthesis of Acenaphthenes via Direct and Rearranged Intramolecular Friedel-Crafts Cyclialkylations of Intermediate Carbinols. *Polycycl Aromat Compd* **2013**, *33* (4), 331–346. https://doi.org/10.1080/10406638.2013.781041.

(2) Mitchell, R. H.; Lai, Y.-H.; Williams, R. V. N-Bromosuccinimide-Dimethylformamide: A Mild, Selective Nuclear Monobromination Reagent for Reactive Aromatic Compounds. *J Org Chem* **1979**, *44* (25), 4733–4735. https://doi.org/10.1021/jo00393a066.

(3) Pigulski, B.; Ximenis, M.; Shoyama, K.; Würthner, F. Synthesis of Polycyclic Aromatic Hydrocarbons by Palladium-Catalysed [3 + 3] Annulation. *Organic Chemistry Frontiers* **2020**, *7* (19), 2925–2930. https://doi.org/10.1039/d0qo00968g.

(4) Koch, K.-H.; Müllen, K. Polyarylenes and Poly(Arylenevinylene)s, V. Synthesis of Tetraalkyl-Substituted Oligo(1,4-Naphthylene)s and Cyclization to Soluble Oligo(Peri-Naphthylene)S2). *Chem Ber* **1991**, *124* (9), 2091–2100. https://doi.org/10.1002/cber.19911240935.

(5) Ehrlice, H. W. W. A Refinement of the Crystal and Molecular Structure of Acenaphthene. *Acta Cryst* **1957**, *10*, 699–705. https://doi.org/10.1107/S0365110X5700242X.

(6) Simmons, G. L.; Lingafelter, E. C. The Crystal Structure of Pyracene. *Acta Crystallogr* **1961**, *14* (8), 872–874. https://doi.org/10.1107/S0365110X61002515.

(7) Hsieh, C. T.; Chen, C. Y.; Lin, H. Y.; Yang, C. J.; Chen, T. J.; Wu, K. Y.; Wang, C. L. Polymorphic Behavior of Perylene and Its Influences on OFET Performances. *Journal of Physical Chemistry C* **2018**, *122* (28), 16242–16248. https://doi.org/10.1021/acs.jpcc.8b02199.

(8) Tanaka, J. The Electronic Spectra of Aromatic Molecular Crystals. II. The Crystal Structure and Spectra of Perylene. *Bull Chem Soc Jpn* **1963**, *36* (10), 1237–1249. https://doi.org/10.1246/bcsj.36.1237.

(9) Li, T.; Zhang, C. Z.; Su, Y. X.; Niu, M. X.; Gu, C. Y.; Song, M. X. Crystal Structure and Optoelectronic Properties of Antiaromatic Compound 3,4,9,10-Tetrahydrodicyclopenta[Cd,Lm]Perylene. *Crystallography Reports* **2017**, *62* (6), 885–888. https://doi.org/10.1134/S1063774517060165.

(10) Hall, C. L.; Andrusenko, I.; Potticary, J.; Gao, S.; Liu, X.; Schmidt, W.; Marom, N.; Mugnaioli, E.; Gemmi, M.; Hall, S. R. 3D Electron Diffraction Structure Determination of Terrylene, a Promising Candidate for Intermolecular Singlet Fission. *ChemPhysChem* **2021**, *22* (15), 1631–1637. https://doi.org/10.1002/cphc.202100320.

(11) Spackman, M. A.; Jayatilaka, D. Hirshfeld Surface Analysis. *CrystEngComm* **2009**, *11* (1), 19–32. https://doi.org/10.1039/b818330a.

(12) McKinnon, J. J.; Spackman, M. A.; Mitchell, A. S. Novel Tools for Visualizing and Exploring Intermolecular Interactions in Molecular Crystals. *Acta Crystallographica Section B: Structural Science*. December 2004, pp 627–668. https://doi.org/10.1107/S0108768104020300.

(13) Seki, S.; Saeki, A.; Sakurai, T.; Sakamaki, D. Charge Carrier Mobility in Organic Molecular Materials Probed by Electromagnetic Waves. *Physical Chemistry Chemical Physics* **2014**, *16* (23), 11093–11113. https://doi.org/10.1039/C4CP00473F.

(14) Honsho, Y.; Miyakai, T.; Sakurai, T.; Saeki, A.; Seki, S. Evaluation of Intrinsic Charge Carrier Transport at Insulator-Semiconductor Interfaces Probed by a Non-Contact Microwave-Based Technique. *Sci Rep* **2013**, *3* (1), 3182. https://doi.org/10.1038/srep03182.